DEVELOPMENT OF A NEW DUAL DIFFUSER MODULATION TECHNIQUE TO ALLEVIATE THE SCINTILLATION EFFECT IN FREE SPACE OPTICAL COMMUNICATION

By

ABDUL RAHMAN BIN KRAM
(1040810527)

A thesis submitted
In fulfillment of the requirements for the degree of
Doctor of Philosophy

School of Computer & Communication Engineering

UNIVERSITI MALAYSIA PERLIS

2014

ACKNOWLEDGEMENTS

Alhamdullilah, for the first and foremost, all praises and thanks to Allah the Almighty, for gracing me with strength to complete my thesis. I would like to express my deepest gratitude to my supervisor Prof. Dr. Syed Alwee Aljunid Bin Syed Junid who willingly accepted me as a student without doubt, and believes in me in finishing this study with full support and encouragement. To my co-supervisors, Ir Dr. Anuar Bin Mat Safar and Dr. Hilal Adnan Fadhil, thank you for the words of guidance, advice and encouragement throughout the completion of my thesis. My heartiest thank to both my beloved parents, who continuously pray for my success and giving me their unconditional support all along the way, especially in taking care of my children when I have no one else to turn to. I would also like to acknowledge my siblings for their utmost moral support. My endless thanks and greatest appreciation to the one, who always cares about me and at my side during my ups and downs, the one and only, my beloved wife Rapidah Binti Mustapha. I could have never completed this journey without her unconditional love and support. To Dr. Amir Razif Arief, Dr. Zahereel Ishwar and Dr. Junita I would like to extend special word of thanks for their endless support and guidance. My sincere appreciation also goes for my colleague and my best friend Mohd. Rashidi Che Beson, who always supports and assists me since my degree study until now. Last but not least I would like to acknowledge the Ministry of Higher Education and University Malaysia Perlis for supporting my studies financially.

Abdul Rahman Kram

TABLE OF CONTENTS

CHAPTER 3: RESEARCH METHODOLOGY

CHAPTER 4: DEVELOPMENT OF DUAL DIFFUSER MODULATION TECHNIQUE (DDM) IN FSO SYSTEM

LIST OF FIGURES

LIST OF TABLES

Pembangunan Satu Teknik Baharu Dwi Peresap Pemodulatan Untuk Mengurangkan Kesan Pergolakan Atmosfera Dalam Komunikasi Ruang Bebas Optik

ABSTRAK

Tesis ini membentangkan pendekatan baharu untuk teknik modulasi dalam ruang bebas komunikasi optik disebabkan oleh pergolakan atmosfera. Teknik modulasi baharu adalah berdasarkan pengubahsuaian konvensional modulasi intensiti untuk mengesan langsung hidup-padam memasukkan not (CIM/DD-OOK) yang mampu untuk mengoptimumkan kesan fasa peresap skrin, meningkatkan kuasa yang diterima dan meningkatkan tahap paras ambang isyarat. Pembatasan yang utama bagi CIM/DD-OOK ialah menderita dengan proses pengesanan ambang kerana berlakunya isyarat turun naik dan oleh kerana itu mengguna penyesuaian ambang untuk mendapatkan prestasi yang optimum yang mana memerlukan proses yang sangat kompleks. Menggunakan peresap boleh mengurangkan indeks sintilasi walau bagaimanapun ia boleh melemahkan kuasa isyarat. Pembangunan teknik modulasi baharu terdiri daripada tiga bahagian utama. Bahagian yang pertama adalah membangunkan analisis saluran atmosfera Gaussian bagi menentukan hala tuju kajian penyelidikan. Bahagian kedua ialah pembangunan terbitan matematik di mana untuk menganalisis secara teori teknik modulasi baharu dengan teknik modulasi konvensional. Analisis prestasi akan menyiasat kuasa isyarat, isyarat tahap ambang, isyarat kepada nisbah bising dan kadar ralat bit. Akhir sekali, bahagian ketiga adalah mengsimulasi teknik modulasi yang baharu dengan menggunakan perisian OptiSystem. Dengan ini boleh mengukur keupayaan DDM secara dekat hampir dalam keadaan FSO sebenar dan pada masa yang sama boleh mengesahkan dengan bahagian teori. Keputusannya menunjukkan bahawa untuk prestasi kuasa penerima pada hanya penerimaan BER 10^{-9} di bawah keadaan pergolakan yang kuat, teknik DDM dapat mengesan isyarat yang lemah sehingga - 18dBm. Sementara itu, bagi CIM/DD-OOK dengan dan tanpa peresap adalah pada - 14dBm dan 0dBm masing-masing dengan kuasa yang berbeza diterima kira-kira 4dBm dan 18dBm atau bersamaan 66 peratus dan 99 peratus peningkatan . Dalam menganalisis kadar bit , kadar data penilaian adalah dari 622Mbps sehingga 10Gbps. Analisa menunjukkan bahawa apabila sistem FSO beroperasi di bawah kesan pergolakan yang kuat dan jika kuasa menerima ditetapkan pada-10dBm, dengan jelas teknik DDM menunjukkan prestasi unggul jika dibandingkan dengan teknik modulasi OOK konvensional. Pada 2.5Gbps, magnitud BER untuk DDM teknik meningkat dengan 12 magnitud atau bersamaan peningkatan 100 peratus dan CIM/DD-OOK dengan peresap hanya 2 magnitud dimana memberikan peningkatan 33 peratus sahaja. Sementara itu, bagi keputusan analisis kuasa menerima DDM pada jarak 3km perambatan dengan mempertimbangkan 0dBm kuasa menghantar, panjang gelombang 1550nm dan kekuatan peresap l_c = 0.01, kuasa yang diterima adalah -4.59dBm dan dibandingkan dengan konvensional OOK yang menggunakan peresap hanya -7.6dB yang sama dengan 3dBm perbezaan atau kira-kira 100 peratus peningkatan. Dari segi prestasi BER, DDM boleh meluaskan penyebaran jarak dengan peningkatan kira-kira 42 peratus. Oleh itu perlaksanakan teknik modulasi DDM baharu adalah lebih baik daripada teknik modulasi keamatan konvensional untuk mengesan langsung hidup-padam memasukkan not (CIM/DD-OOK) bagi mengatasi degradasi isyarat pudar disebabkan keadaan pergolakan yang kuat.

Development of A New Dual Diffuser Modulation Technique To Alleviate Atmospheric Turbulence Effect In Free Space Optic Communication

ABSTRACT

This thesis presents new approach for modulation technique in free space optical communication due to atmospheric turbulence. The new modulation technique is based on the modification conventional intensity modulation for direct detection on off keying (CIM/DD-OOK) which capable to optimize the phase screens diffuser effect, enhance power received and improve threshold signal level. The main limitation of the CIM/ DD-OOK is suffering with the threshold detection for the occurrence of signal fluctuations and therefore the use of adaptive threshold for optimum performance of which requires a very complex process. The using of diffuser can reduced the scintillation index however it can attenuate the signal power. The development of new modulation technique consists of three major parts. The first part is developing the Gaussian atmospheric channel analysis to determine the direction of research study. The second part is the mathematical derivation development where to analyze theoretically the new modulation technique based on conventional modulation technique. The performance analysis will investigate the signal power, threshold signal level, signal to noise ratio and bit error rate. Lastly, the third part is simulating the new modulation technique by using the OptiSystem software. This can measured the capability of DDM in close in real FSO situation and at same time can validate with the theoretical part. The result shows that for the receiving power performance at acceptable BER 10^{-9} under strong turbulence condition, the DDM technique able to detect weak signal up to -18dBm. Meanwhile for CIM/DD-OOK with and without diffuser are at -14dBm and 0dBm respectively with different received power approximately 4dBm and 18dBm or equivalent to 66 percent and 99 percent improvement. In a bit rate analysis, the evaluation data rate from 622Mbps up to 10Gbps. Analysis shows that when the FSO system operate under strong turbulence effect and if the power receive is set fix at -10dBm, clearly the DDM technique shows the superior performance if compare to conventional OOK modulation technique. At 2.5Gbps, the magnitude of BER for DDM technique increase with 12 magnitudes or equivalent to 100 percent improvement and the CIM/DD-OOK with diffuser only 2 magnitudes which give the 33 percent improvement. Meanwhile for the analysis result of receiving power DDM at 3km distance propagation with consider 0dBm power transmit, wavelength 1550nm and diffuser strength at l_c = 0.01, the received power is -4.59dBm compare with conventional OOK that using diffuser only -7.6dBm which equal to 3dBm different or around 100 percent improvement. In term of BER performance, the DDM can further the distance propagation with approximately 42 percent improvement. Thus the new modulation DDM technique performs better than the conventional intensity modulation for direct detection on off keying (CIM/DD-OOK) to overcome the degradation of signal fading due to strong turbulence condition.

LIST OF ABBREVIATION

APD	Avalanche Photodiode
AWGN	Addictive White Gaussian Noise
BER	Bit Error Rate
CIM/DD-OOK	Conventional Intensity Modulation Direct Detection On Off Keying
CW	continuous wave laser
DDM	Dual Diffuser Modulation
DFB	Distributed-Feedback Lasers
FCC	Federal Communication Commission
FEC	Forward Error Control
FP	Fabry–Perot
FSO	Free Space Optic
FWHM	Full Width Half Maximum
Gbps	giga bit per second
LED	Light-Emitting Diodes
Mbps	mega bit per second
PCB+OOK	Partially Coherent Beam On Off Keying
PDF	Probability Density Function
SDH	Synchronous Digital Hierarchy
SNR	Signal to Noise Ratio
VCSEL	Vertical-cavity Surface-Emitting Laser

CHAPTER 1

INTRODUCTION

1.1 Background

The Free Space Optics (FSO) can be defined as an optical communication technology that uses light which usually uses a LASER source and propagate via free space to transmit data between two points (FSO, 2009). Alexander Graham Bell, who the first discovered it in the late nineteenth century with his experiment to convert voice sounds into telephone signals and transmitted them between receivers through free air space along a beam of light for a distance of some 600 feet (fSONA, 2009). In the year 1960's, the scientists have successfully developed Light Amplification by Stimulated Emission of Radiation (LASER) technology which after that is used in the optical communication (FSO, 2003 & Johnson, 2002). This technology has the same characteristic with the fiber optic communications but only distinguished interm of medium propagation. The data of optic fiber communication are transmitted by modulated laser light in cable, while FSO data are transmitted in a narrow beam through the atmosphere. Light travels through air faster than it does through glass, so it is fair to classify FSO as optical communications at the speed of light. The stability and quality of the link is highly dependent on atmospheric factors such as fog, haze, scintillation and heat. Maximum range of terrestrial links is limited (less than10 km). Nowadays, the FSO communication systems are increasingly being considered as an attractive option for the rapid provisioning of multi-gigabit per second links (Willebrand, 2002 & Nykolak, 2001 & Carbonneau, 1998).

Various applications can be applied in an FSO system today such as the last mile high bandwidth internet connectivity, the temporary high bandwidth data links, the mobile telephony backhaul (3G), satellite links as well as the various applications where the optical fibers cannot be used. There has been exponential growth in the use of FSO technology over the last few years, primarily for "last mile" applications, because FSO links provide the transmission capacity to overcome information bottlenecks (Dennis, 2002). This high data rate application can send voice, video conference and real-time image transmission, and also to achieve affordable communication for everyone, at any time and place (Hamed Al-Raweshidy, 2002). The communication capabilities allow not only human to human communication and contact, but also human to machine and machine to machine interactions. The communication will allow our visual, audio, and touch sense, to be contacted as a virtual 3-D presence (Govind, 2001).

1.2 Problem Statement and Motivation

The FSO communication is strongly influenced by the atmospheric channel effect which can cause the beam signal fading and wander. There are two main effects that can deterior the quality signal of FSO that are atmospheric attenuation and atmospheric turbulence as report in (D. Kedar, 2004 & X. Zhu, 2002& S. Karp, 1988& S. Bloom, 2003&D. Kedar, 2003). In the atmospheric attenuation will causes the signal scattering and absorption, need modification on an FSO system design to transmit higher power without exceeding the safety limits or has to reduce the propagation link (Isaac I, 2001& A. A. Farid 2007). Meanwhile for the atmospheric scintillation is caused by the atmospheric temperature inhomogeneity as presented in (Li, 2003&I. Kim, 1999). The scintillation effect will cause the signal fading due to constructive and

destructive interference of the optical beam traversing the atmosphere. Typical scintillation fade margins for short propagation link is around 2 to 5 dB which is less than the margins for atmospheric attenuation (I. I. Kim, 1997), making scintillation insignificant for short range FSO systems. Nevertheless if the range is exceeding more than 1 km the scintillation will impairs the FSO link availability and degrade the FSO performance significantly (X. Zhu, 2002& S. Bloom, 2003& I. Kim, 1999& S. Chan, 2006).

The OOK modulation technique is one simple modulation technique to be implemented and it has become the most popular for the commercially modulation technique available terrestrial FSO systems currently (H. Willebrand, 2002&X. Zhu, 2002& S. Bloom, 2003& J. T. Li, 2003). The major problem with OOK is suffering from the threshold signal level. The threshold level/point in the decision circuitry used to distinguish between bits zero and one is always fixed midway between the expected levels of data bits one and zero (I. B. Djordjevic, 2007). This will produce an optimum less error performance in non-fading channels. However when the presence of turbulence, the received signal level will fluctuate and at the same time the threshold detector has to track this fluctuation in order to determine the optimum decision point (H. Yamamoto & T. Ohtsuki, 2003). As a result this will need a great design challenge, as the channel noise and fading will have to be continually tracked for the OOK in FSO to perform optimally. If ignoring the signal fluctuation and just let the OOK FSO system operate with a fixed threshold level will cause the increment of detection error (E. J. Lee & V. W. S. Chan, 2004).

By using a phase screen diffuser which is mounted at the laser exit of transmitter, it can reduce the scintillation index and enhance the FSO performance. Nevertheless the use of the phase screen diffuser will attenuate the power transmit due to the expended of

beam divergence cause by the diffuser effect. Consequently more less power will be received at the receiver detector. The effect of diffuser also will become less effective when increase to strong turbulence. This condition will not give the advantage over FSO to improve the overall performance. Therefore the new DDM overcomes this limitation of CIM/DD-OOK where optimizes the diffuser effect, increases the power received and fix to zero threshold level signal to create robust modulation against atmospheric turbulence effect.

1.3 Research Objectives

The new DDM technique designed is because of the limitation CIM/DD-OOK in threshold detection process which cause the increasing of BER when experiencing scintillation effect. The use of diffuser can reduce the scintillation index but it limitation can weak the signal power. Therefore the DDM aim to improve threshold detection signal, enhance the signal power and increase the reduction of scintillation index. Therefore the main objectives of this research are stated below:

a) To develop a new modulation technique with optimize the diffuser effect, increase the power received and improve the threshold signal level
b) To develop a mathematical derivation for a new modulation technique
c) To analyze the theoretically and simulated performance of a new modulation technique

1.4 Scope of Work

Figure 1.1 shows the scope of research to develop the new modulation technique. This can be effectively guided the direction of research and can focus on the research contribution. Basically this research is under the terrestrial FSO and can divide into three main challenges that are effect of absorption and scattering (fog, aerosol, and smog), the effect of atmospheric turbulence and eye and skin safety. We focus on the atmospheric turbulence effects which focus on the scintillation effect that cause the FSO experiencing signal fading. In order to mitigate the scintillation effect five methods can be implemented. The first is adaptive optics where this approach does not require wavefront measurements which are difficult to obtain under strong scintillation conditions typical for many communication scenarios. It is based on the direct optimization of a performance quality metric such as the communication signal strength. The second is forward error control (FEC) which aims to manage the bound error variability within certain limits to improve the link reliability. The third is diversity technique which can be divided into two parts; a) spatial domain technique and b) temporal domain technique. The fourth method by using the modulation technique and lastly, employ the partially coherent beam (PCB) over the FSO system. A new modulation technique is based on the modulation technique with using partial coherent beam.

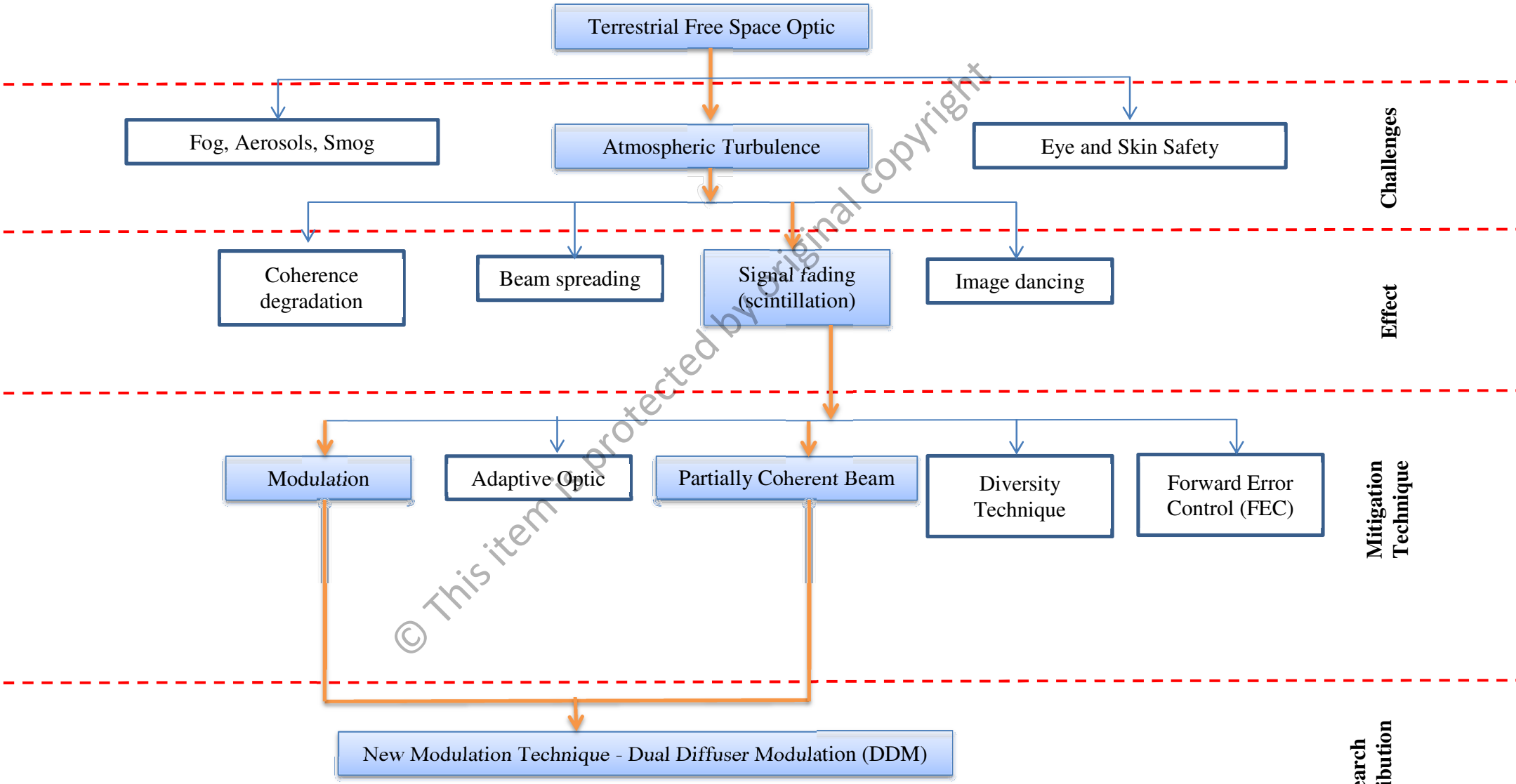

Figure 1.1: Scope of research

1.5 Thesis Organization

The remainder of this dissertation is organized as follows. Chapter 2 provides an overview of free space optic to concentrate the effect of atmospheric turbulence, atmospheric attenuation and eye and skin laser safety. This chapter is more focused on literature to mitigate the effecst of atmospheric turbulence. There are five mainly effects due to turbulence which will be discuss briefly that are coherence degradation, beam spreading, image dancing, and signal fading. Literature on FSO strengths and issues will be also reviewed in this chapter. Other than that the fundamental of modulation and partially coherent beam will be highlighted in the case study. Chapter 3 discusses the methodology to implement the research. In this chapter will discuss briefly on the research methodology, designing parameters analysis and simulation analysis. This chapter also discuss the noise consideration in research and fundamental on partial coherent beam (PCB) which relate to diffuser part.

Chapter 4 can be divided into two main parts. The first part discusses the development of new modulation technique which will briefly highlight the elements of light source, inverter, phase screen diffuser, photodetector and subtractor. The second part is devoted to a thorough investigation into the new dual diffuser modulation (DDM) technique. The performance of new modulation will analyze interm of signal power, threshold detection, signal to noise ratio (SNR) and bit error rate (BER). It will be compared with the conventional intensity for direct detection on-off keying (CIM/DD-OOK). The mathematical model for DDM also covered. The Chapter 5 is more focus on the performance of the DDM technique in the presence of turbulence and concentrate under strong turbulence effect. The mathematical model with presence of

turbulence will be included to analyze the new modulation technique. The simulation result is discussed also in this chapter to compare and validates the theoretical results. Finally, a review of all investigated systems in this dissertation is conducted and the results obtained for the new modulation technique are also summarized in the Chapter 6. In addition, the contribution of the research will be highlight as well and also the future work are discussed in this chapter.

CHAPTER 2

LITERATURE REVIEW

2.1 Introduction

This chapter delivers the review of contemporary research, theories and principles of FSO systems of study. It encircles the overview of terrestrial free space optical, the effect of atmospheric channel such as atmospheric attenuation, atmospheric turbulence and laser safety. In this chapter we also discuss in brief the mitigation methods to reduce turbulence induce fading effect. The overall of the background study can be described in Figure 2.1.

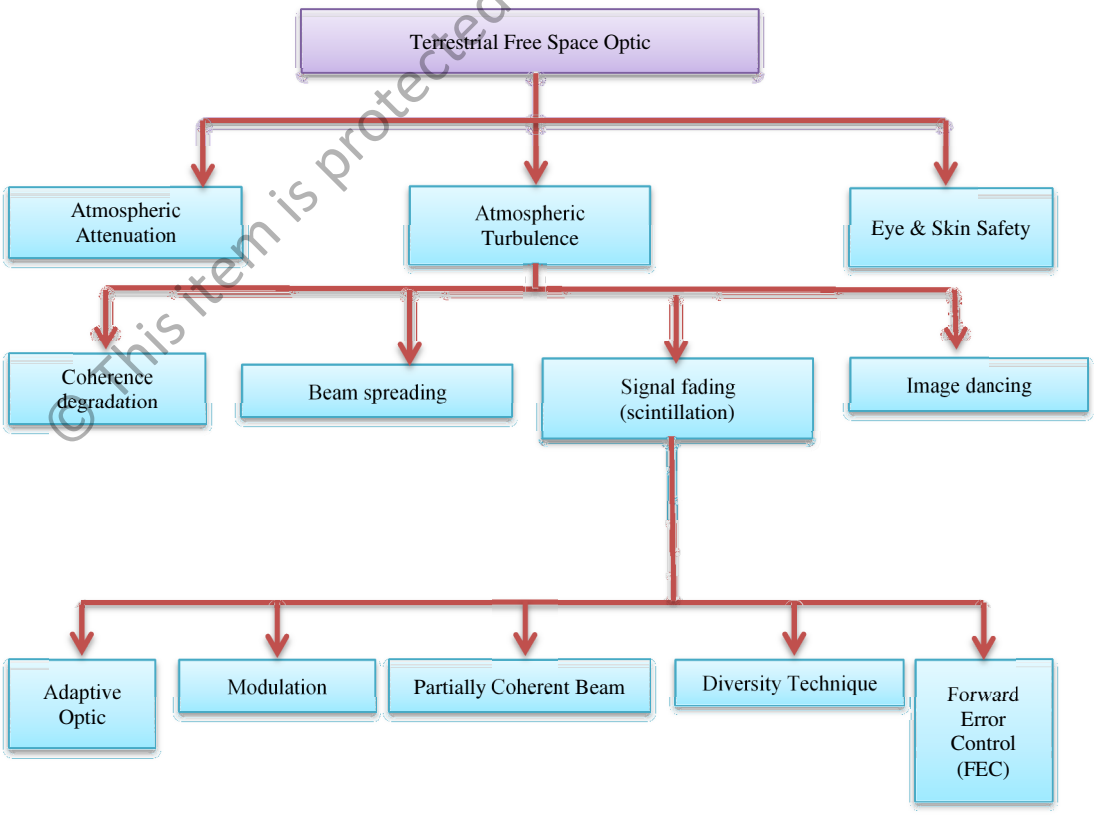

Figure 2.1: Literature background of study

2.2 Overview of Terrestrial Free Space Optic Communications (FSOC)

The terrestrial FSO communication is a line-of-sight (LOS) technology that transmits a modulated beam of visible or infrared light through the atmosphere for broadband communications. In a manners similar fiber optic communication, FSO uses Light Emitting Diode (LED) or laser (Light Amplification by Stimulated Emission of Radiation) point source of data communication. The basis of FSO communication is illustrated in block diagram Figure 2.2.

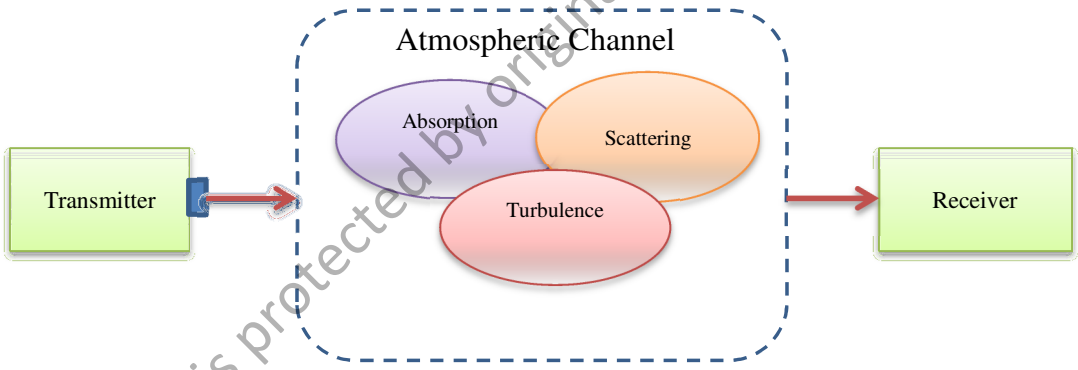

Figure 2.2: Basic FSO diagram (Weichel H., 1990)

Basically the FSO communication can be divided into three main parts which consist of a transmitter, atmospheric channel and a receiver (O. Bouchet, 2005). The transmitter part has the primary duty of modulating the source data onto the optical carrier, which then propagates through the atmosphere to the receiver. The most widely used modulation type is the intensity modulation (IM), in which the source data is modulated onto the intensity of the optical radiation. In the atmospheric channel part consists of three main effects. Firstly is absorption, which occurs primarily in response to water particles and also contribute by gases, but quite a small effect when compared with

water absorption (B. Bova & S. Rudnicki, 2001). This effect causes a decrease in the power density of the FSO beam and directly affects the availability of a system. However, the use of appropriate power, based on atmospheric conditions, and use of spatial diversity helps maintain the required level of network availability (Z. Kolka, 2007). Secondly is scattering which occur when the wavelength collides with the scattered. The scattering will not cause the loss of energy but only a directional redistribution of energy will may have significant reduction in beam intensity for longer distances (Earl J. McCartney, 1997; E.B. Zyambo, 2001). Lastly is a turbulence effect where occur when radiation strikes the Earth from the Sun. Some of the radiation is absorbed by the Earth's surface and yielding heating up the Earth surface air mass. This mass of warmer and lighter air will mix turbulently with the surrounding cooler air mass which causes the fluctuation over signal transmission (N. Araki & H. Yashima, 2005).

Interms of advantages of FSO technology communication over fiber communication, the FSO is not requiring the licensing from the Federal Communications Commission (FCC). Unlike the RF communication need the licensing for frequency allocation due to RF use the frequency that less than 300 GHz (Lumenlink, 2003). Apart from that the FSO can support the bandwidth up to 2.5Gbps if compare to RF limited to 622Mbps. The further study has successfully tested 160Gbps in laboratories and speed could potentially be able to reach Terabit range (Rockwell, 2001). The FSO also has an attractive alternative to the excessively high cost of digging the street to lay the fiber and requiring permission from authorities for installation. This technology transmission only needs a place on a roof or behind a window to set up a transceiver. The duration of installation can be made over within a few hours or one day (Sona, 2001).

Behind the advanced of this technology, the obvious limitation in FSO is vulnerable to weather condition. This led this technology not applicable for long distance in terrestrial FSO. This technology also needs a line of sight (LOS) transmission to operate. Any blocking over the laser light will cause the receiver not received the signal and drag to loss of communication data. For instance the flying bird across the laser beam propagation is most normal cases that block the laser light. Moreover, the building movement also can impair the link performance. This is because the arising of pointing error in FSO system (Arnon, 2003).

2.2.1 FSO Characteristics

There are several fundamental of FSO technology that are different with other wireless communication system.

a) **Narrow beam size -** The optical radiation is known for its extremely narrow beam, a typical laser beam has a diffraction limited divergence of between 0.01 – 0.1 mrad (Dennis Killinger, (2002). This implies that the transmitted power is only concentrated within a very narrow area, thus providing an FSO link with adequate spatial isolation from its potential interferers. The tight spatial confinement also allows for the laser beams to operate nearly independently, providing virtually unlimited degrees of frequency reuse in many environments and makes data interception by unintended users difficult. Conversely, the narrowness of the beam implies a tighter alignment requirement.

b) **Weather dependent** – The performance of terrestrial FSO is tied to the atmospheric conditions. Fog is among the biggest challengest wheather in FSO which produce the high attenuation.

c) **Unlicensed spectrum** – Due to the congestion of the RF spectrum, interference from adjacent carriers is a major problem facing wireless RF communication. To minimise this interference, regulatory authorities, such as the Federal Communication Commission (FCC) in US and Office of Communication (Ofcom) in the UK, put stringent regulations in place. To be allocated a slice of the RF spectrum therefore requires a huge fee and several months of bureaucracy. At present, the optical frequencies are free from all of this. The absence of a license fee and its bureaucratic time delay implies that the return on investments in FSO technology begins to trickle in far more quickly since the initial set-up cost is lower and the deployment time shorter.

d) **Large bandwidth capacity** – In any communication system, the amount of data transported is directly related to the bandwidth of the modulated carrier. The allowable data bandwidth can be up to 20 % of the carrier frequency. Using an optical carrier whose frequency ranges from 1012 – 1016 Hz could thus permit up to 2000 THz data bandwidth. Optical communication therefore guarantees an increased information capacity compared to radio frequency based communication systems. This is simply because on the electromagnetic spectrum, the optical carrier frequency, which includes infrared, visible and ultra violet frequencies, is far greater than the radio frequency. The usable frequency bandwidth in RF range is comparatively lower by a factor of 105.

e) **Fast installation** – The time it takes for an FSO link to become fully operational, starting from installation down to link alignment, could be as low as four hours. The key requirement is the establishment of an unimpeded line of sight between the transmitter and the receiver. It can also be taken down and redeployed to another location quite easily.

f) **Cost effectiveness** – The cost of deploying FSO is lower than that of an RF with a comparable data rate. FSO can deliver the same bandwidth as optical fibre but without the extra cost of right of way and trenching. Based on a recent findings by fSONA, an FSO company based in Canada, the cost per Mbps per month based on FSO is about half that of RF based systems (D. Rockwell, A,2009).

2.2.2 Basic Block Diagram FSO system

The block diagram of a typical terrestrial FSO link is shown in Figure. 2.2. As same other communication technology, an FSO system essentially consist three main parts: transmitter, channel and receiver. The channel part is explained detail begin Section 2.3.

2.2.2.1 Transmitter

The primary duty of this first part is modulating the source data onto the optical carrier, which is then propagated through the atmosphere to the receiver. The intensity modulation (IM) is the most widely used in FSO modulation where the source data is modulated onto the intesity of the optical radiation. In order to perform the modulation it can be executed by varying the driving current of the optical source directly in sympathy with the data to be transmitted or via an external modulator, such as the

symmetric Mach-Zehnder interferometer. The external modulator is one of the main part in the transmitter. It enables to produce the higher data rate if compare with direct modulation. However the weakness of external modulator has a nonlinear response. Other properties of the radiated optical field such as its phase, frequency and state of polarisation can also be modulated with data through the use of an external modulator. After via the modulator, the signal will move to transmitter telescope. This part is the end of transmitter part before the signal enter to transmission channel. It functions to collects, collimates and directs the optical radiation towards the receiver telescope at the other end of the channel.

The other important criteria in transmitter part is the selection light source of optical wavelength. Each of wavelength range has their different ability. The commercially available FSO systems operate roughly between 750 nm and 1600nm, with one or two systems being developed to operate at the wavelength of 10,000 nm. In these range wavelength experiencing different severe absorption. In the shorter wavelength, the absorption occurs primarily in response to water particles suah as moisture, which are an inherent part of the atmosphere even under clear weather conditions (S. Bloom, E. Korevaar, J. Schuster, & H. Willebrand (2003). The contribution of gas absorption to the overall absorption coefficient is not considered here because the gas-specific absorption coefficients are quite small when compared with water absorption. However, in the longer wavelength range above 2000 nm, gas absorption can dominate the absorption properties of the atmosphere. The brief of general optical wavelength in FSO are given below.

a) Wavelength range 780 to 850 nm

This wavelengths has been use widely in commercial FSO operation, and available in higher power laser sources that operate in this region. The wavelength for 780 nm is available with low cost laser but the average lifespan of these lasers can be an issue. Meanwhile for the laser wavelength at 850 nm, reliable, low cost, high-performance transmitter and detector components are readily available and commonly used in network and transmission equipment (S. Bloom, E. Korevaar, J. Schuster, & H. Willebrand (2003). Highly sensitive silicon (Si) avalanche photodiode (APD) detector technology and advanced vertical-cavity surface-emitting laser (VCSEL) technology can be used for operation in this wavelength.

b) Wavelength range 1520 nm to 1600 nm

This wavelengths are well suited for free space transmission but nowadays it also has been design for terrestrial FSO where the high quality transmitter and detector components is readily available as well in order to adapt this high performance wavelength. The combination of low attenuation and high component availability in this wavelength makes the development of wavelength-division multiplexing (WDM) FSO systems feasible. However, components are generally more expensive, and have a smaller receive surface area when compared with Si APD detectors that operate in the 850 nm wavelength. This wavelengths also become the optional of many companies to be used in long-haul fiber systems due to it high performance. In addition, this wavelengths are compatible with erbium-doped fiber amplifier (EDFA)

technology, which is important for high power more than 500 mW and high data rate can support more than 2.5 Gbps systems. Finally interm of eye safety, approximately 50 times as much power can be transmitted at 1520 nm –1600 nm than can be transmitted compared at 780–850 nm, owing to the low transmission of the human eye at this wavelengths (S. Bloom, E. Korevaar, J. Schuster, & H. Willebrand (2003).

c) Wavelength range 10,000 nm

This wavelength is new to the commercial FSO arena and is being developed due to better performance under the fog transmission. However there is some considerable debate regarding this characteristics which claim dependent upon fog type and duration. Generally, only few components available at 10 μm which is the reason it is not widely used in telecommunications equipment. At this wavelength it does not penetrate glass and making this component not suitable, to deploy behind the window. However, the poor glass penetration will cause not to be concentrated by optical aids and enables for high power operation in unrestricted environments (S. Bloom, E. Korevaar, J. Schuster, & H. Willebrand (2003).

2.2.2.2 Receiver

This part mainly function to helps recover the transmitted data from the incident optical field. Inside the receiver consist of several main parts to process the data. It begin with receiver telescope which function to collects and focuses the incoming optical radiation onto the photodetector. The large receiver telescope aperture is better

as it collects multiple uncorrelated radiations and focuses their average on the photodetector. This is referred to as aperture averaging but a wide aperture also means more background noise will arise. Then, follow up with optical bandpass filter which help to reduce the amount of background noise. After that the signal will go through to photodetector. Basically there are two type of photodetector, p-i-n diode (PIN) and avalanche photodiode (APD) which will act to converts the optical signal into an electrical signal. The post-detection processor or well known as decision circuit will process the output signal from photodetector. Under this process, it will involve the amplification, filtering and signal processing. As a result the high fidelity data recovery can be produced.

Generally the receiver detection process can be classified into two categories. The first is direct detection receiver which detects the instantaneous intensity or power of the optical radiation impinging on the photodetector. The output of the photodetector is proportional to the power of the incident field. Its implementation is very simple and most suitable for intensity modulated optical systems (W. K. Pratt. 1969). The second is coherent detection receiver. This tye of detection will involve the photo-mixing phenomenon. The incoming optical field is mixed with another locally generated optical field on the surface of the photodetector. The coherent receiver can be further divided into homodyne and heterodyne receivers. In homodyne receivers the frequency/wavelength of the local (optical) oscillator is exactly the same as that of the incoming radiation (W. K. Pratt., 1969), while in heterodyne detection the incoming radiation and the local oscillator frequencies are different (S. Betti, G. De marchis, & E. Iannone (1995).

2.2.3 FSO Applications

Among the areas of application of terrestrial FSO can be listed below:

a) **Last mile access** – FSO is used to bridge the bandwidth gap (last mile bottleneck) that exists between the end-users and the fibre optic backbone. Links ranging from 50 m up to a few km are readily available in the market with data rates covering 1 Mbps to 10 Gbps (I. Kim, 2009).

b) **Multi-campus communication network** – FSO has found applications in interconnecting campus networks and providing back-up links at Fast-Ethernet or Gigabit-Ethernet speeds (A. K. Majumdar & J. C. Ricklin, 2008).

c) **High definition television** – In view of the huge bandwidth requirement of high definition cameras and television signals, FSO is increasingly being used in the broadcast industry to transport live signals from high definition cameras in remote locations to a central office (I. Kim, 2009).

d) **Optical fibre back up link** – Used to provide back-up against loss of data or communication breakdown in the event of damage or unavailability of the main optical fibre link (H. Willebrand and B. S. Ghuman, 2002).

e) **Difficult terrains** – FSO is an attractive data bridge in such instances as across a river, a very busy street, rail tracks or where right of way is not available or too expensive to pursue.

f) **Cellular communication back-haul** – Can be used to back-haul traffic between base stations and switching centres in the 3rd and 4th generation (3G/4G) networks, as well as transporting IS-95 code division multiple access (CDMA) signals from macro and micro-cell sites to the base stations (H. Willebrand & B. S. Ghuman, 2002).

g) **Disaster recovery/Temporary links** – The technology finds application where a temporary link is needed, be it for a conference or ad-hoc connectivity in the event of a collapse of an existing communication network (A. K. Majumdar & J. C. Ricklin, 2008).

2.3 Atmospheric Attenuation

The atmospheric attenuation effect can be defined as a process in which the flux density of a parallel beam of energy decreases with increasing distance from the source as a result of absorption or scattering by the atmosphere (B. Flecker, 2006). It can be divided into two main categories that are attenuation by absorption and attenuation by scattering.

2.3.1 Absorption

Absorption occurs when suspended water molecules in the terrestrial atmosphere extinguish photons. It has resulted in the attenuation over signal during the propagation transmission. As the increase of the humidity in the environment, the absorption will increase and causes the attenuation to rise high (M. Naboulsi, 2004).

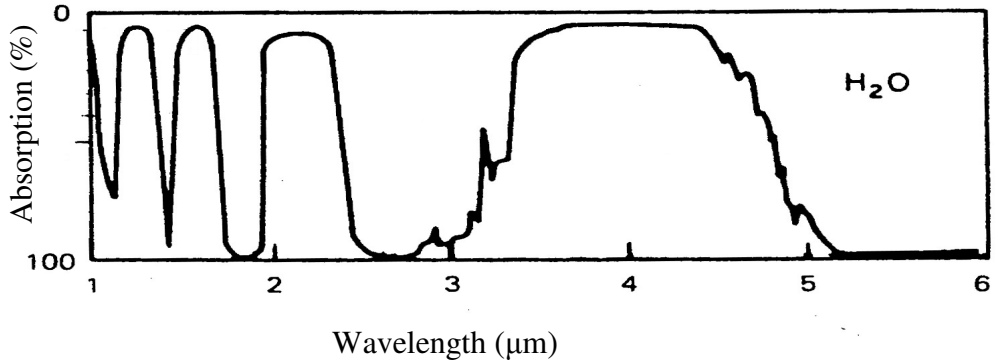

Figure 2.3: Absorption curve for water vapor (H_2O) (Schlessinger, 1994)

The water vapor (H_20) and carbon dioxide (CO_2) are responsible for most of the absorption of radiant energy by earth's atmosphere as shows in Figure 2.3 and Figure 2.4. These gases have absorption bands in the infrared spectrum (Willebrand, 2002). From Figure 2.3 shows that the strong absorption of H_2O occurs near the region of 2.7 μm and 4.3 μm. Meanwhile the Figure 2.4 shows the absorption of CO_2 occur in the wavelength region 1.4, 1.9, 2.7 and 6.3μm (Schlessinger, 1994).

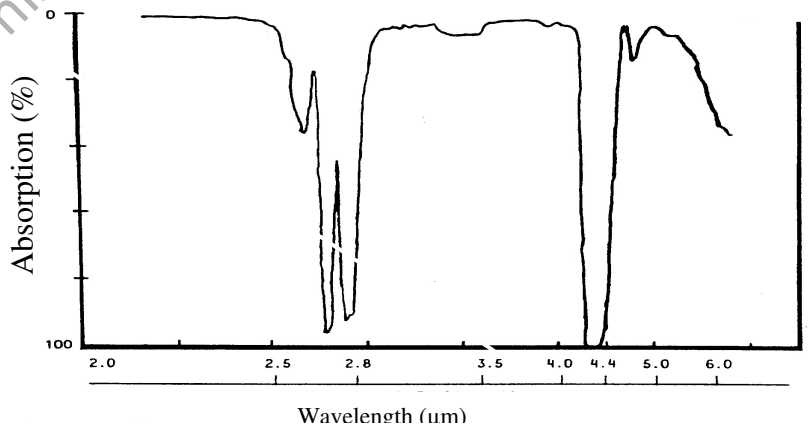

Figure 2.4: Absorption curve for CO_2 (Schlessinger, 1994)

2.3.2 Scattering

The scattering affected over in FSO is with taken the energy from beam when the beam encounters particles or molecules of different sizes and shapes. This process will weaken the signal in the transmission process. This leads to the attenuation of laser power in the atmosphere. The scattering is produced by particles in the atmosphere such as dust or liquid particles of air. If there any irregularities in the entering surface, this also can produce the scattering. The scattering also has a greater effect than absorption.

The Figure 2.5 described the general behavior of Rayleigh, Mie and Non-Selective scattering in the atmosphere.

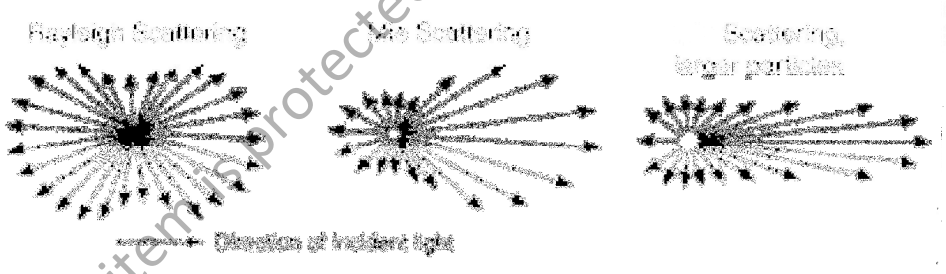

Figure 2.5: General behavior of Rayleigh, Mie and Non-selective scattering

Generally the scattering can be divided into three types. The first is Rayleigh scattering. It occurs when the particles are small compared to the incident wavelength. Similar to absorption, this light scattering is strongly wavelength dependent. Particles that are small in comparison with the wavelength scuh as air molecules and haze will produce Rayleigh scattering, which has a symmetrical angular distribution. At ultraviolet and visible wavelengths Rayleigh scattering is quite pronounced, while scattering for wavelengths greater than 3 μm is basically nonexistent.

The second type scattering is Mie scattering which occurs when the small particles or molecules are similar or greater than the incident wavelength. Fog and aerosol particles are the major contributors to the Mie scattering process. Meanwhile, the third is non-selective scattering which occurs when the particles are much larger than the incident wavelength. Water droplets such as like rain is among this region scattering. This type scattering also can be describe using geometrical optics. Unlike Rayleigh scattering, this type of scattering is more concentrated in the forward direction.

Molecular absorption and scattering effects are often combined and can be described by a single attenuation coefficient α which can be written as

$$\alpha(\lambda) = \alpha_A(\lambda) + \alpha_S(\lambda) \tag{2.1}$$

where α_A and α_S are the coefficient parameters describing molecular absorption and scattering processes, respectively. The transmittance of laser radiation that has propagated a distance L is related to the attenuation coefficient α as described by

$$\tau = exp[-\alpha(\lambda)L] \tag{2.2}$$

where the product αL is called the optical depth. Both absorption and scattering are deterministic effects that are quite well known and can be predicted based on a variety of conditions.

2.4 Eye and Skin Safety

The optical beams can cause injury to both the skin and eye, but the damage to the eye is far more significant because of the eye's ability to focus and concentrate optical energy. The laser communications systems can be designed to be eye safe which means there is no danger over people who might happen to encounter the communications beam. Lasers of higher power can be used more safely with 1550nm system compared to 850nm and 780nm. This is because wavelengths less than 1400nm allow the light to go through the cornea and lens, and focus on the retina, which can cause eye damage. The Figure 2.6 shows the absorption of the human eye at different wavelengths.

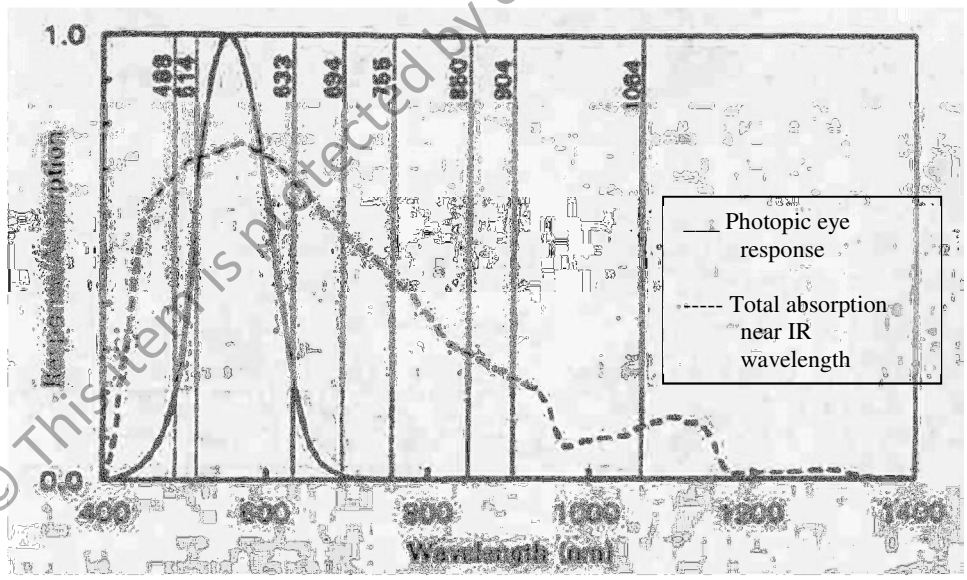

Figure 2.6: Human eye absorption at various wavelengths (S. Bloom, E. Korevaar, J. Schuster, & H. Willebrand, 2003)

The International Electrotechnical Commission (IEC) who is one of the international standard bodies which provide guidelines on safety of optical beams. They have been publishing some of international standards which related to all electrical equipment, including lasers and laser equipment (IEC60825-1). Figure 2.5 shows the classifications for laser standard provide by IEC.

Table 2.1: Comparison Maximum Permissible Exposure (MPE) limit for 850nm and 1550nm

Wavelength	**850nm**	**1550nm**
Maximum Permissible Exposure (MPE)	2.0 mW/ cm^2	100 mW/ cm^2

Table 2.1 shows the MPE for wavelength 850nm and 1550nm respectively. As we can see the shorter wavelength (850nm) only permissible 2 mW/cm^2 but the longer wavelength (1550) nm can support up to $100mW/cm^2$. In practical terms, the allowable safe laser power is about 50 times higher at 1550nm compared to 850nm. The factor of 50 is able to provide up to 17dB additional margin to propagate over longer distances, through heavier attenuation, and to support higher data rates. The higher data rate available with commercial 850nm is 622Mbps and 2.5Gbps for 1550nm systems.

In order to provide a better protection to the eye or skin of anybody that might come in contact with the radiation of laser equipment, the MPE limits have been stipulated by standard organizations. It is the highest radiation power or energy, measured in W/cm2 or J/cm2 that is considered safe with a negligible probability of causing damage. The MPE is measured at the cornea of the human eye or at the skin, for a given wavelength and exposure time. It is usually about 10 % of the dose that has a 50 % chance of creating damage under worst-case conditions (K. Schroder, 2000).

Lasers classified as Class 1 is most desirable for optical wireless communication systems since their radiation are safe under all conditions and circumstances. Class 1 lasers require no warning labels and can be used without any special safety precautions. This explained detail in Table 2.2.

Table 2.2: IEC 60825-1 standard for classification of lasers categories

Category	Description
Class 1	Low power device emitting radiation at a wavelength in the band 302.5–4000 nm. Device intrinsically without danger from its technical design under all reasonably foreseeable usage conditions, including vision using optical instruments (binoculars, microscope, monocular)
Class 1M	Same as Class 1 but there is possibility of danger when viewed with optical instruments such as binoculars, telescope, etc. Class 1M lasers produce large-diameter beams, or beams that are divergent.
Class 2	Low power device emitting visible radiation (in the band 400–700 nm). Eye protection is normally ensured by the defence reflexes including the palpebral reflex (closing of the eyelid). The palpebral reflex provides effective protection under all reasonably foreseeable usage conditions, including vision using optical instruments (binoculars, microscope, monocular).
Class 2M	Low power device emitting visible radiation (in the band 400–700 nm). Eye protection is normally ensured by the defence reflexes including the palpebral reflex (closing of the eyelid). The palpebral reflex provides an effective protection under all reasonably foreseeable usage conditions, with the exception of vision using optical instruments (binoculars, microscope, monocular).
Class 3R	Average power device emitting a radiation in the band 302.5–4000 nm. Direct vision is potentially dangerous
Class 3B	Average power device emitting a radiation in the band 302.5–4000 nm. Direct vision of the beam is always dangerous. Medical checks and specific training required before installation or maintenance is carried out.
Class 4	High power device There is always danger to the eye and for the skin, fire risk exists. Must be equipped with a key switch and a safety interlock. Medical checks and specific training required before installation or maintenance is carried out.

2.5 Atmospheric Turbulence

One of the major challenges of FSO is the presence of atmospheric turbulence. Atmospheric turbulence affects the propagation of a beam of light within the channel in three ways. Firstly, the wavefront is distorted by the variation due to scintillation index, thus creating the fluctuations in the intensity of the optical signal. Secondly, the beam wandering takes place due to the diffraction of the laser beam, when the diameter of the beam is smaller/equal to the size of the eddies. Thirdly, the atmospheric turbulence makes the laser beam to spread beyond the diffraction limit. Scintillation is a severe problem and can result in a significant deterioration of the link BER performance.

Atmospheric turbulence produces temporary pockets of air with slightly different indices of refraction. If the size of the turbulence cells is larger than the beam diameter, the whole laser beam bends. This effect is illustrated in Figure 2.7. The turbulence in the atmosphere causes variation in the spatial intensity distribution of the laser beam which causes the laser wander and laser beam spreading (H. Manor, 2003). The turbulence effect on the laser beam occurs because of small-scale dynamic changes in the index of refraction of the atmosphere.

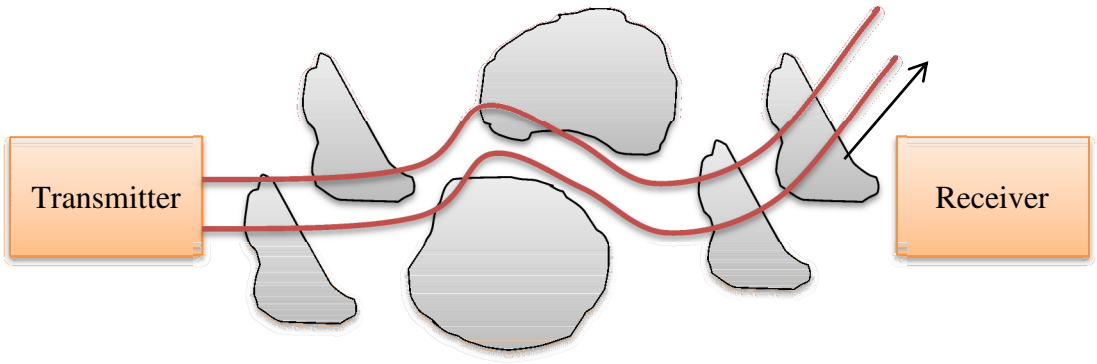

Figure 2.7: Laser beam wanders due to turbulence cells that are larger than the beam diameter

It is common that the sizes of the turbulence cells are smaller than the beam diameter and so the laser beam bends and become distorted. Small variations in the arrival time of various components of the beam wave front produce constructive and destructive interference and result in temporal fluctuations in the laser beam intensity at the receiver. Figure 2.8 graphically examines what happens in this occurrence.

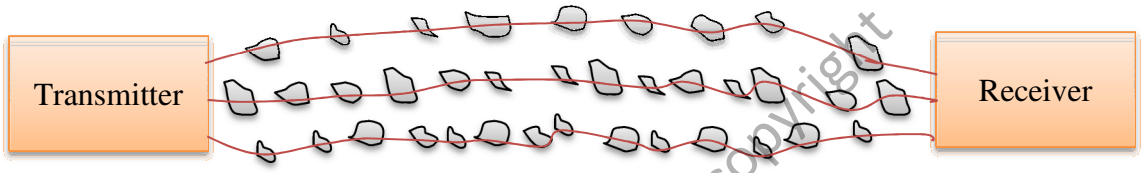

Figure 2.8: Scintillation or fluctuations in beam intensity at the receiver due to turbulence cells that are smaller than the beam diameter

The atmospheric turbulence can be alleviated by using several techniques such as:-

1) Adaptive Optics
2) Forward Error Correction (FEC)
3) Diversity Technique
4) Modulation Technique
5) Partially Coherent Beam (PCB)

2.5.1 Adaptive Optics

The wavefront distortions induced by the atmospheric turbulence can severely impact the performance of free space optical communication causing signal fading on a millisecond time scale. The bit error rate (BER) is the major communication performance is depends on both short-term errors resulting from electronic-circuit

related noise and the turbulence induced long-term random breaks in communication data traffic known as atmospheric signal fading. This can be mitigating using the adaptive optics (AO) (D. L. Fried, 1998).

The main advantage using AO is the active prevention of long-term data loss rather than data recovery. This could be accomplished by mitigating the atmospheric turbulence induced wave front distortions (Tyson, 2005). However the challenge is the real-time control of the active/adaptive optical elements incorporated in the receiver or transmitter optics in order to make the communication signal fading less likely.

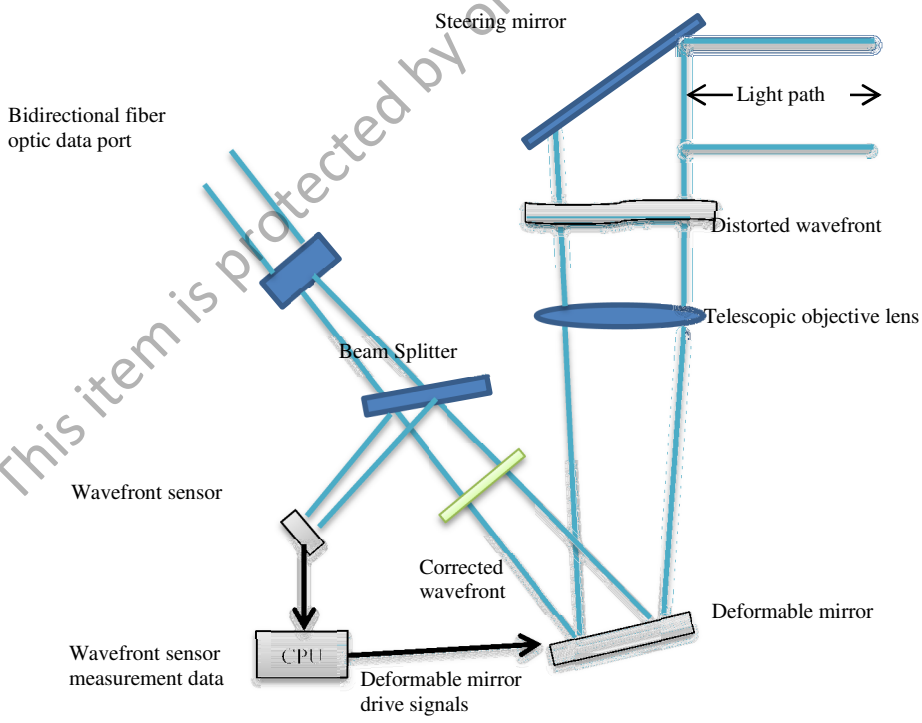

Figure 2.9: Adaptive optics systems unite several technologies to remove noise from optical signals-precision optics, wavefront sensors, deformable mirrors, and lasers-tied together with high-speed control systems (J. Elon Grave & S. Drenker, 2002)

There are two general approaches for AO technique:

a) Conventional adaptive approach- based on wavefront sensing and reconstruction (J.W. Hardy, 1998; F. Roddier, 1999). The part of the received beam has to be directed to a wave front sensor

b) Blind optimization approach- used the received signal which determined from the communication signal after low-pass filtering for feedback

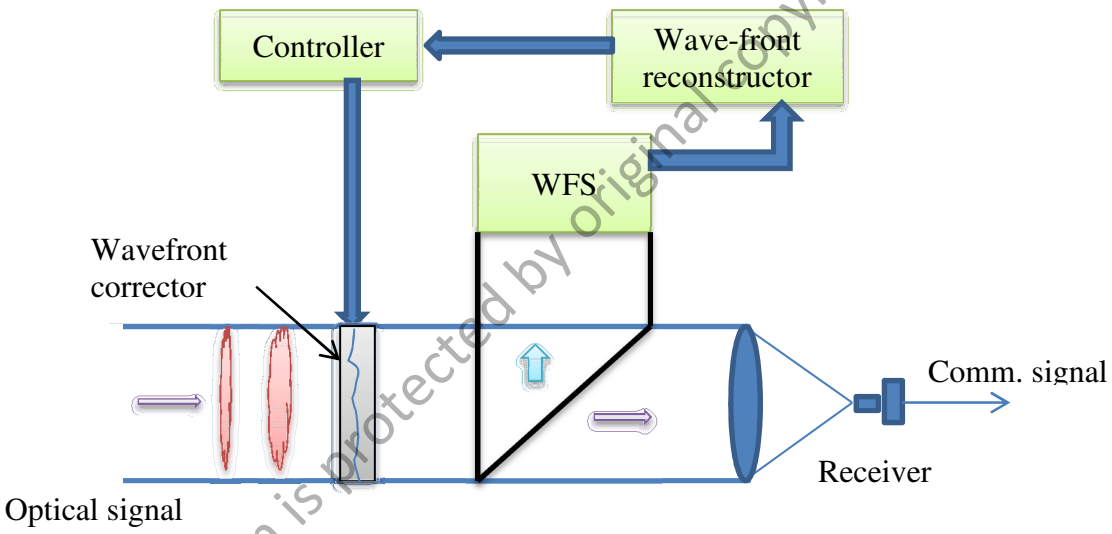

Figure 2.10: Conventional adaptive optics approach uses a wavefront sensor (WFS) and wave front reconstruction (Arun K. Majumdar & Jennifer C. Ricklin, 2007)

Nevertheless the several novel technologies of AO have emerged and one of them is stochastic parallel gradient descent (SPGD) (J. C. Spall, 2003& M. A. Vorontsov & V. P. Sivokon, 1998& M. A. Vorontsov; G.W. Carhart & J. C. Ricklin, 1997). This AO technique using parallel processing hardware based on VLSI micro-electronics and the emergence of high-bandwidth wave front phase controllers (R. T. Edward, M. Cohen & G. Cauwenberghs, 1999).

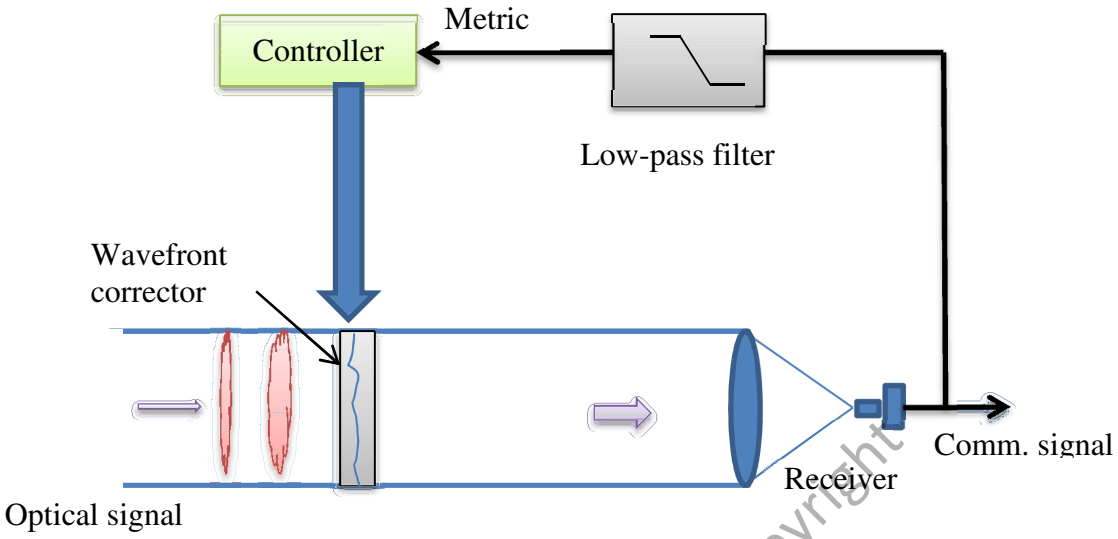

Figure 2.11: Wavefront distortion compensation based on blind optimization of a system performance metric (Arun K. Majumdar & Jennifer C.Ricklin, 2007)

The SPGD can be divided into four techniques.

1) Using the signal strength (J) as a feedback signal
2) An adaptive transmitter reduces the turbulence-induce beam spreading originating from the transmitter (TX). It uses the signal strength remote by the receiver (R_{x2}) as a feedback signal (J_2).
3) Received and transmitted optical signals share the same adaptive optical elements in an adaptive transceiver.
4) Use the fiber optics components reduces the complexity of FSO setup in an adaptive transceiver.

2.5.2 Forward Error Correction (FEC)

The forward error correction technique used for controlling errors in data transmission over unreliable or noisy communication channels (Charles Wang, Dean Sklar & Diana Johnson, 2002). This can be implemented by applying the sufficient

redundancy to the information bits and at the receiver by using these redundancies the bits in error are detected and corrected by using an error-correcting code (ECC). The redundancy allows the receiver to detect a limited number of errors that may occur anywhere in the message, and often to correct these errors without retransmission. FEC gives the receiver the ability to correct errors without needing a reverse channel to request retransmission of data, but at the cost of a fixed, higher forward channel bandwidth. FEC is therefore applied in situations where retransmissions are costly or impossible, such as one-way communication links and when transmitting to multiple receivers in the multicast. FEC information is usually added to mass storage devices to enable recovery of corrupted data, and is widely used in modems.

The theoretical error performance of coded systems over time varying channel has been under research for many years which reported in (Gideon Kaplan & Shlomo Shamai, 1994; Tolga M.Duman & Masaoud Salehi, 1999). Reported in (J. L. Pamart, E. LeFranc, 1994& S. Yamamoto, H. Takahira & M. Tanaka, 1994), the FEC provides an improved margin against noise and pulse distortion in long-haul optically amplified transmission systems. There are several forward error correction (FEC) schemes have been proposed:

a) Reed-Solomon (RS) codes (Y. T. Koh & F. M. Davidson, 1989)

b) Convolutional codes (F. M. Davidson & Y. T. Koh, 1988)

c) Turbo codes (J. Li & M. Uysal, 2003)

d) Trellis-coded modulation (H. Park & J. R Barry, 2004)

2.5.3 Diversity Technique

These techniques are applicable in the regime in which the receiver aperture is smaller than the correlation length of the fading and the observation interval is shorter than the correlation time of fading. The receiver is assumed has no knowledge of the instantaneous fading state. This technique also is based on the statistical properties of fading as a function of both temporal and spatial coordinates.

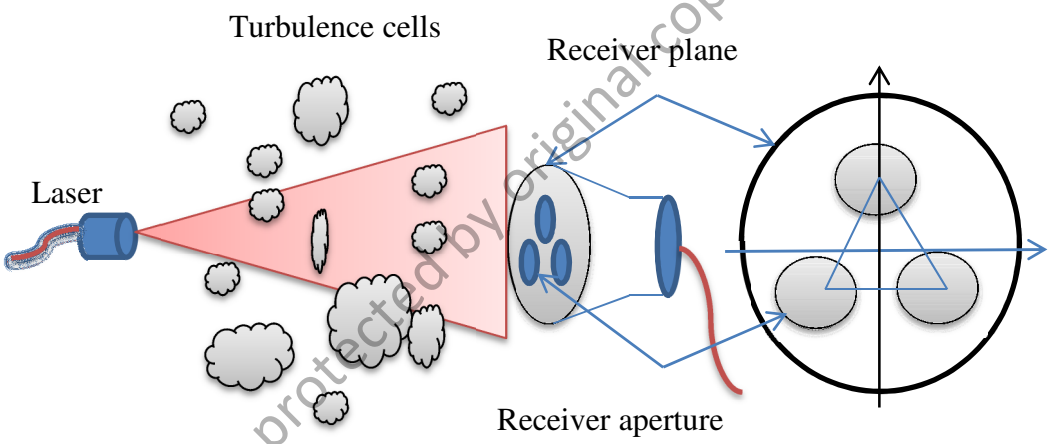

Figure 2.12: Schematic of an FSO link with a triple-aperture receiver. The receiver geometry is depicted on the right (G. Yang, M. Khalighi, Z. Ghassemlooy, & S. Bourennane, 2013)

The study of diversity technique has been many investigate by the researchers reported in (S. M. Haas, J. H. Shapiro, & V. Tarokh, 2002; E. Lee & V. W. Chan, 2004& S. G. Wilson, M. Brandt-Pearce, Q. Cao, & J. H. Leveque, 2005). Among diversity technique, the spatial diversity is particularly attractive with its lower complexity (S. Trisno, 2005). Spatial diversity can be easily implemented in FSO systems since the optical wave front coherence length in the atmosphere is of the order of centimeters. Therefore, multiple transmitters only needs to be placed centimeters apart to experience independent fading channels (S. M. Navidpour, M. Uysal, & M.

Kavehrad, 2007). Besides its role as a fading-mitigation tool, multiple-aperture structure reduces the potential for temporary blockage of the laser beam by obstructions (E. Lee & V. W. Chan, 2007; E. Lee & V. w. Chan, 2009).

Generally, this technique can be divided into two categories:

a) Temporal diversity technique - one must employ a single receiver. When the receiver knows only the marginal statistic of the fading, a symbol-by-symbol ML detector can be used to optimize performance. When the receiver also knows the temporal correlation of the fading, maximum-likelihood sequence detection (MLSD) can be employed, yielding a further performance improvement, but the cost of very high complexity.

b) Spatial diversity technique – one must employ at least two receivers to collect the signal light at different positions or from different spatial angles. Spatial diversity reception with multiple receivers can be used to overcome turbulence-induced fading. When it is not possible the receiver sufficiently far apart, the fading at different receivers is correlated, reducing the diversity gain. The maximum-likelihood (ML) detection can be used to reduce the diversity gain penalty caused such fading correlation.

2.5.4 Modulation

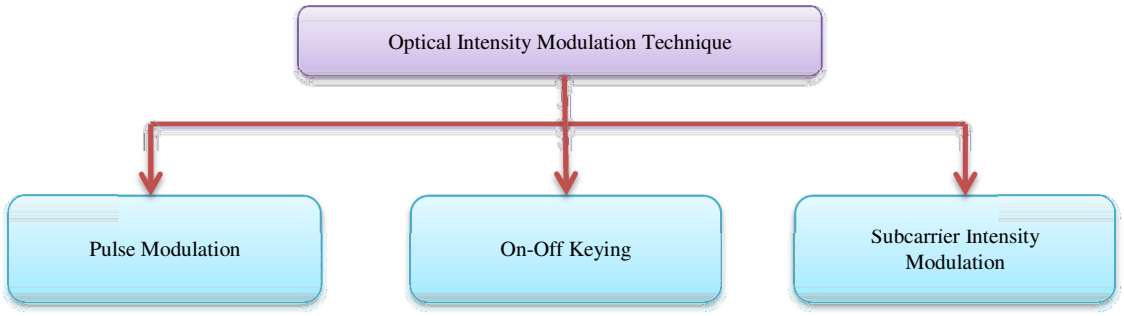

Figure 2.13: Digital modulation technique in FSO communication

The performance of the FSO link due to the turbulence effect can also be improved by employing an appropriate modulation scheme that makes a good compromise between complexity and performance. The modulation tree can be viewed in Figure 2.13 which shows the category of digital modulation. Generally, digital modulation can be divided into three main techniques:

(a) Pulse Modulation

(b) Subcarrier Intensity Modulation (SIM)

(c) On-Off Keying (OOK)

2.5.4.1 Pulse Modulation

The pulse modulation can be defined as the process of transmitting signals in the form of pulses by using special techniques. Among the technique in pulse modulation are:-

(a) Pulse amplitude modulation (PAM)

(b) Pulse width modulation (PWM)

(c) Pulse position modulation (PPM)

(d) Pulse code modulation (PCM)

The pulse position modulation (PPM) is one of the famous pulse modulation techniques which have the interesting advantage of being average energy efficient (F. Xu, M.A. Khalighi & S. Bourennane, 2009). The PPM modulation technique improves on the power efficiency of OOK but at the expense of an increased bandwidth requirement and greater complexity. The previous research in Q-ary PPM proposed a simple soft-remapping method of low complexity. The receiver complexity is one major problem in view of the implementation of a terrestrial FSO system. In the PPM receiver it requires both slot and symbol synchronization in order to demodulate the information encoded on the pulse position. Nevertheless, because of its superior power efficiency, PPM is an attractive modulation technique for optical wireless communication systems, particularly in deep space laser communication applications (H. Hemmati, 2007).

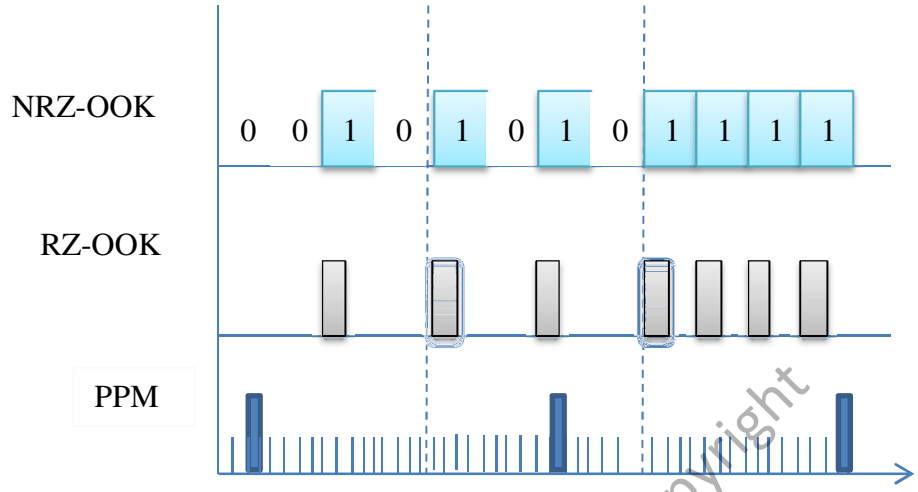

Figure 2.14: Example time waveforms for 16-PPM and 4-bit OOK (W. O. Popoola & Z. Ghassemlooy, 2009)

2.5.4.2 Subcarrier Intensity Modulation (SIM)

Subcarrier intensity modulation is a technique borrowed from the very successful multiple carrier radio frequency (RF) communications. Various applications have been used such as (I. B. Djordjevic & B. Vasic, 2006& T. Ohtsuki, 2003);

a) Digital television

b) Local area networks (LANs)

c) Asymmetric digital subscriber line (ADSL)

d) 4G communication systems

e) Optical fiber communications

In optical fiber communication networks for example, the subcarrier modulation techniques have been commercially adopted in transmitting cable television signals and have also been used in conjunction with wavelength division multiplexing (G. P. Agrawal, 2002). There are however some challenges in the implementation of SIM, these are:

a) Relatively high average transmitted power due to:

I. The optical source being ON during the transmission of both binary digits "1" and "0", unlike in OOK where the source is ON during the transmission of bit "1" only.

II. The multiple subcarrier composite electrical signals being the sum of the modulated sinusoids requires a DC bias. This is to ensure that this composite electrical signal, that will eventually modulate the laser intensity, is never negative. Increasing the number of subcarriers leads to increased average transmitted power, because the minimum value of the composite electrical signal decreases (becomes more negative) and the required DC bias therefore increases (R. You & J. M. Kahn, 2001). This factor results in poor power efficiency and places a bound on the number of subcarriers that can be accommodated when using multiple SIM.

b) The possibility of signal distortions due to: inherent laser non-linearity and signal clipping due to over-modulation.

c) Stringent synchronization requirements at the receiver side.

Reported in (X. Song & J. Cheng, 2013) the SIM performance over atmospheric turbulence interm of BER and SER can be increase using the moment generating function (MGF) approach. It applied the non-coherent and differently coherent subcarrier modulation to produce the high accurate series of BER and SER solution which particularly for large SNR analysis. The spectral efficiency in SIM has been investigated in with using technique

adaptive subcarrier PSK intensity (N. D. Chatzidiamantis, A. S. Lioumpas, G.K. Karagiannidis & S.Arnon, 2011).

2.5.4.3 On-Off Keying (OOK)

The OOK signaling is the dominant modulation scheme employed in commercial terrestrial wireless optical communications systems. This is primarily due to its simplicity and resilience to the innate nonlinearities of the laser and the external modulator (H. Willebrand & B. S. Ghuman, 2002; S. Bloom, E. Korevaar, J. Schuster, & H. Willebrand, 2003). Nevertheless, in the atmospheric turbulence channels, the OOK scheme requires adaptive threshold to perform optimally (J W. Huang, J. Takayanagi, T. Sakanaka, & M. Nakagawa, 1993& T. Ohtsuki, 2002).

The performance of FSO systems on turbulence atmospheric channels can be evaluated using the bit error probabilities which is based on on-off keying (OOK) modulated FSO systems for all turbulence regimes. The typical scintillation fades last between 1 μs and 100 μs, and when the link is operated at multi-gigabits per second data rate, the loss of potentially up to 10^9 consecutive bits may occur, thus causing a devastating effect on the throughput of the network due to interactions with the upper layer protocols (Chan, 2006). Therefore, the turbulence induced fading duration and strength has to be mitigated. The forward error controls (FEC) mechanisms have been suggested in order to reduce the signal fading (X. Zhu, 2003& A. Garcia 2007& M. Uysal, 2004). However report in (M. Razavi, 2005& X. Zhu, 2001) shows that implementation error control coding causes the huge processing delays and drop the efficiency in view of the number of redundant bits that will be required. Some of the researcher also suggests using an array receiver analyzed in

(Q. Cao, 2006& S. M. Navidpour, 2007& I. I. Kim, 1997) to lessen the atmospheric turbulence induced channel fading. Semiconductor amplifiers operated in saturation mode also have been proposed in to mitigate the turbulence effect (M. Abtahi, 2006). The investigation study of adaptive optics to correct the wavefront deformation caused by atmospheric turbulence has been carried out but this technique is very expensive and complex to be implemented on terrestrial FSO systems (J. Elon Grave, 2002).

Generally there are two type of photodetection in OOK modulation technique that are direct detection and coherent detection.. The photodetection can be defined as a process to convert the optical signal into electrical signal with the aim of recovering the transmitted information. Begin from the transmitter the information is encoded either in the frequency, phase or the intensity of the radiation from an optical source whether LED or laser. Then, this encoded radiation is transmitted to the receiver through the free-space channel. At the receiver, the front-end devices focus the filtered radiation onto the photo detecting surface in the focal plane.

The basic feature of OOK modulation can be described as

a) Simple to implement and easy detection
b) The common technique for intensity modulation/direct detection
c) Require threshold to make an optimal decision due to the problem time-varying fading
d) Return –to-Zero (RZ) pulse, only the partial duration bit will used
e) Non-return-to-zero (NRZ) pulse, equal to 1 bit duration transmitted

2.5.4.3.1 Direct Detection

This detection technique is the simplest type of optical receiver in detecting the signal power due to only respond the instantaneous power of the collected field. In the direct detection technique, the local oscillator does not require recovering the encoded information, but only associated with the intensity variation of the transmitted field (R. M. Gagliardi & S. Karp, 1995). Hence this type of detection is also called envelope detection. The basis of direct detection technique is illustrated in Figure 2.15.

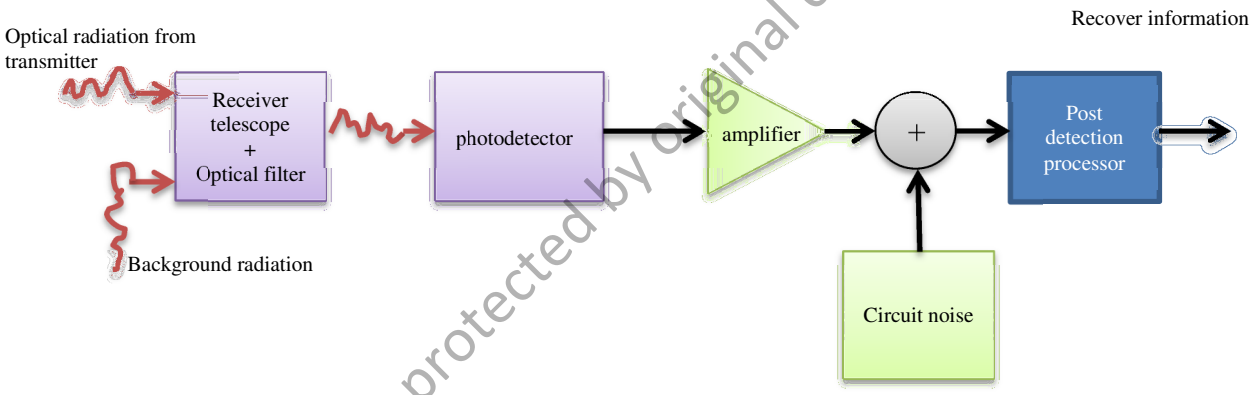

Figure 2.15: Typical FSO block diagram for direct detection technique (W. O. Popoola, Z. Ghassemlooy, & E. Leitgeb, 2007)

Unfortunately, the optical field always detects the presence of an additional sources and noises at the receiver (N. Perlot, 2007). The noises the occur during the detecting process such as shot noise, dark current noise, background noise and thermal noise which generate from circuit system itself. All of this can contribute to corrupt the receiving signal. This will become worse when the presence of turbulence especially when associate with the threshold signal level.

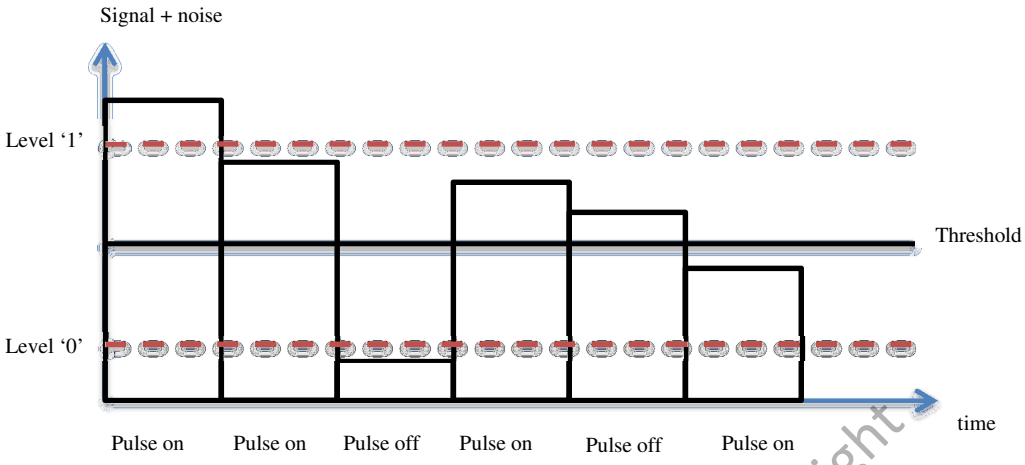

Figure 2.16: OOK threshold level behavior (Arun K. Majumdar & Jennifer C.Ricklin, 2007)

The Figure 2.16 shows the behavior of OOK level for digital signal. The level '1' is indicating the pulse on condition whereas the level '0' is indicates pulse off condition. It can be summarized as shows in Table 2.3.

Table 2.3: OOK threshold behavior for digital signal

Pulse condition	Threshold	Description
Pulse On	Above	Signal presence
	Below	Miss detection
Pulse Off	Above	False alarm
	Below	No signal

The miss detection condition is occurring when the signal being send but not beyond the threshold level. Meanwhile the false alarms arise when the noise alone exceeds the threshold level and as a result interpreted as a signal (L. C. Andrews, R. L. Phillip, 2005). This condition can be described in Figure 2.17.

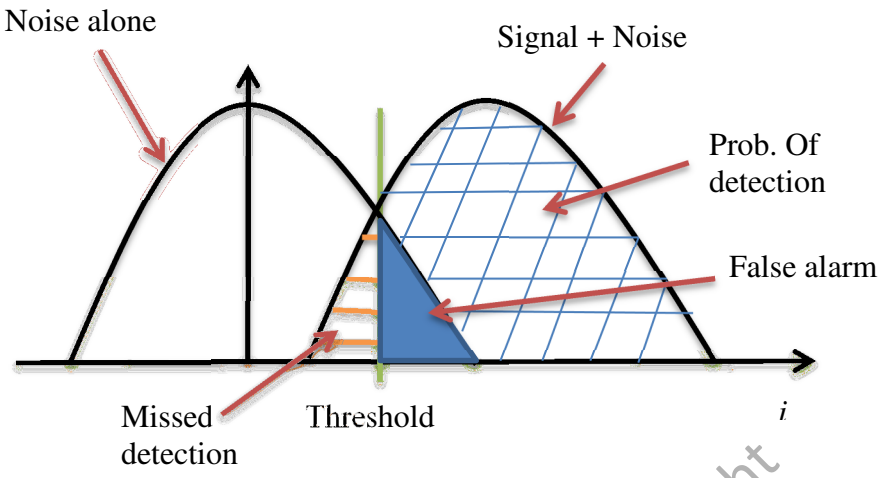

Figure 2.17: Signal condition to represent the region of miss detection and false alarm (L. C. Andrews, R. L. Phillip, 2005)

As reported in (X. Zhu & 1. M. Kahn, 2002), stated that the major challenge OOK is requires adaptive threshold to perform optimally in atmospheric turbulence condition. This fact among others has led to the increased interest in the study of SIM in FSO systems (W. O. Popoola, Z. Ghassemlooy, & E. Leitgeb, 2007&M. Uysal, L. Jing, & Y. Meng, 2006). Therefore it is unsurprising that the majority of the work reported in literature (S. M. Navidpour, M. Uysal, & M. Kavehrad, 2007) is based on this signaling technique.

2.5.4.3.2 Coherent Detection

An optical local oscillator is used here to generate optical radiation at a certain wavelength/frequency (W. K. Pratt, 1969). The frequency of the local oscillator does not have to be the same as that of the incoming information-bearing radiation. This possibility is thus responsible for the two variants of coherent detection discussed below. The block diagram of a coherent receiver is shown in Figure 2.18. It is pertinent to clarify that the term coherent detection in optical detection is not synonymous with coherent detection in radio

frequency (RF) parlance. In contrast to RF coherent detection, the output of the local oscillator in optical coherent detection is not required to have the same phase as the incoming radiation.

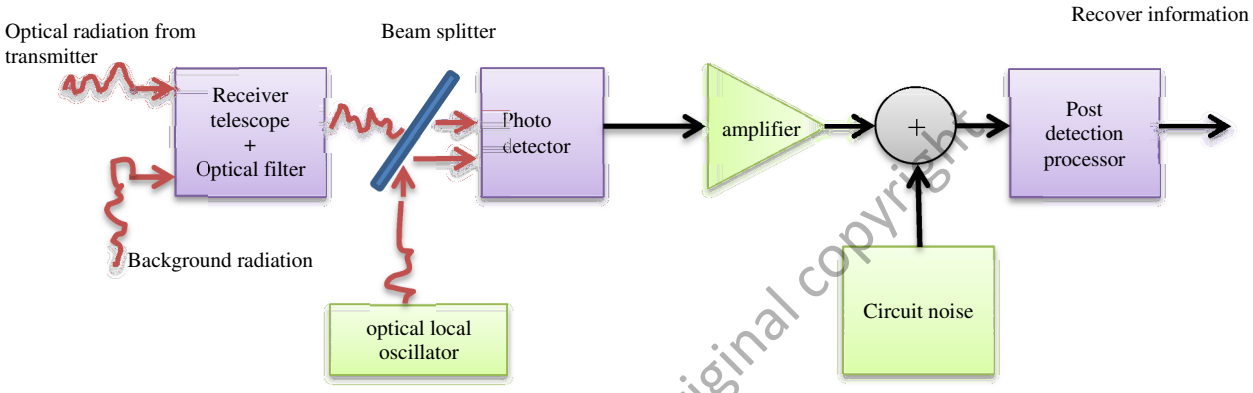

Figure 2.18: FSO basic block diagram for coherent detection (W. O. Popoola, Z. Ghassemlooy, & E. Leitgeb, 2007)

2.5.5 Partially Coherent Beam (PCB)

The using of phase screen diffuser at the transmitter is one of the alternatives to alleviate the atmospheric turbulence effect. It is well known as a partially coherent beam in FSO laser communication. The interest in the spatially partially coherent beam as a tool improving the performance of laser communication systems was indicated recently in a number of reported in (R. K. Tyson, 2002& A. Dogariu, 2003& T. Shirai, 2003& M. Salem, 2003& V. G. Sidorovich, 2002& G. Gbur, 2002& H. Yamamoto, 2003, T. Shirai & A. Dogariu, 2003). Studies of the propagation of a partially coherent beam wave through atmospheric turbulence have been conducted over the past three decades by numerous researchers (Y. Baykal, 1985& T. Yoshimura, 1986). A partially coherent

source can be generated in a number of different ways, including the placement of a diffuser at the laser transmitter of a quasi-monochromatic source. Most theoretical studies concerning a spatially partially coherent beam wave rely on a Gaussian Schell model for describing the partial coherence of the source beam (L. Mandel, 1995& A. C. Schell, 1961). This model utilizes a Gaussian correlation function to describe the surface roughness of the diffuser, often leading to simplifications. However the partially coherent beam causes the more expanding of beam divergence (Yaqing, Zhensen, Rui & Jinpeng, 2011). Consequently it can reduce the power transmit and resulting in the degrade of the signal received. Sometime the diffuser also is used as a tool to control the power (Korotkova, Andrews and Phillips, 2000 & Ricklin and Davidson 2002*).*

The beginning study of PCB has been investigated over the past three decades by researchers (L. Mandel & E. Wolf, 1995& A. C. Schell, 1961& S. Wandzura, 1980; R. L. Fante, 1980& V. A. Banakh & V. M. Buldakov, 1983). One of the ways study in this area, is by placing the diffuser at the laser exit aperture of a laser transmitter which can reduce the scintillation at the receiver. The free space second order statistical characteristics of a PCB are investigating detail in (L. Mandel & E. Wolf, 1995) by using the Gaussian Schell model (GCM).

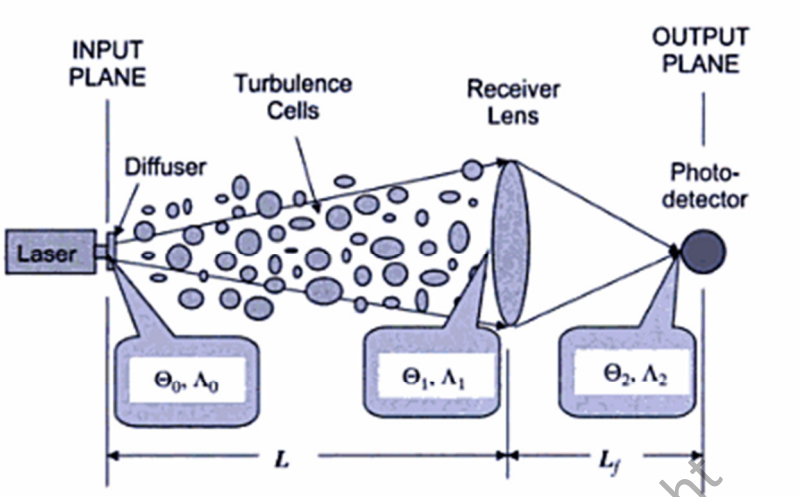

Figure 2.19: PCB parameters with a diffuser at laser exit of collimate beam (L. C. Andrews, R. L. Phillip. 2005)

The Figure 2.19 shows the PCB parameters by placing a thin phase screen diffuser at the laser exit of a climate beam. The Θ and Λ represent the Curvature and Fresnel ratio respectively which will discuss detail in Chapter 4. The capability of PCB has been studied in (Oztan, M.A., Baykal, Y. 2010) to decrease the scintillation noise effect for longer FSO above 5km. Apart from the advantage PCB reduce the scintillation index, the report from (E. Lee, Z. Ghassemlooy, W. P. Ng & M.A. Khalighi, 2013) has investigated the benefit of PCB to mitigate the pointing error in FSO. This is because the diffuser will cause the beam to spread more and thus reduce the pointing error effect. However, due to increase in beam spreading will cause the power signal decrease (O. Korotkova, L. C. Andrews & R. L. Phillips, 2000). Due to that, sometime the diffuser can become a power control tool to reduce the power when the signal light power is setup fix (O. Korotkova, L. C. Andrews, R. L. Phillips, 2003). In addition, reported in (O. Korotkova, L. C. Andrews, R. L. Phillips, 2004) analyze that the effects of diffuser are becoming less when in strong turbulence. As a result, the combination diffuser with other technique such as multi receiver or large collecting could provide sufficient high quality data transfer (Mahon, R., et al 2008).

2.5.6 Effect of Atmospheric Turbulence

The most practical implementation for FSO communication involves the use of an intensity modulation/direct detection (IM/DD) system. The transmitted data is on-off keying (OOK) intensity modulated and goes through an atmospheric channel to the receiver. The receiver aperture collects the received optical signal and focuses it onto a photodetector, which converts the instantaneous optical power into electrical current for the detection process. In the presence of atmospheric turbulence between transmitter and receiver, the received signal exhibits random intensity fluctuations.

The instantaneous received signal power P_R as expressed in Equation 2.3 is a random quantity. The observed quantity is now the averaged or mean received signal power $\langle P_R \rangle$ given by

$$\langle P_R \rangle \cong \frac{\pi}{8} D^2 \langle I(0,L) \rangle = \frac{P_R}{1+1.33\sigma^2 \Lambda^{5/6}} \tag{2.3}$$

Furthermore, it follows that the mean signal current is $\langle i_s \rangle = \Re \langle P_R \rangle$, where $\Re$ is the photodetector responsivity. The output current from the detector $i = i_S + i_N$ in the case is a random variable, which has the mean value $\langle i_s \rangle$ and the variance $\sigma_i^2 = \sigma_S^2 + \sigma_N^2$, , where σ_s^2 represents fluctuations in the signal that become a contributor to the detector noise and related to the normalized intensity variance σ_I^2 by

$$\sigma_s^2 = \langle i_S^2 \rangle - \langle i_s \rangle^2 = \langle i_s \rangle^2 \sigma_I^2 \tag{2.4}$$

Using the relations given in Euation 2.3 and Equation 2.4 and the averaged SNR $\langle \Gamma_0 \rangle$ at the output of the detector assumes the form

$$\langle \Gamma_0 \rangle = \frac{\langle i_S \rangle^2}{\sigma_i^2} = \frac{\Gamma_0}{\left(1+1.33\sigma_I^2 \Lambda^{5/6}\right)^2 + \Gamma_0 \sigma_I^2} \tag{2.5}$$

The BER can be expressed as

$$P_r(e)_{OOK} = \frac{1}{2} erfc\left(\frac{i_s}{2\sqrt{2}\sigma_N}\right) = \frac{1}{2} erfc\left(\frac{1}{2\sqrt{2}}\sqrt{\Gamma_0}\right) \tag{2.6}$$

In the presence of optical turbulence the expression in Equation 2.6 must be modified to incorporate the effects of signal fluctuations. In this case, the threshold level is now set to half the average signal corresponding to a received pulse ($i_T = \langle i_S \rangle / 2$).

The false alarm probability P_f does not depend on the random received signal and can be written as

$$P_f = P_R|(1|0) = \frac{1}{2} erfc\left(\frac{1}{2\sqrt{2}}\sqrt{\Gamma_0}\right) \tag{2.7}$$

However the miss probability p_m is now

$$P_m = P_R|(0|1) = \frac{1}{2} erfc\left(\left[\frac{2i_s}{\langle i_s \rangle} - 1\right]\frac{1}{2\sqrt{2}}\sqrt{\Gamma_0}\right) \tag{2.8}$$

where i_s is the random detecror dignal corresponding to the instantanrous received intensity. To compute the average BER $\langle P_R(e) \rangle$, these question must average over the intensity fluctuation spectrum. This gives

$$\langle P_r(e)\rangle = \frac{1}{4}\left\{erfc\left(\frac{1}{2\sqrt{2}}\sqrt{T_0}\right) + \int_0^{\infty} P_I(i_s)\left(\left[\frac{2i_s}{\langle i_s\rangle} - 1\right]\frac{1}{2\sqrt{2}}\sqrt{T_0}\right) di_s\right\} \quad (2.9)$$

where $P_I(i)$ is the PDF of the intensity fluctuations.

The limiting performance of average BER can be achieved by assuming the threshold level is dynamically set at half instantaneous received signal level i_t, which lead to expression

$$\langle P_r(e)\rangle_L = \frac{1}{2}\int_0^{\infty} P_I(i_s) erfc\left(\frac{i_s}{2\sqrt{2\langle i_S\rangle}}\sqrt{\langle T_0\rangle}\right) di_s\} \quad (2.10)$$

This shows that the turbulence will deterior the signal performance FSO and the most problem OOK signaling is relating threshold ability as discussed further in Chapter 4. In Chapter 5 will discuss the probility of error for DDM technique.

2.6 Summary

This chapter provides an overview of terrestrial FSO communication. The mainly challenges of FSO can be divided into atmospheric attenuation, atmospheric turbulence and skin & laser safety are described. This chapter also more emphasis on the scintillation effect and focus modulation and PCB technique to mitigate the atmospheric turbulence effect. The OOK modulation technique is briefly explained and it's a major limitation highlighted. In addition, the implementation PCB in OOK can enhance the FSO performance but still have weakness arise. The aim of this dissertation is to improve the modulation technique via enhance the threshold detection process and increase the reduction of scintillation index.

CHAPTER 3

RESEARCH METHODOLOGY

3.1 Introduction

This chapter describes the flow of methodology of development of Dual Diffuser Modulation (DDM) technique. The brief research methodology is explained in Section 3.2. The parameters considering in an evaluation such as effective power, bit rate and propagation are discussed in Section 3.3. Meanwhile, the Section 3.4 elaborate the analysis in simulation approach. The noise consideration in FSO analysis is dicussed in Section 3.5 and the detail about the diffuser is explained under the PCB in Section 3.6.

3.2 Research Methodology

The development of new modulation can divide into three approaches. The first approach is to develop the model of modulation technique. In this part, develop theoretically the structure of new modulation technique. It encircles the transmitter and receiver part. The components that are discussed are light source, inverter, phase screen diffuser, photodetector and subractor. This part is explained detail in Section 4.2 in Chapter 4.

The second approach discusses the theoretical design and performance analysis of new modulation technique. This part also explained the PCBs parameters which will be use in theoretical analysis. Among the relate topic for PCBs are beam spreading, mean intensity and flux variance. The detail explaination about PCBs in Section 3.6. The

performance of the modulation will be presented also interm of signal to noise ratio (SNR) and bit error rate (BER). Mathematical derivation of new modulation technique will be discussed in two conditions which relate to SNR and BER. The first condition is considered without the presence of atmospheric turbulence and the second condition with the presence of turbulence. After completing the mathematical derivation, the performance of this modulation is analyzed and compared to the conventional intensity modulation for on-off keying (CIM/DD-OOK) to distinguish the significance of the modulation in FSO communication.

The last approach is analyzing the new modulation through the aid of a simulator which is known as *Optiwave* software (*Optisystem Ver.11*). This will assist further the investigating the findings which are set up to be close as real FSO condition. At this stage also, it can validate the theoretical results that presented in earlier work. Apart from that, the simulations enable the modulation design to operate optimally in an FSO system network. This is because the implementation in simulator specifically considers the practical factors such as scintillation index, attenuation effect and geometrical loss which is become important role to evaluate the FSO performance. The overall research methodology is illustrated in Figure 3.1.

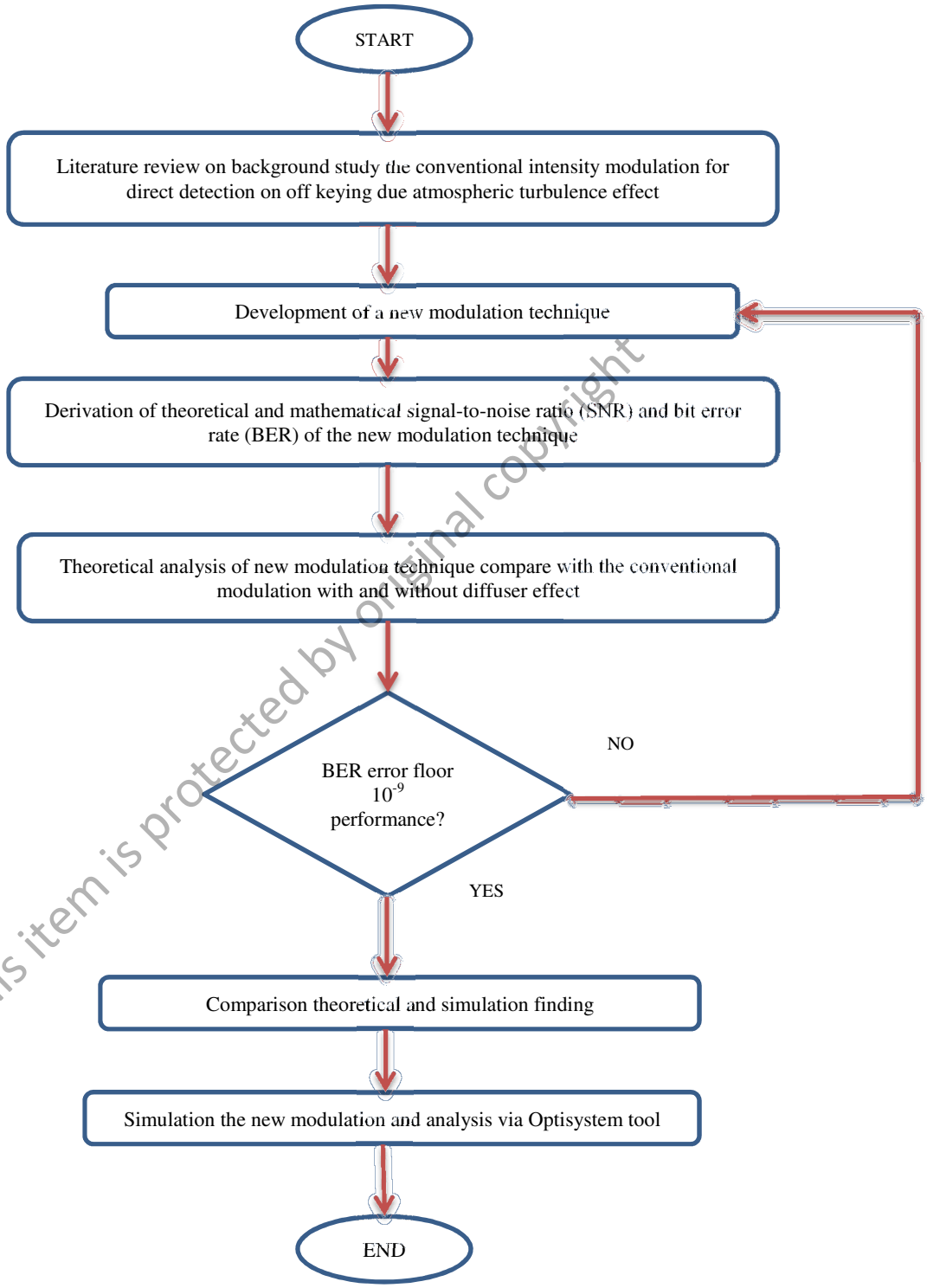

Figure 3.1: Flow chart of methodology the development of new DDM technique

3.3 Design Performance Parameters

The design parameter is one of the crucial parts in order to evaluate the effectiveness of the new modulation technique. It allows the designer to change or make the parameters variable to analyze the capability of the new system. In this work study, the design parameters that will be used are consists of:

a) **Diffuser strength** - in weak to moderate turbulence regime, the using of diffuser is very effective. As a result, the reduction of scintillation index is huge. This reduction can be increased more with employs the higher diffuser strength. However, when turbulence turns to strong regime, the effect of diffuser becomes less but still contribute to reduction of scintillation index in small amount decreasing. The variable of diffuser strength parameter will produce a different value of scintillation index.

b) **Receiver Aperture** - this design parameter can be related to aperture averaging effect and at the same time play a role to add the coverage of collecting the intensity signal. The variable value of the receiver aperture will result the effective signal power also variable. There are two major effects when considering this parameter that are reduction the scintillation index and increase the effective signal power. In this work, the comparison of receiver aperture between three sizes: $W_G = 0.01$m, $W_G = 0.02$m and $W_G = 0.03$.

c) **Propagation distance** - in terrestrial FSO communication, the propagation distance is very important in order to have the optimal performance. The short distance for FSO is very popular in currently commercialization. One of the main reasons is due to robust again the atmospheric channel effect. However, the ever increasing demands in FSO need this technology able to operate more long distance. Consequently, it can become the cost effective for this technology without the need any router or regenerator for long distance propagation. In the case study the propagation distance is compared up to 3km.

d) **Bit rate** - bit rate can be defined as a rate of data transfer for one bit. In other word it can be said as an ability speed of the system to transmit one bit data over channel transmission. Basically the higher bit rate will increase bit error as well but at the same time if the system can operate at high bit rate gives more advantage over a system. Nowadays, the commercial FSO can easily to operate at 2.5Gbps but lately from the continuous study of researchers show that this advance of technology can support the bit rate up to 10Gbps and even more. This is one of the major advantages of FSO if compare other mode communication technology such as fiber and radio frequency which usually limit to 622Mbps for optimal performance. In this study, four main bit rates STM-1 (155 Mbps), STM-4 (622 Mbps), STM-16 (2.5 Gbps), STM-64 (10 Gbps) are used, according to the Synchronous Digital Hierarchy (SDH) standard, typically used for metro applications.

e) **Effective power** - the effective power in FSO is vital in determining the highest quality signal. The signal power from the transmitter and receiver power at receiver influence the performance system. Therefore it is important to determine the effective power in FSO where normally measured interm of dBm. In this work, the effective power is mainly determined by the signal power that associate with SNR and the signal power is related to the power received at the receiver which relate to power transmit at the transmitter. For the power transmit, the comparison is between three levels of power starting from -5 dBm, then 0 dbm and finally 5 dBm. This variation level power transmits to analyze the capability of new modulation technique is able to operate at low power transmit. Meanwhile for the power received, the range is set between -50 dBm to 0 dBm.

3.3.1 Signal to Noise Ratio (SNR)

The SNR can be defined as the ratio of signal power to the noise power. It will compare the level of a desired signal to the level of background noise and normally expressed in decibels (dB). In FSO system, the SNR are generated from the power received over the presence noises such as shot noise, background noise, dark current noise and thermal noise which is generated from the system itself.

3.3.2 Bit Error Rate (BER)

The BER of a digital communication system can be defined as the probability of incorrect bit identification by the decision circuit. In FSO communication, the goal is to transmit the maximum number of bits per second over the maximum possible range with less error. The performance of FSO can be predicted by computing the BER of the system which depend on the modulation format and the SNR. Interm of modulation, for instance OOK the transmitter sends a pulse of light into a channel to represent a '1' and not send any light for '0'. When a signal plus noise is present at the receiver input, there are two ways in which error occurs. The first is error '1' when the receiver decides to '0' but actually '1' was transmitted. The second is the errors for '0' occur when receiver decides '1' but '0' was sent actually.

In the presence of turbulence, the SNR is considered as an average, $\langle SNR \rangle$ due to the fluctuation of the signal and thus the BER also will consider an average to include the factor of the probability distribution of irradiance or intensity. Most of FSO communication, have set the standard the minimum for BER is 10^{-9} and will be use same in this research of study for the worst case scenario. It can define as a one error can only allow in 1 billion bits transmitted.

3.4 Simulation Analysis

The simulation approach in investigating the performance system is one of the wise alternative when the limitation in hardware and experimental availability arise and also can become the preliminary stage before implement in real condition. The use of the

simulation software can be exploited to make the validations and optimization analysis. In this work, the *Optisystem Version 11* was employed for simulation software tool. Through the simulation it allows each of the design modulation sequence system will be tested using varying specific sets of designing parameters such as scintillation index, power transmits, receiver aperture, propagation distance and bit rate. Performance is characterized mainly by the BER, effective power, eye diagram shape and oscilloscope pattern.

3.5 Noise Detection Analysis

There are various noise sources in FSO communication. All of this noise contributes to deteriorate signal performance.. This noises will limit the ability photodetector to detect the incoming signal. If the signal power is less than the noise power, the signals will not be able to be distinguished clearly. The two most important sources of noise in the optical receiver are the shot noise resulting from the statistical nature of the photon-to-electron conversion process and the thermal noise associated with the amplifier circuitry. These sources of noise always accompany the optical signal. Another type of noise involved in the detection of optical radiation is dark current noise and background illumination noise, which may cause deleterious effects in FSO communication systems.

3.5.1 Shot Noise

The only significant noise that affects its performance is that associated with the quantum nature of light itself. The principal noise associated with a photodetector is

called quantum or shot noise. When an unmodulated lightwave is measured using a photodetector, two current components are obtained at the output. The first one is DC current, and the second one is the undesired shot noise signal. The shot noise arises from the statistical nature of the production and collection of discrete photoelectrons when an optical signal is incident on a photodetector. It has equal power density at all frequencies. If the electronic circuit after the photodetector only handles the frequency bandwidth Δf , the mean-square current amplitude of the shot noise i_{Shot}^2 is given by

$$i_{shot}^2 = 2e\Re(i_s)B \tag{3.1}$$

where *e* is electron charge, $\Re$ is the responsivity and B is the bandwidth. For an APD, in addition to the primary source of shot noise, there is a noise figure associated with the excess noise generated by the random avalanche process. This noise figure F(M) is defined as the ratio of the actual noise generated in an avalanche photodiode to the noise that would exists if all carrier pairs were multiplie2d by exactly M and is given by $F(M) = \frac{\langle m^2 \rangle}{M^2}$, where $\langle m^2 \rangle$ is the mean square gain and can be approximated as M^{2+x} with x varying between 0 and 1 depending on the material and structure. Thus, the meansquare current amplitude of the shot noise for APD $\langle i_{SN}^2 \rangle_{APD}$ is given by $\langle i_{SN}^2 \rangle_{APD} = 2qi_sM^2F(M)\Delta = 2q_M\Delta f$ where i_S is the average value of total multiplied output current, i_M is the average unmultiplied photocurrent, and M factor APD.

3.5.2 Dark Current Noise

The dark current is the photocurrent generated when no photon is impinging on the photodetector. The dark current is the current that continues to flow through the bias circuit of the device even if no light is incident on the photodiode. It arises from electrons and/or holes that are thermally generated in the p-n junction of the photodiode. The dark current strongly depends on the type of semiconductor, operating temperature, and bias voltage. Depending on the materials, their values range from 100 pA for Si up to 100 nA for Ge.

$$i_{dark}^2 = 2e(i_d)B \tag{3.2}$$

3.5.3 Background Noise

This type of noise is due to the detection of photons generated by the environment. Background illumination noise is caused by the light that is not part of the transmitted signals, such as ambient light. If the photodetector is not isolated from the background radiation, the appearance of this noise is inevitable. Due to the discreteness and randomness of both the dark current and background radiation, these noise sources are similar to the shot noise. There are two types of sources contribute to background radiation noise; a)Sun and b) the sky

$$i_{background}^2 = 2e\Re\langle i_{sky} + i_{sun}\rangle B \tag{3.3}$$

where, $i_{sky} = \frac{N(\lambda)\Delta\lambda\pi\Omega_{FOV}^2}{4}$ and $i_{sun} = W(\lambda)\Delta\lambda$. The $N(\lambda)$ is spectral radiance of sky W(λ) = spectral radiant emmittance of sun, $\Delta\lambda$ = bandwidth of an optical bandpass filter (OBPF) and Ω_{FOV}^2 = photodetector field of view angle (FOV) in radians.

3.5.4 Thermal Noise

Thermal noise also called Johnson noise or Nyquist noise. This is the noise caused by the thermal fluctuation of electrons in any receiver circuit of equivalent resistance R_L, and temperature T_n.

$$i_{thermal}^2 = \frac{4k_bT_nB}{R_L} \tag{3.4}$$

where k_b is the Bolztman's constant, T_n is the temperature of receiver noise, B is the electrical equivalent noise bandwidth of the receiver and R_L is the load resistance. At temperatures above absolute zero, the thermal energy of the charge carriers in any resistor leads to fluctuations in local charge density. These fluctuating charges cause local voltage gradients that can derive a corresponding current into the rest of the circuit.

3.6 Partially Coherent Beam (PCB)

The study in the spatially PCBs has an attractive number of researchers due to the capability for improving the performance of laser communication systems was indicated recently in a number of publications (J. C. Ricklin & F. M. Davidson, 2002; G. Gbur & E. Wolf, 2002; V. G. Sidorovich, V. V. Ragulsky, M. V. Vasil'ev, A. A. Leshchev, &

M. A. Sadovnikov, 2002; T. Shirai, A. Dogariu, & E. Wolf, 2003). In this work, the theoretical model for PCB focus on the scintillation index calculation in turbulence. This is because scintillation index is the most important statistic for practical application FSO systems. In this research study, the Kolmogorov spectrum model will be used in the case of weak atmospheric turbulence. By using the theory of Andrews (L. C. Andrews, R. L. Phillips, & A. R. Weeks, 1997; L. C. Andrews, R. L. Phillips, & C. Y. Hopen, 2001) the weak scintillation index of a PCB can be used in all atmospheric conditions. Therefore, the scintillation index depends on the strength of the diffuser and the strength of the atmospheric turbulence.

3.6.1 Basic Model Beam and Parameters

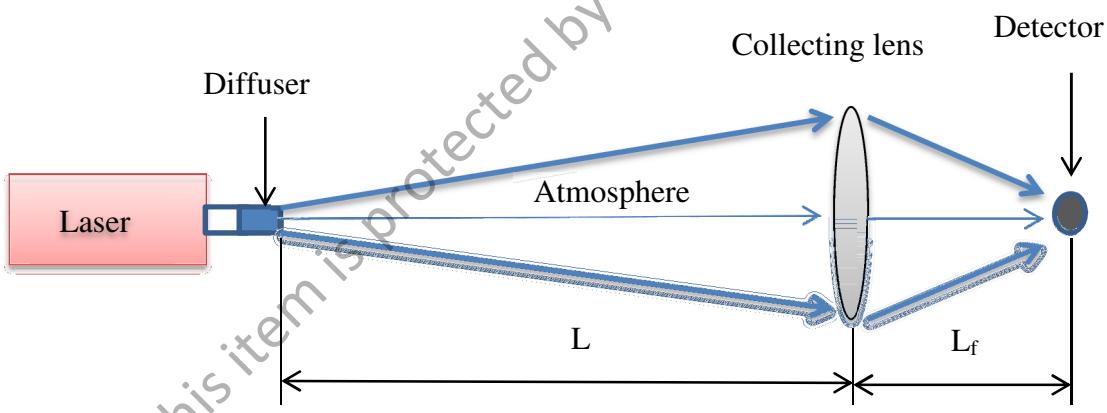

Figure 3.2: PCBs model and configuration (O. Korotkova, L. C. Andrews, R. L. Phillips, 2004))

The Figure 3.2 shows the diffuser model for PCB with propagation channel. For the transmitted beam wave of the diffuser is characterized by TEM_{00} Gaussian beam wave parameters.

$$\Lambda_0(L) = \frac{2L}{kw_0^2} \tag{3.5}$$

$$\Theta_0(L) = 1 - \frac{L}{F_0} \tag{3.6}$$

where the $\Lambda_0(L)$ represent the initial Fresnel ratio and the $\Theta_0(L)$ represent the initial phase curvature. The $k = \frac{2\pi}{\lambda}$ is the laser wave number, λ (in meters) is wavelength, L (in meters) is propagation distance to the collecting (Gaussian) lens, F_0 (in meters) is the phase front radius of curvature, and W_0 (in meters) is the laser exit aperture radius. From the Andrews and Phillips, (L. C. Andrews, R. L. Phillips, & A. R. Weeks, 1997), the parameters Θ_1 and Λ_1 for the beam incident on the collecting lens can be written as:

$$\Lambda_1 = \frac{2L}{kW_1^2} = \frac{\Lambda_0}{\Theta_0^2+\Lambda_0^2} \tag{3.7}$$

$$\Theta_1 = 1 + \frac{L}{F_1} = \frac{\Theta_o}{\Theta_0^2+\Lambda_0^2} \tag{3.8}$$

The Gaussian lens at the receiver assume has radius W_G and phase front radius of curvature F_G . After propagating through the lens to the detector located in the image plane at distance L_f behind the lens, the beam has radius W_2 and radius of curvature F_2 , which are characterized by beam parameters:

$$\Lambda_2 = \frac{2L_f}{kW_2^2} = \frac{L}{L_f}\left[\frac{\lambda_1+\Omega_G}{\left(L/L_f-L/F_G+\bar{\Theta}_1\right)^2+(\Lambda_1+\Omega_G)^2}\right] \tag{3.9}$$

$$\Theta_2 = 1 + \frac{L_f}{F_2} = \frac{L}{L_f}\left[\frac{L/L_f-L/F_G+\bar{\Theta}_1}{\left(L/L_f-L/F_G+\bar{\Theta}_1\right)^2+(\Lambda_1+\Omega_G)^2}\right] \tag{3.10}$$

where $\bar{\Theta}_1 = 1 - \Theta_1$ and the nondimensional parameter Ω_G is defined by

$$\Omega_G = \frac{2L}{kW_G^2} \tag{3.11}$$

The model the diffuser in front of the laser transmitter by a thin random phase screen diffuser (L. C. Andrews & R. L. Phillips, 1998; J. W. Goodman, 1985) can be characterized by a single-scale Gaussian spectrum model:

$$\Phi_s(k) = \frac{\langle n_1^2 \rangle l_c^3}{8\pi\sqrt{\pi}} exp\left(-\frac{1}{4} l_c^2 k^2\right) \tag{3.12}$$

where k is wave number, and l_c is directly related to the variance σ_g^2 (J. C. Ricklin & F. M. Davidson, 2002) to describe the partial coherence properties of the source:

$$l_c^2 = 2\sigma_g^2 \tag{3.13}$$

The parameter $\langle n_1^2 \rangle$ is the fluctuation in the index of refraction induced by the diffuser and the nondimensional parameter analogous that relating the strength of diffuser is defined as:

$$q_c = L/kl_c^2 \tag{3.14}$$

Therefore the 'new' Gaussian beam from the diffuser effect can be characterized by an effective set of beam that are Θ_e, $\Lambda_e$and N_s represent the number of speckles cells.

$$N_s = 1 + \frac{2W_0^2}{l_c^2} = 1 + \frac{4q_c}{\Lambda_0} \tag{3.15}$$

$$\Lambda_e = \frac{\Lambda_0 N_S}{\Theta_0^2 + \Lambda_0^2 N_S} \tag{3.16}$$

$$\Theta_e = \frac{\Theta_0}{\Theta_0^2 + \Lambda_0^2 N_S} \tag{3.17}$$

For the effective spot beam $W_e(L)$ for PCB is described by (Yaqing Li, Zhensen Wu, Rui Wu & Jinpeng Zhang, 2011) to consider the global coherent parameter ξ. It can be written as

$$W_e(L) = w_o\sqrt{\left(\Theta_o^2 + \xi\left(\frac{2L}{kw_o}\right)^2\right)} \tag{3.18}$$

$$\xi = \xi_s + \frac{2w_o^2}{\rho_o} \tag{3.19}$$

where the $\xi_s = 1 + \frac{w_o^2}{\sigma_\mu^2}$ represent the source of the coherence parameter of the laser beam emitted by the transmitter, $\rho_0 = [0.545C_n^2k^2L]^{-3/5}$ is the coherence length through turbulence atmosphere and σ_μ^2 is the variance of the Gaussian describing the ensemble average of the random phases which relate to diffuser strength. If the $\xi_s = 1$, the beam is categorized as a perfectly coherent beam and the beam is categorized as a partially coherent beam if the $\xi_s > 1$ (Wang, S. C. H. & Plonus, M. A., 1979). If without diffuser effect the beam spot radius at the receiver can be expressed as (Ricklin, J. C., Bucaille, S. & Davidson, F. M., 2004)

$$W(L) = W_o(\Theta_o + \Lambda_o)^{1/2} \tag{3.20}$$

where the Θ_o and Λ_o are the initial phase curvature and initial Fresnel ratio respectively as shows in Equation 3.5 and Equation 3.6.

3.6.2 Scintillation Index

The PCBs scintillation index is produced by the combination of diffuser and atmospheric turbulence. In the weak turbulence regime, the scintillation index of PCBs was calculated in (O. Korotkova, L. C. Andrews, & R. L. Phillips, (2003).)

$$\sigma_B^2 = 3.86\sigma_I^{\,2}\left\{\begin{array}{l}0.4\left[(1+2\Theta_{ed})^2+4(\Lambda_{ed})^2\right]^{5/12}\\ \mathrm{X}\left(\cos\left[\frac{5}{6}\tan^{-1}\left(\frac{1+2\Theta_{ed}}{2\Lambda_{ed}}\right)\right]\right)\\ -\left(\frac{11}{6}(\Lambda_{ed})^{5/6}\right)\end{array}\right\} \tag{3.21}$$

where σ_I^2 is the Rytov variance that can written as

$$\sigma_I^{\,2} = 1.23\,C_n^{\,2}k^{\,7/6}L^{11/6} \tag{3.22}$$

Meanwhile for strong turbulence, the scintillation index of PCBs can be used in the strong fluctuation theory developed by Andrews (J. W. Goodman, 1985; L. C. Andrews & R. L. Phillips, 1998).

$$\sigma_{strong}^2 = exp\left[\frac{0.49\sigma_B^2}{\left(1+0.56\sigma_B^{12/5}\right)^{7/6}}+\frac{0.51\sigma_B^2}{\left(1+0.69\sigma_B^{12/5}\right)^{5/6}}\right]\text{-}1 \tag{3.23}$$

which σ_B^2 is given in Equation 3.21.

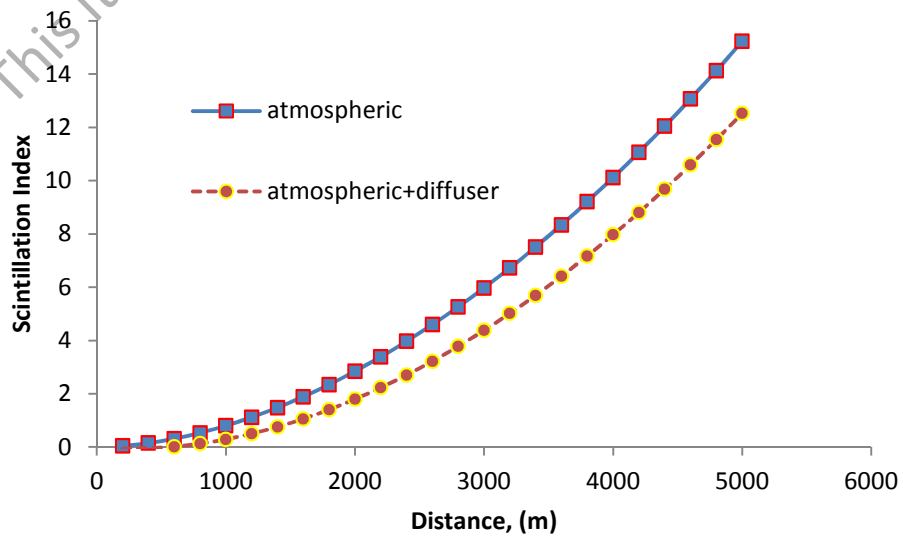

Figure 3.3: Comparison scintillation index due to weak turbulence between with and without diffuser

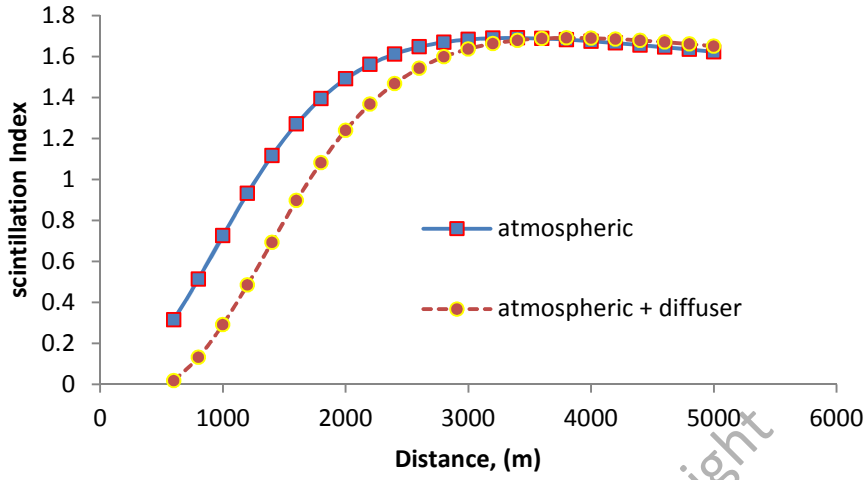

Figure 3.4: Comparison scintillation index due to strong turbulence between with and without diffuser

The Figure 3.3 shows the effect of the diffuser in order to reduce the scintillation index under the weak turbulence. The diffuser is more effective under this regime turbulence. Meanwhile the Figure 3.4 shows the reduction scintillation index due to a diffuser for strong turbulence. The effect of the diffuser becomes less but still reduces the scintillation index in small amount.

3.6.3 Flux Variance

The reduction of the scintillation index due to PCB alone would not be sufficient for the high-quality data transfer calculated interms of the bit error rate (BER) in communication systems. However, the combination of partial coherence with large enough collecting lens (aperture averaging effect) can provide the required BER level. The flux variance of the intensity fluctuations at the detector plane that calculated for the collecting lens with normalized radius Ω_G is valid for all atmospheric conditions as given in (L. C. Andrews, 2001):

$$\sigma^2_{flux}\left(L+L_f,\Omega_G\right)=\exp\left[\sigma^2_{\ln x}\left(L+L_f,\Omega_G\right)+\sigma^2_{\ln y}\left(L+L_f,\Omega_G\right)\right]-1 \tag{3.24}$$

where $\sigma^2_{\ln x}$ is the flux variance associated with large-scale fluctuations (O. Korotkova, 2003).

The effect of aperture averaging can be describe as when the receiving aperture is larger than a spatial scale size that produces the intensity fluctuations, the receiver will average the fluctuations over the aperture and the scintillation will be less compared to scintillation measured with a point receiver (J. H. Churnside, 1991; Vetelino, 2007). It has been shown that aperture averaging causes a shift of the relative spatial frequency content of the inensity spectrum toward lower frequencies, since the fastest fluctuations caused by small-scale sizes average out (L. C. Andrews, 2000; Mahon, R., et al 2008). Hence, the scintillation measured by a receiving aperture is produced by scale sizes larger than the aperture. The obvious advantage of increasing the aperture size is collecting more light. However, as the aperture size exceeds several times the coherence length of incident light on it, the scintillation index gets reduced, a phenomenon known as aperture averaging (D. L. Fried, 1967; J. Richard Kerr, 1973).

In strong turbulence, there is two-scale behaviour in the intensity flux variance obtained by a finite size receiving aperture. A sharp decrease in scintillation is observed for increasing aperture sizes up to the coherence scale, ρ_o, after which there is a levelling effect, followed by a second decrease in the intensity flux variance when the aperture exceeds the scattering disk $L/\kappa p_o$ (J. H. Churnside, 1991; L. C. Andrews, 2000). The levelling effect arises since medium-scale sizes are inefficient in producing scintillation in strong turbulence. Hence, if a receiving aperture is larger than ρ_o in

strong turbulence, the small-scale scintillation is mostly averaged out. This should affect the PDF of the intensity fluctuations since existing models, developed for point receivers, are obtained by modulating the small and large scale distributions. Therefore in this thesis we use the Gamma Gamma distribution and suitable for all fluctuation regime (M. A. Al-Habash, 2001). The detail Gamma Gamma distribution function is discussed in Chapter 5 for BER performance under the presence of atmospheric turbulence effect.

The log intensity due to large scale eddies is given as;

$$\sigma_{\ln x}^2\left(L+L_f,\Omega_G\right)=0.49\sigma_R^2\left(\frac{\Omega_G-\Lambda_e}{\Omega_G+\Lambda_e}\right)^2 XR\left[\frac{\eta_x}{1+0.4\eta_x\dfrac{(1+\Theta_e)}{(\Lambda_e+\Omega_G)}}\right]^{7/6} \tag{3.25}$$

where $R=\frac{1}{3}-\left(\frac{1}{2}\right)(1-\Theta_e)+\left(\frac{1}{5}\right)(1-\Theta_e)^2$. The quantity η_x in Equation 4.2 is the normalized large-scale cutoff frequency determined by the asymptotic behavior of $\sigma_{\ln x}^2$ in weak turbulence and saturation regime (L. C. Andrews, (1998); O. Korotkova, 2003):

$$\eta_x=\frac{R^{-6/7}\left(\dfrac{\sigma_B}{\sigma_R}\right)^{12/7}}{1+0.56\,\sigma_B^{12/5}} \tag{3.26}$$

Meanwhile log intensity due to small scale eddies is given as;

$$\sigma_{\ln y}^2\left(L+L_f,\Omega_G\right)=\frac{1.27\,\sigma_R^2\eta_y^{-5/6}}{1+0.4\dfrac{\eta_y}{(\Lambda_1+\Omega_G)}} \tag{3.27}$$

where the corresponding cutoff frequency is

$$\eta_y = 3\left(\frac{\sigma_R}{\sigma_B}\right)^{12/5}\left(1 + 0.69\,\sigma_B^{12/5}\right) \tag{3.28}$$

The Figure 4.4 shows the comparison of flux variance versus the various of collecting lens radius, W_G between weak and strong turbulent condition. The propagation distance L = 2000m and for weak and strong turbulent strength $C_n^2 = 10^{-15}m^{-2/3}$ and $C_n^2 = 10^{-13}m^{-2/3}$ respectively which leading to Rytov variance $\sigma_I^2 = 0.07$ and $\sigma_I^2 = 7.09$. The significant reduction of the flux variance occurs in weak turbulent the flux varies from 0 to 0.05 but for the strong turbulence the flux value varies from 0 to 0.4. This illustrated that the effect of flux variance is greater when the strength of turbulence increase and the reduction flux become less. From the graph also shows that the effect of flux variance can be reduced by increase the collecting lens radius. As the collecting lens radius increase the value of flux variance will decrease.

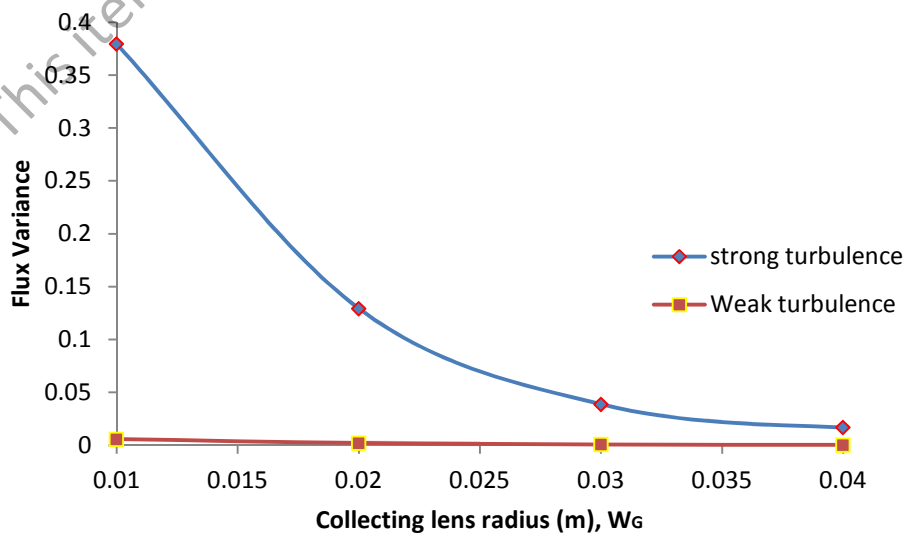

Figure 3.5: Comparison of flux variance $\sigma_I^2(L + L_f, \Omega_G)$ versus the collecting lens radius, W_G between weak and strong turbulence condition for partially coherent beam (diffuser effect)

Interms of the effect of diffuser strength relating aperture averaging effect, the Figure 3.5 shows the effect normalize collecting lens, Ω_G versus the several partially coherent beams with q_c = 0.1, 1and 10 and coherent beam for the weak turbulent condition. The propagation distance L= 1000m, wavelength, λ = 1μm, W_G = 0.01m and $C_n^2 = 10^{-15} m^{-2/3}$. As we can see, the flux variance value is low when under this region turbulent with the highest flux is at 0.136 for coherent beam. Meanwhile the lowest flux is at 0.0054 for q_c = 10. This indicates the flux variance reduce when the q_c increase which relating to the strength of the diffuser.

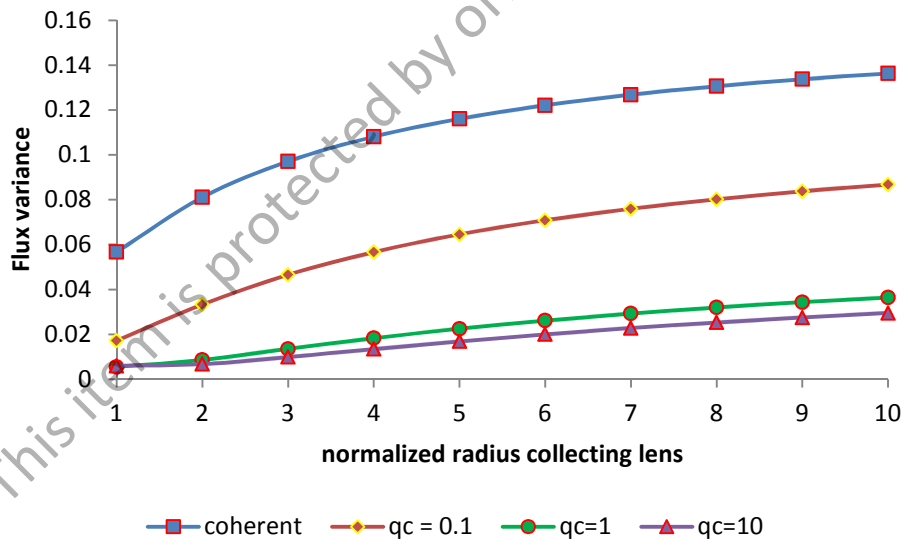

Figure 3.6: Effect of normalizing collecting lens, Ω_G vs. flux variance for q_c = 0.1,1 and 10 and coherent beam in weak turbulence regime

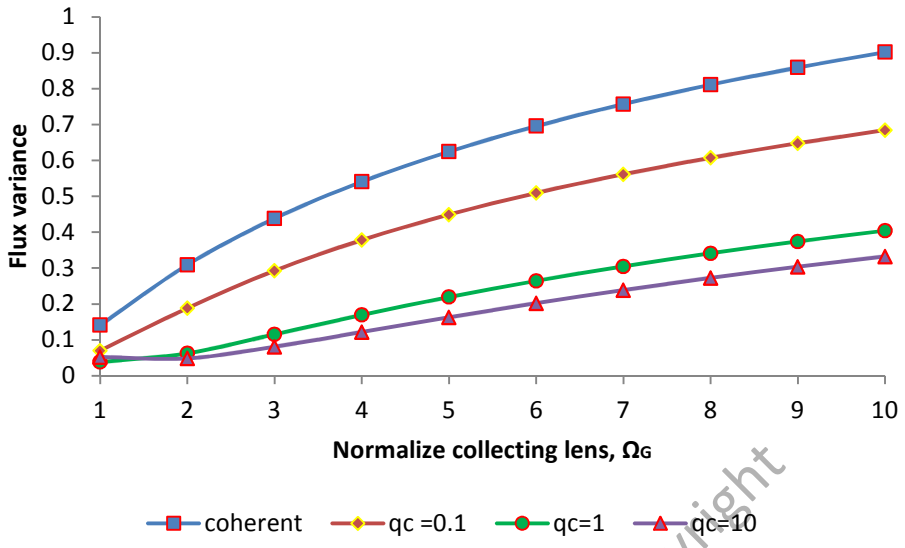

Figure 3.7: Effect of normalize collecting lens, Ω_G vs. flux variance for q_c = 0.1,1 and 10 and coherent beam in strong turbulence regime

Nevertheless, when in strong turbulence the effect of the diffuser is less as shown in Figure 3.6. Consequently the flux variance value is high and can lead to increase of signal to noise ratio (SNR). If compare with Figure 3.7, the highest value of flux is at 0.09 for coherent beam and the lowest flux is produced by q_c = 10 with value 0.052. This indicates that the reduction of flux is reduced even the increasing of Ω_G.

3.7 Gaussian atmospheric optical channel analysis

In this work, the analysis is based on the Gaussian atmospheric optical channel. Basically there are two methods for analysis that are a) Poisson analysis and b) Gaussian analysis (J. Alda, 2003). The Poisson analysis involves the photoelectron count but when consider the large signal photoelectron counts, and by taking the detection thermal noise into account as explained in Section 3.5, the Gaussian analysis can be used to generate signal current probability distribution. Assume the condition without any loss of generality, the receiver area may be normalized to unity that

represented by the optical intensity, *I*. If $\Re$ represents the responsivity of the PIN photodetector, the received signal in an OOK system is therefore given by:

$$i(t) = \Re I + n(t) \tag{3.29}$$

where $n(t) = N(0, \sigma^2)$ can be represented by the additive white Gaussian noise (AWGN), $[g(t - jT)]$ is the pulse shaping function and *dj* = [-1, 0].

The received signal at the receiver is fed into a threshold detector which compares the received signal to a pre-determined threshold level. If the receiver determines the binary '1' so than the received signal is above of the threshold level and '0' otherwise. The probability of error is therefore given as:

$$P_e = P(1) \int_{-\infty}^{i_{th}} P(0|1)dI + P(0) \int_{i_{th}}^{\infty} P(1|0)di \tag{3.30}$$

where i_{th} is the threshold signal level and the marginal probabilities are defined as:

$$P(i|0) = \frac{1}{\sigma^2\sqrt{2\pi}} ex(-i^2/2\sigma^2) \tag{3.31}$$

$$P(i|1) = \frac{1}{\sigma^2\sqrt{2\pi}} exp\left[\frac{-(i-\Re I)^2}{2\sigma^2}\right] \tag{3.32}$$

For equiprobable symbols, p(0)= p(1)=0.5, hence the optimum threshold point is at $i_{th} = 0.5\Re I$ and the conditional probability of error reduces to:

$$\mathrm{P_{ec}} = \mathrm{Q}\left(\frac{\mathrm{i_{th}}}{\sigma}\right) \tag{3.33}$$

where $Q(x) = 0.5erfc\left(x/\sqrt{2}\right)$.

3.8 Summary

In this chapter, the flow of research methodology is discussed. Generally there are three approaches to develop the DDM technique. The first approach is develop theoretically the model of this new technique. The second approach is develop theoretically mathematical derivation and the third approach is verify the theoretical part with simulation by using OptiSystem software. In this chapter also discuss the noise consideration that presence in FSO calculation. Among the noise that take into account are shot noise, background noise, dark current noise and thermal noise. Apart from that, the detail explaination about partially coherent beam (PCB) that relate to diffuser part is discussed as well. It will covered the basic model and parameter for PCB, scintillation index and flux variance. In order to succesfull the research, the Gaussian atmospheric channel analysis is utilized due to large signal photoelectron count considered.

CHAPTER 4

DEVELOPMENT OF DUAL DIFFUSER MODULATION TECHNIQUE (DDM) IN FSO SYSTEM

4.1 Introduction

In this chapter, it described the development of Dual Diffuser Modulation (DDM) technique. The model of this new modulation technique encircle the parts of light source, inverter, phase screen diffuser, photodetector and subtractor are discussed in Section 4.2. In order to analyze this new technique modulation, the comparison analysis between DDM technique and CIM/DD-OOK technique will be discussed in Section 4.4. There are four significant indicator performance will be exploited in the comparison analysis interm of signal power, threshold detection , signal to noise ratio and bit error rate.

4.2 Proposed System Model

The development of DDM which is based on modifying the CIM/DD-OOK consists of two parts. The first part is transmitter which can be listed three main components that are laser source, inverter data and phase screen diffuser. The second part is receiver which consists of two main components that are photodetector and subtractor.

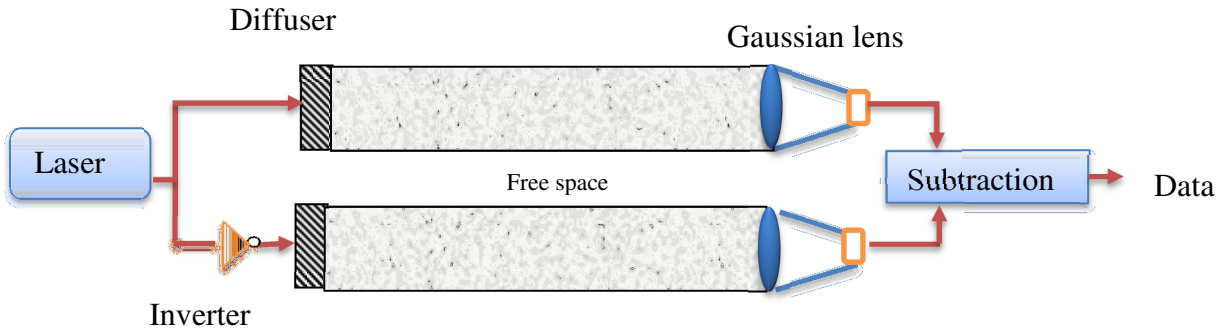

Figure 4.1: Proposed setup for Dual diffuser modulation (DDM) technique

Figure 4.1 shows the proposed setup of a new DDM technique. Generally, this new modulation technique employs two transmitters and two receivers. The first transmitter will send the original data and the second transmitter will send the complement of the original data. The both transmitters will mount the diffuser to create the new laser beam characteristic in order to combat with atmospheric turbulence effect on medium propagation. The laser source that uses the phase screen diffuser at the transmitter is well known as partially coherent beam and without phase screen diffuser usually recognized as a perfectly coherent beam. The inverter that using here is assume to be ideal inverter which considered no delay output or signal.

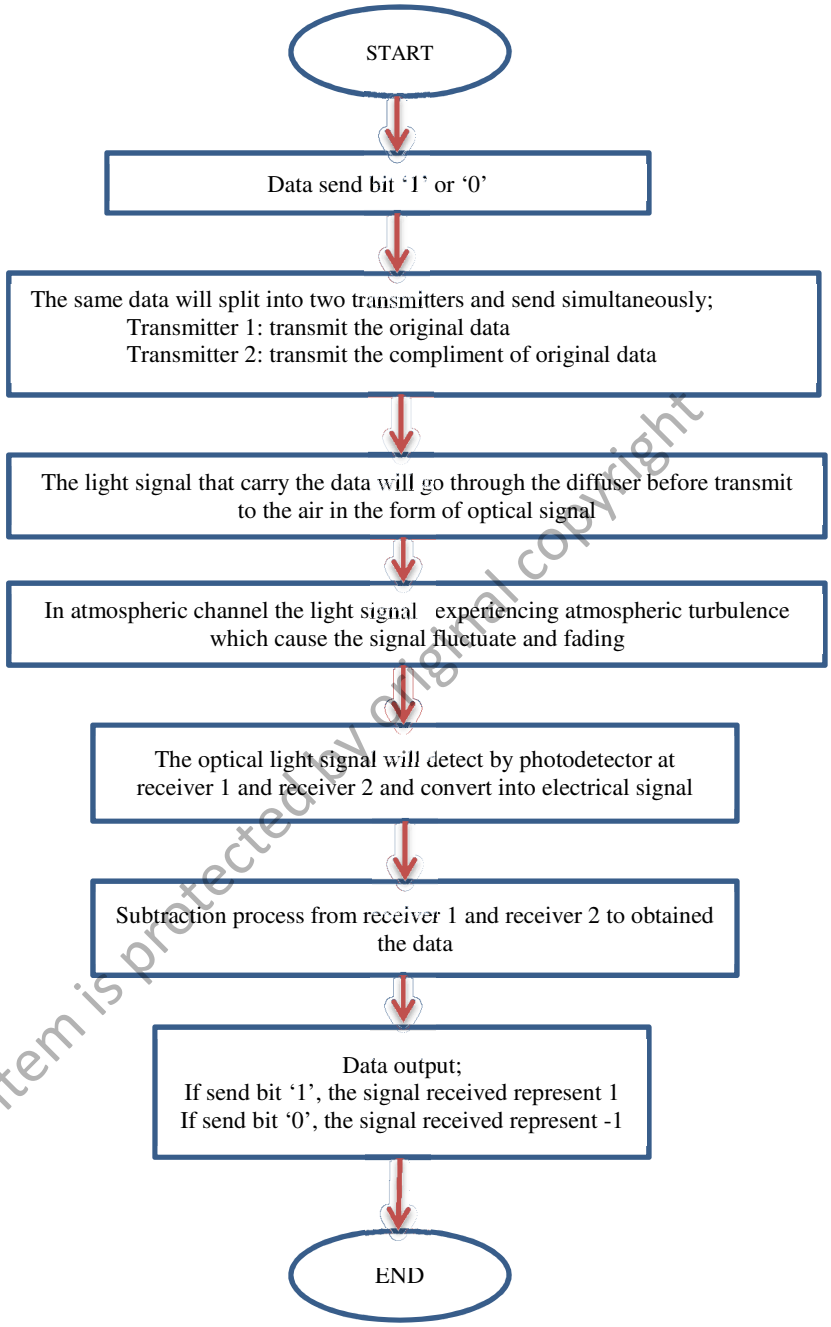

Figure 4.2: Flowchart of a new modulation technique of DDM

In receiver part, the received signal from the photodetctor 1 and photodetector 2 for original and compliment respectively will go through the subtraction process. The subtractor is assumed to be an ideal subtractor were no current losses when

implementing the subtraction signal. The flowchart for the DDM signal process can be seen in Figure 4.2.

4.2.1 Light Source

The modulated light source, which is typically a laser or light-emitting diode (LED), provides the transmitted optical signal and determines all the transmitter capabilities of the system. Only the detector sensitivity plays an equally important role in total system performance.

4.2.1.1 LED

Light-Emitting Diodes (LEDs) are semiconductor light-emitting structures. Due to their relatively low transmission power, LEDs are typically used in applications over shorter distances with moderate bandwidth requirements up to 155 Mbps. Depending on the material system, LEDs can operate in different wavelength ranges. When compared to narrowband or single wavelength laser transmission sources, LEDs have a much broader spectral range of operation. The Figure 4.3 shows the sample output of LED from the optical spectrum. The typical full width half maximum (FWHM) emission spectrum varies between 20 and 100 nm around the designed center wavelength of operation. Infrared LEDs are also used as transmission sources in household remote controls. The advantages of LED sources include their extremely long life and low cost. Recently the LED has been study as a light source in the airplane cabine for short distance FSO communication inside the aircraft. As the aircraft cabin presents the larger number of nodes to interconnect, free-space optical (FSO) communication appears to be

one of the best solutions for weight and power saving solutions. In addition FSO communication systems provide safer operation than radio frequency solutions as they do not interact or affect with the on board communication equipment. High throughput point to multipoint free-space optical links is presented hereafter. The conceptual architecture, main performances and limitations are described and compared with avionics requirements and standards.

4.2.1.2 Laser

In the common field of telecommunication, only lasers that are capable of being modulated at 20 Mbps to 2.5 Gbps can meet current marketplace demands. In addition, how the device is modulated and how much modulated power is produced are both important to the selection of a device. The sample output for laser shown in Figure 4.5.

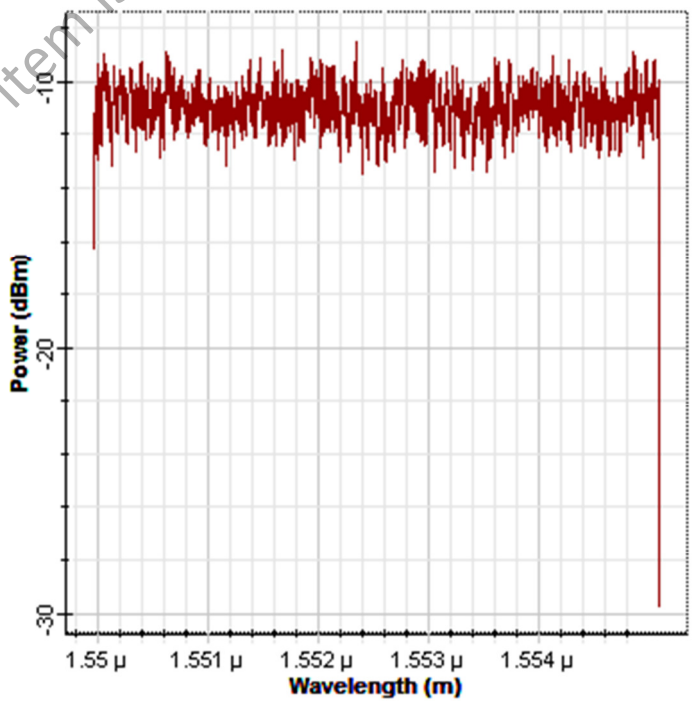

Figure 4.3: Power versus wavelength spectrum of LED

Among the familiar laser for range wavelength 850 nm to 1550nm

- The VCSEL 850nm wavelength is an outgrowth of fiber communications development and has many attractive features. VCSELs revolutionized the transmission component market because of their exceptional cost and performance advantages over previously available technology. Most notably, VCSELs have a reasonable, nominal average power level of several milliwatts of output at high-speed operation and high reliability numbers for MTBF. The average power, not the peak power, determines the link margin. Inasmuch as the 850nm VCSEL is cheaper than many of its alternatives, the 850-nm products dominate the low-price FSO systems because operation speeds are generally below 1 Gbps for off-the-shelf systems. Because of their high efficiency, power dissipation is typically not an issue for VCSELs, and active cooling is not required. In addition, VCSELs emit light in the form of a circular beam instead of an elliptical beam. The round shape of the beam pattern perfectly matches the round core of an optical fiber, facilitating the coupling process and improving coupling efficiency. The success of VCSEL technology has been so tremendous that many VCSEL manufacturers can produce shorter-wavelength 850 nm laser structures with direct modulation speeds beyond 3 Gbps (S. Bloom, E. Korevaar, J. Schuster, & H. Willebrand (2003).

- Fabry–Perot (FP) and Distributed-Feedback Lasers (DFB) lasers based on InGaAs/InP semiconductor technology with operating wavelengths around 1550 nm were developed specifically for fiber optic communications systems because of the low attenuation characteristics of optical fiber in this wavelength range.

With the development of these lower-power laser sources came high modulation speed, wavelength stability, reliability, and long life spans. Today's lower-power 1550 nm DFB lasers have demonstrated excellent lifetime performance that satisfies the stringent requirements of the telecommunications industry. DFB lasers can drive fiber networks capable of 1–40 Gbps of modulation under highly controlled environmental conditions (S. Bloom, E. Korevaar, J. Schuster, & H. Willebrand (2003).

In this thesis, we choose the continuous wave laser (CW) as show in Figure 4.4 with a wavelength selection at 1550nm for the case research study. This is because at 1550nm wavelength the FSO systems should able to:

a) Operate at higher power levels which is important for longer-distance FSO systems
b) Support the high-speed modulation in FSO systems
c) Produce small footprint and low power consumption
d) Can operate over a wide temperature range without major performance degradation especially for outdoor systems

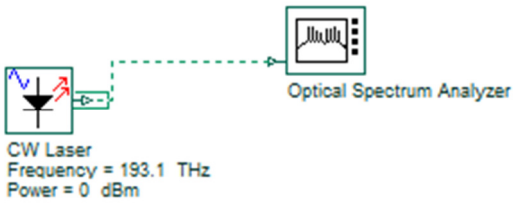

Figure 4.4: Continuous Wave (CW) laser configuration

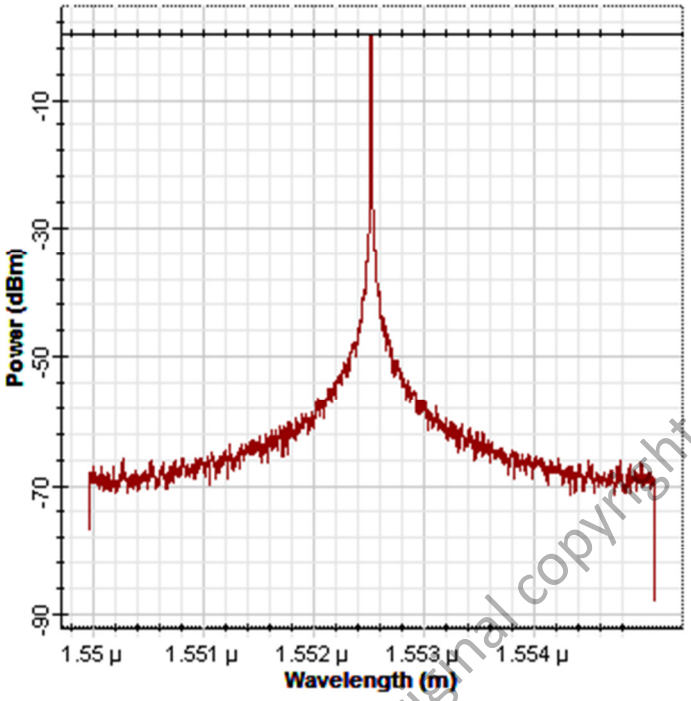

Figure 4.5: Power versus wavelength spectrum of laser

4.2.2 Inverter

The inverter can be defined as a logic gate that converts the input to the opposite state for output. If the input is true, the output is false, and vice versa. An inverter performs the Boolean logic NOT operation. In FSO communication system, the inverter converts the output electrical signal from the pulse generator before via the modulator as show in Figure 4.6. The inverter that employs in DDM technique is assume an ideal inverter where no output delay will produce.

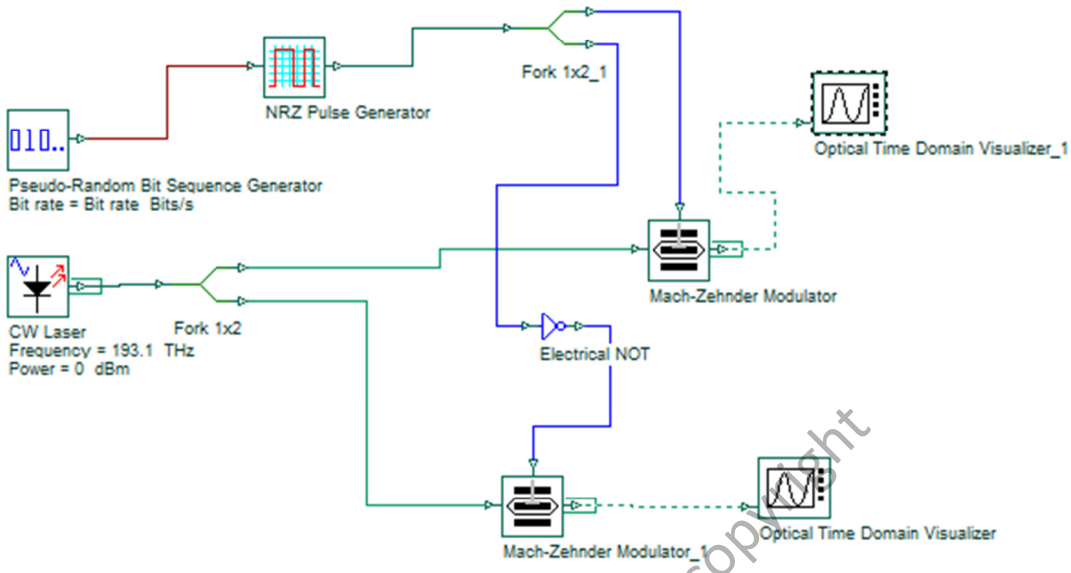

Figure 4.6: Inverter configuration in DDM technique

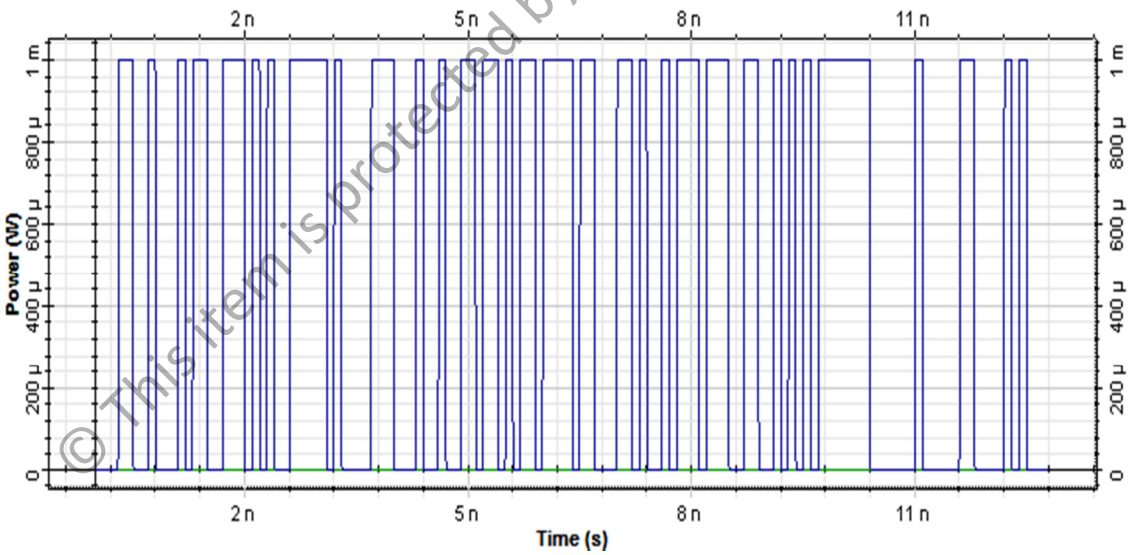

Figure 4.7: Output optical domain for original data without inverter effect

The Figure 4.7 and Figure 4.8 shows the output signal for condition with and without inverter effect respectively.

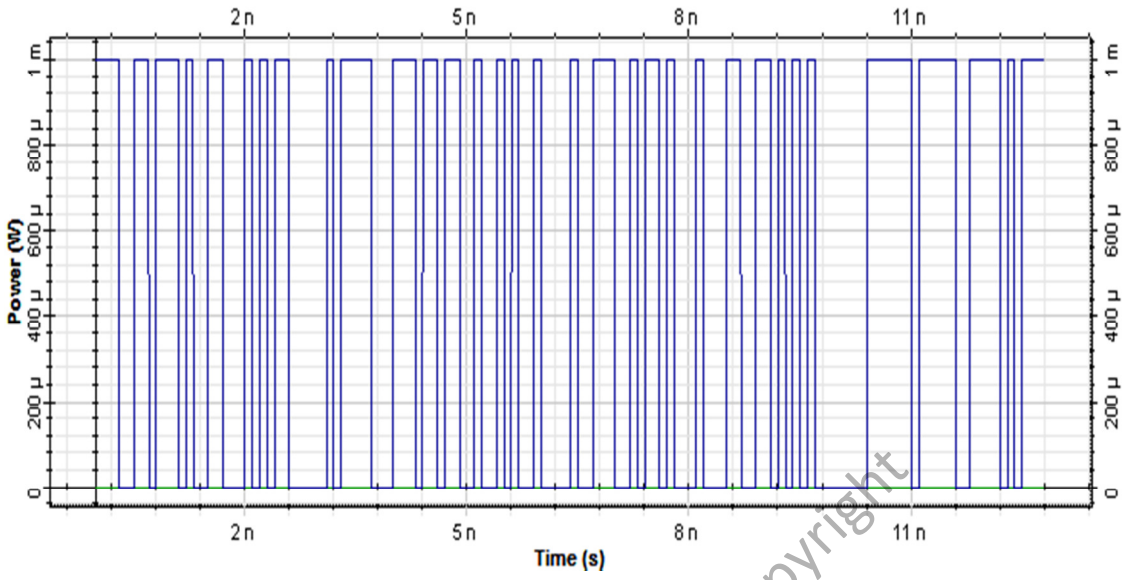

Figure 4.8: Output optical domain for compliment of original data with inverter effect

4.2.3 Random Phase screen diffuser

The diffuser that is placed at the laser exit is to create the partially coherent beam in order to reduce the scintillation effect. This section discusses details in partially coherent beam at Section 3.6 in Chapter 3.

4.2.4 Photodetector

Basically made of semiconductor is either photo resistances or current or voltage generators. When the photodetector in illuminated state, the value of resistance, the current or the voltage depends on the incident radiant power. In FSO system application, the photodetectors received images of the near fields of the transmitter after propagation along trajectories, optical beams through the atmosphere and some optics elements (Sorensen, 1979). Generally the photodetector consist of two types PIN photodetector and APD photodetector. In this thesis, we only consider the PIN

photodetector as shown in Figure 4.9 where for the new DDM technique setup is placed at both receivers.

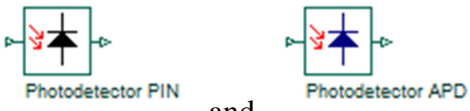

(a) and (b)

Figure 4.9: PIN and APD photodetector component

The PIN photodiode consists of '*p*' and '*n*' regions separated by a very lightly n-doped intrinsic i region. In normal operation, a sufficient reverse bias voltage is applied across the device so that the intrinsic region is fully depleted. When an incident photon has energy greater than the bandgap energy of the material, the photon can give up its energy and excite an electron from the valence band to the conduction band. This generates free electron-hole pairs called photocarriers. The PIN photodetector is designed so that these photocarriers are generated mainly in the depleted region, where most of the incident light is absorbed (A. Nordbotten (2000). The high electric field present in the depletion region causes the photocarriers to separate and be collected across the reversed-bias junction. This produces a current flow in an external circuit, with one electron flowing for every photocarrier generated. The current flow is known as photocurrent.

The Avalanche Photodiode (APD) internally multiplies the primary signal photocurrent before it enters the input circuitry of the following amplifier. This increases the receiver sensitivity, since the photocurrent is multiplied before encountering the thermal noise associated with the receiver circuit. In this structure, photocarriers are created initially mostly in the lightly p-doped intrinsic layer called *a p*

-layer, because the *n*+-*p* junction is very thin. When there is sufficient voltage across the p -layer, the photocarriers can drift rapidly across it. Therefore, at the *n*+-*p* junction near the positive electrode, a large field gradient is created and efficient avalanche multiplication occurs. The avalanche mechanism is a is also a function of the bias voltage. For practical applications, Si APD is operated typically with M =100. The reverse bias voltage ranges from 10 to 100 V. If the bias voltage is too high, the photodiode may be in danger of creating self-sustaining avalanche current without photoexcitation, leading to extra noise from the photodiode (A. Nordbotten (2000).

Since an APD has much larger gain, it offers a better sensitivity than pin photodiode. The sensitivity increase may be on the order of 4 to 7 dB. However, they also have serious drawbacks, such as: a high operating voltage is required to provide a strong electric field, there is a strong temperature dependent of the multiplication factor, and there is additional noise due to saturation effects at high radiation levels (A. Nordbotten (2000). Although these problems can be addressed and compensated, cost is increased. In contrast, a pin photodiode followed by an electronic amplifier could also provide good sensitivity margin with the expense of slower response time. For data transmission below one gigabit per second, the configuration of a pin photodetector and electronic amplifier may be advantageous over APD because of its low cost.

4.2.5 Subtractor

An electrical subtractor is a function to subtract the electrical signal from the output photodetector 1 and photodetector 2 which is illustrated in Figure 4.10. Here we assume the ideal electrical subtractor where no current loss during the subtraction process and also to simplify the calculation.

$$P_0 = (P_1) - (P_2) \tag{4.1}$$

where the output from the subtractor is in electrical signal form. Consequently the signal output of DDM technique results the double magnitude of power at receiver as shows in Figure 4.11.

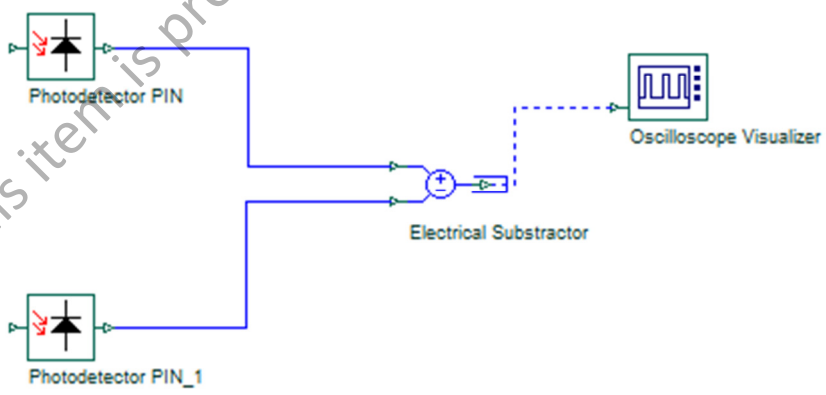

Figure 4.10: Electrical subtractor configuration in DDM technique

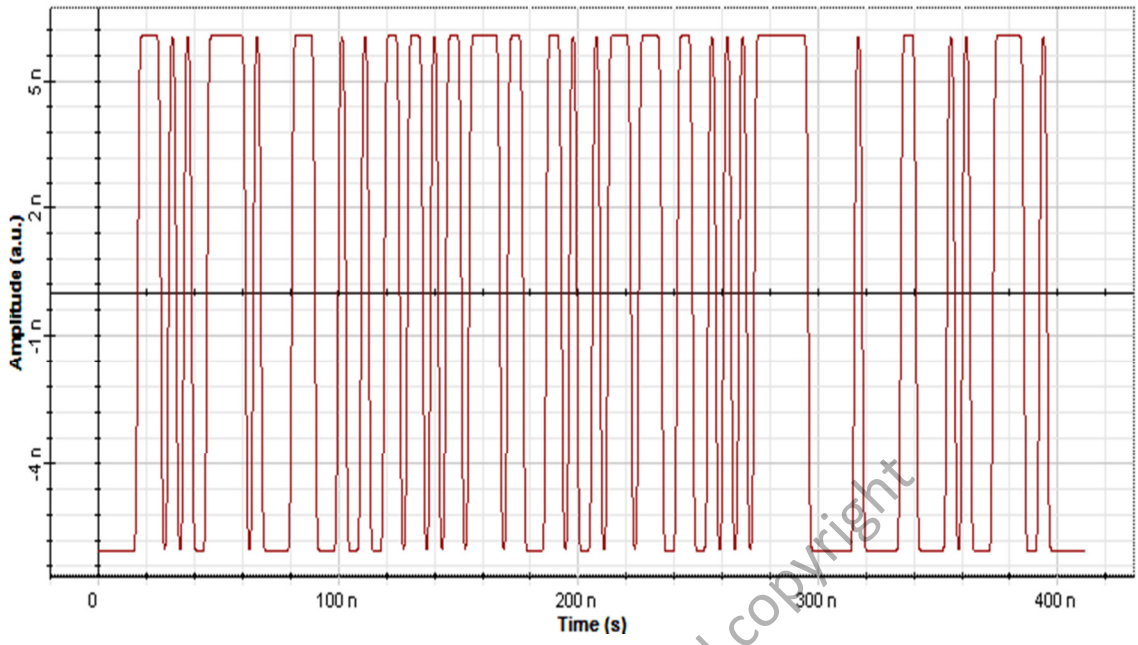

Figure 4.11: Sample output for DDM technique via the subtraction process

In Figure 4.11 show the increment of the amplitude level as compared with conventional OOK signaling in Figure 4.7 and Figure 4.8. Now, every bit of data has the full cycle wave pattern from 1 to -1 for bit '1' and bit '0'. The next chapter will discuss in detail the analytical performance of DDM and compare with CIM/DD-OOK.

4.3 Comparison performance between Dual Diffuser Modulation and Conventional Intensity Modulation/Direct Detection for On Off Keying technique

The comparison analytical involves the signal power, threshold detection, SNR and BER for case absence of turbulence. Then, the performance will compare with the conventional modulation (CIM/DD-OOK). The Table 4.1 shows the parameters that use to calculate the comparison modulation.

Table 4.1: Parameters for modulation comparison performance

Parameters	Symbols	Value
Wavelength	λ	1550 nm
Distance	L	2000 m
Electron charge	e	1.6 x 10^{-19} C
Plank constant	h	6.6 x 10^{-34} J.s
Speed of light	c	3 x 10^{8} Km/s
Photodetector efficiency	η	0.7
Power transmitt	P_o	0 dBm
Receiver aperture diameter	l_c	0.1
Radius of curvature	F_o	∞
Spot beam at transmitter (z=0)	W_o	0.025 m

4.3.1 Signal power

The intensity of the optical beam can be defined as the square amplitude of the optical field (Andrews, L. C., 1998). When considering the radial distance r from the optical axis, the intensity can be written as

$$I^{o}(r, L) = I_{o}\left[\frac{W_{o}}{W(L)}\right]^{2} \exp\left[-\frac{2r^{2}}{W^{2}(L)}\right] \tag{4.2}$$

where the $I^{o} = (0,0)$ is the transmitter output intensity at the center line of the beam, $W(L)$ is beam spot radius and the superscript o denotes the intensity in a free space without the presence of turbulence. The relation between the intensity of the optical beam and the total power in the beam for the case $r = 0$ as expressed by (Saleh, B. E, 1991).

$$I^{o}(0, L) = I_{o}\frac{W^{2}_{o}}{W^{2}(L)} = \frac{2P_{o}}{\pi W^{2}(L)} \tag{4.3}$$

where P_o is the total power transmitted by the beam. The power P incident on the circular receiver lens of aperture diameter D situated at distance L then can be written as

$$P(D, L) = P_o\left[1 - \exp\left(-\frac{D^2}{2W^2(L)}\right)\right] \tag{4.4}$$

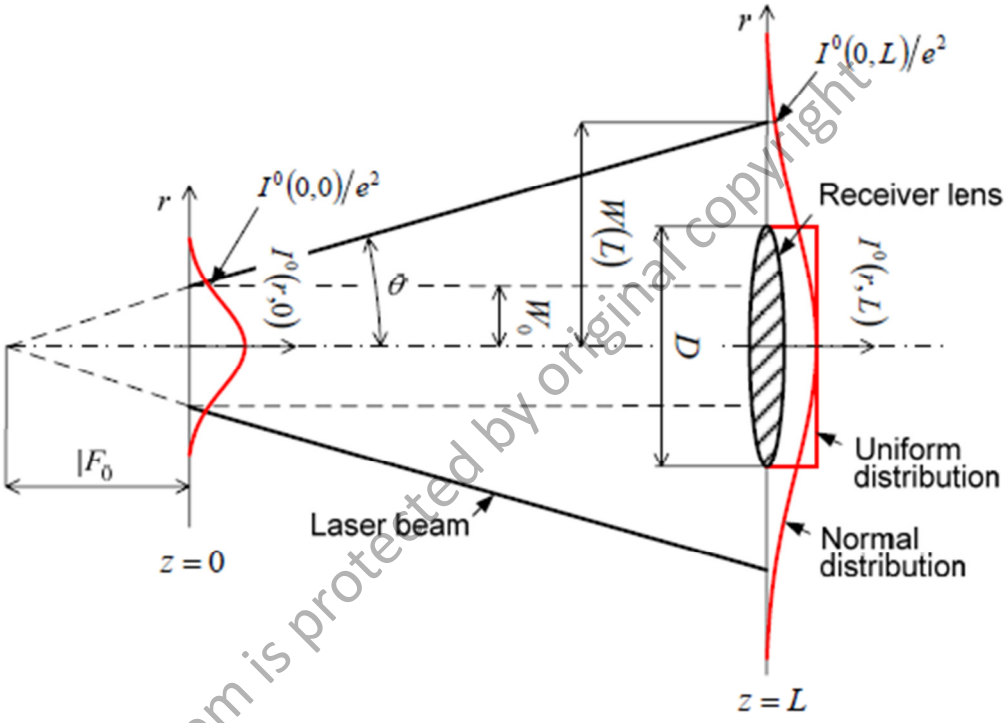

Figure 4.12: Basic parameter Gaussian beam of FSO (A. Prokes, 2009)

However in the real FSO situation, the large divergence angle will occur which normally varies from 1 *mrad* to 10 *mrad*. This will results the value for $kW_o^2/2F_o \gg 1$ and the divergence equation is reduced to $\theta = W_o/|F_o|$. Then the beam spot radius can be simplified and rewrite to become $W = W_o + (L\theta)$. Therefore the received optical power can be written as (A. Prokes, 2009).

$$P(D, L) = I^o(0, L)\frac{\pi D^2}{4} = \frac{D^2 P_o}{2(W_o + L\theta)^2} \tag{4.5}$$

Figure 4.11 illustrates the parameters of the basic Gaussian beam in real FSO condition with assume that the beam radius at the receiver position is much greater than the diameter of the receiver lens. For this case, the optical intensity at the lens can be categorized as uniformly distributed.

4.3.1.1 Conventional Intensity Modulation/Direct Detection –On Off Keying technique

The total signal power at the receiver for CIM/DD-OOK is described in SNR as

$$SNR_0 = \frac{Total\ signal\ power}{Total\ noises}$$

$$= \frac{i_s^2}{\sigma_N^2} \tag{4.6}$$

where (i_s^2) is total signal power and (σ_N^2) is the total signal noises.

$$i_s = \Re P_r \tag{4.7}$$

where the poor represent the power received and then $\Re$ represent the responsivity which can be written as

$$\Re = \frac{\eta e \lambda}{hc} \tag{4.8}$$

Respectively η is the detector quantum efficiency in electrons/photon; e is an electric charge in coulombs; λ is wavelength transmission, h is Plank's constant and c is the speed of light. Recall that free space propagation of a laser beam in the Gaussian model for intensity profile can be described as

$$P_r = \int_0^{2\pi} \int_0^{\infty} I(O,L) r dr d\theta$$

$$= \Re(\frac{\pi D^2}{8} I(0,L)) \quad (4.9)$$

where $I(0,L)$ can be obtained in Equation 4.3.

4.3.1.2 Dual Diffuser Modulation technique

The total signal power at the receiver for DDM after through the subtraction process at the receiver can described as

$$i_s = i_{s1} - i_{s2}$$

$$= i_{s1} - (-\overline{i_{s1}}) \quad (4.10)$$

where i_{s2} is complimentary of i_{s1}

Recall that free space propagation of a laser beam in the Gaussian model for intensity profile as described as

$$P_r = \int_0^{2\pi} \int_0^{\infty} I(O,L) r dr d\theta \quad (4.11)$$

Therefore,

$$i_s = \Re \int_0^{2\pi} \int_0^{\infty} I(O,L) r dr d\theta - (-\Re \int_0^{2\pi} \int_0^{\infty} I(O,L) r dr d\theta))$$

$$= \Re(\frac{\pi D^2}{8} I(0,L)) - (-\Re(\frac{\pi D^2}{8} I(0,L))$$

$$= 2\Re(\frac{\pi D^2}{8} I(0,L)) \quad (4.12)$$

Thus the total signal power of DDM can be written as,

$$i_s = 2\Re P_r \quad (4.13)$$

The Figure 4.13 shows the corresponding of the total signal power over propagation distance in no presence of turbulence. From the graphs, the signal power under diffuser effect experiencing decline condition due to diffractional beam as show curve CIM/DD-OOK+Diffuser. Nevertheless, DDM technique has a better signal power due to double magnitude power yield after subtracting process as shown in Equation 4.12. When the presence of turbulence, the intensity of signal begins to unstable and diffuser help to reduce the scintillation index which can produce better signal power. The Figure 4.14 and Figure 4.15 present the intensity signal power when experiencing the turbulence effect.

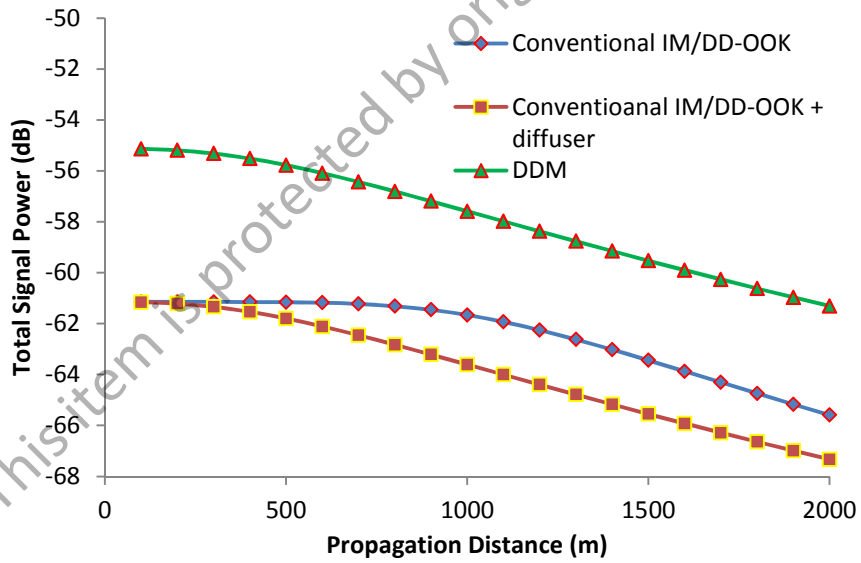

Figure 4.13: Performance of total signal power versus propagation distance in without presence of turbulence

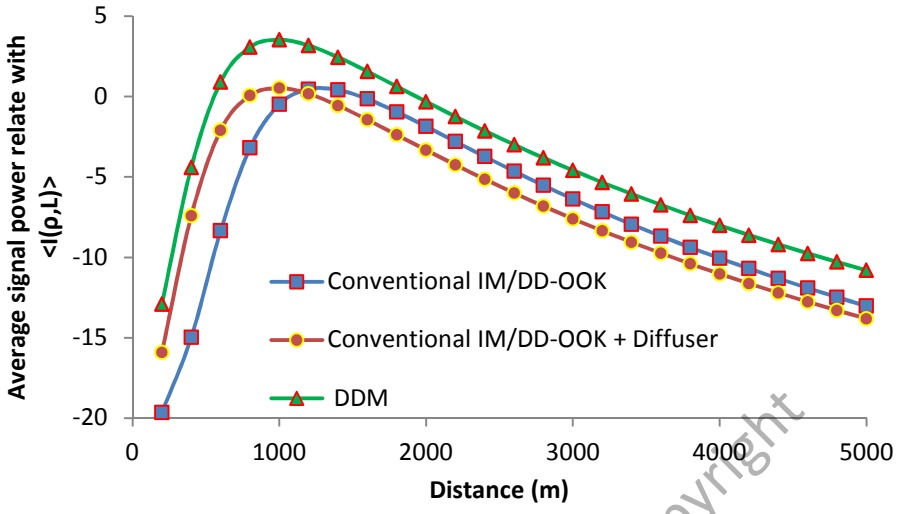

Figure 4.14: Performance of mean intensity signal versus distance under strong turbulence

The Figure 4.14 shows the mean intensity signal power correspond to propagation distance for strong turbulence From the graphs, the DDM increase the mean intensity signal if compare with the CIM/DD-OOK and CIM/DD-OOK+diffuser. However, all the performances of mean intensity decrease as the propagation distance increases.

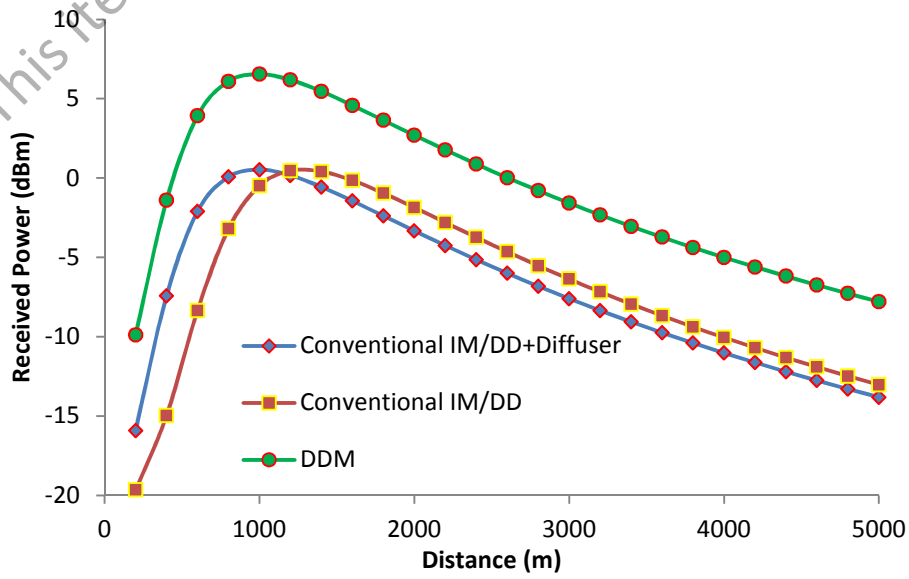

Figure 4.15: Performance of receiving power versus distance under strong turbulence

Meanwhile in the Figure 4.15 shows the power received versus the distance corresponds to mean intensity signal. The curve graphs are generated by using Equation 4.3 and Equation 4.9. As we can see the DDM improves the power received if compare to conventional modulation.

4.3.2 Threshold detection in DDM technique

In receiver part, the threshold detection signal can be illustrated in Figure 4.16. The received signal from the photodetector 1 and photodetector 2 respectively are fed into subtractor. We also assume that the receive signal is perfectly synchronous detect at receiver with no delay condition.

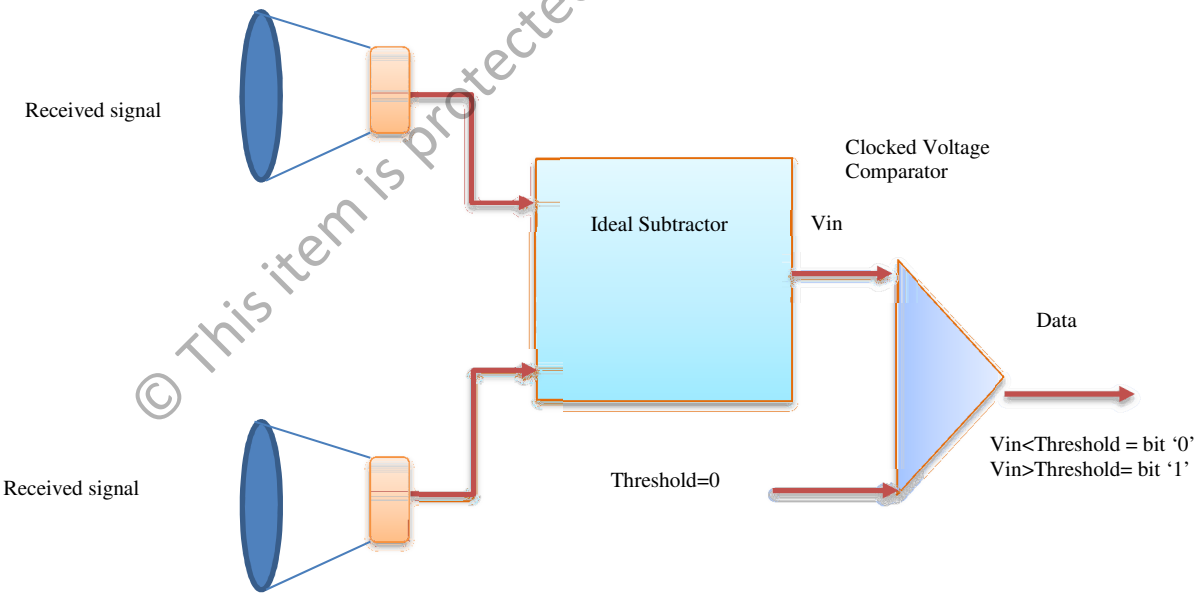

Figure 4.16: Threshold detection for new DDM technique

In the CIM/DD-OOK technique it is assumed that the channel is a zero-mean wide-sense stationary Gaussian process and that the receiver processing circuits, except for the threshold device, are linear. Meanwhile for the case linear-processing receiver circuit with a binary signal plus noise at the input, the sample output can be denoted as

$$r_o = x_o + n_o \tag{4.14}$$

where r_o is the received signal, x_o is a signal being sent whether bit '1' or '0' and n_o is represent Addictive White Gaussian Noise (AWGN) with zero mean Gaussian random variable ($\mu = 0, \sigma_N^2 = \frac{N}{2}$).

Nevertheless, the received signal for DDM technique from photodetector 1 and photodetetor 2 respectively as shown in Figure 4.16 which can be denoted as:

$$r_1 = x_1 + n_1 \tag{4.15}$$

and

$$r_2 = x_2 + n_2 = \overline{s_1} + n_2 \tag{4.16}$$

where $s_2 = \overline{s_1}$ which $\overline{s_1}$ mean complements of s_1 , the x_1 and x_2 are the signal transmitted and n_1 and n_2 are zero mean Gaussian random variable. r_o is an output signal after via the subtraction. The output after subtraction can be derived as:

$$r_o = r_1 + r_2 \tag{4.17}$$

Substitute the Equation 4.15 and Equation 4.16 into Equation 4.17 will produce the output $r_o = (x_1 + n_1) - (\overline{x_1} + n_2)$

$$r_o = x_1 - \overline{x_1} + n_1 - n_2$$

$$r_o = x + n \tag{4.18}$$

where the $x = x_1 - \overline{x_1}$ and $n = n_1 - n_2$

The overall process of binary detection for DDM technique can be denoted in Table 4.2.

Table 4.2: Binary detection for DDM technique at receiver

Transmitter (T_X)		FSO CHALLENGES	Receiver (R_X)		Subtraction process	
Sending bit			Received bit		R_{X1}-R_{X2}	
T_X1	1	Atmospheric turbulence	R_X1	1	Bit '1'	1
	0			0		
T_X2 (Compliment)	0		R_X2	0	Bit '0'	-1
	1			1		

The received signal is a polar signaling format which is also known as anti-podal signal. Since n_1 and n_2 are Gaussian RV with zero mean and variance σ_o^2 then n should be a Gaussian RV as well with zero mean and variance will become $2\sigma_o^2$ for this technique.

4.3.3 SNR in absence of turbulence

4.3.3.1 Conventional Intensity Modulation/Direct Detection –On Off Keying technique

The output SNR in the absence of optical turbulence can be defined as the ratio signal power (i_s^2) over the presence of signal noises (σ_N^2) as show in Equation 4.6. Meanwhile for the total noise power (σ_N^2), we only consider the shot noise and thermal noise for the simplicity calculation purpose.

$$\sigma_N^2 = i_{shot}^2 + i_{thermal}^2 \tag{4.19}$$

The shot noise for CIM/DD-OOK can be rewritten,

$$i_{shot}^2 = 2e(i_s)B$$
$$= 2e(\Re P_r)B$$
$$= 2e\Re((\frac{\pi D^2}{8})(\frac{2P_o}{\pi W^2(L)}))B, \quad (4.20)$$

and for the thermal noise,

$$i_{thermal}^2 = \frac{4k_bT_nB}{R_L} \quad (4.21)$$

The SNR in absence of turbulence without diffuser effect can be written as,

$$SNR_o = \frac{\Re^2((\frac{\pi D^2}{8})(\frac{2P_o}{\pi W^2(L)}))^2}{2e\Re\left(\left(\frac{\pi D^2}{8}\right)\left(\frac{2P_o}{\pi W^2(L)}\right)\right)B+\frac{4k_bT_nB}{R_L}} \quad (4.22)$$

4.3.3.2 Dual Diffuser Modulation technique

The shot noise for DDM can be re-written and become,

$$i_{shot}^2 = 2e(i_s)B$$
$$= 2e(2\Re P_r)B$$
$$= 4e\Re((\frac{\pi D^2}{8})(\frac{2P_o}{\pi W^2(L)}))B, \quad (4.23)$$

and for the thermal noise same as the Equation 4.21. The SNR in absence of turbulence without diffuser effect can be written as,

$$SNR_o = \frac{2^2\Re^2((\frac{\pi D^2}{8})(\frac{2P_o}{\pi W^2(L)}))^2}{4e\Re\left(\left(\frac{\pi D^2}{8}\right)\left(\frac{2P_o}{\pi W^2(L)}\right)\right)B+\frac{4k_bT_nB}{R_L}} \quad (4.24)$$

From the equation above we can obtain the SNR of DDM in absence of turbulence

$$SNRP_o = \frac{SNR_o}{\sqrt{PP_o/P_o}} \quad (4.25)$$

where PP_o is the received power partially coherent beam and P_o is the power of coherent beam. Therefore the SNR of DDM with the effect of the diffuser as shown in Equation 2.6.

$$SNRP_o = \frac{SNR_o}{\sqrt{1+q_c\Lambda_1}}$$

$$SNRP_o = \frac{\left(\frac{2^2\Re^2((\frac{\pi D^2}{8})(\frac{2P_o}{\pi W^2(L)}))^2}{4e\Re\left(\left(\frac{\pi D^2}{8}\right)\left(\frac{2P_o}{\pi W^2(L)}\right)\right)B+\frac{4k_bT_nB}{R_L}}\right)}{\sqrt{1+q_c\Lambda_1}} \quad (4.26)$$

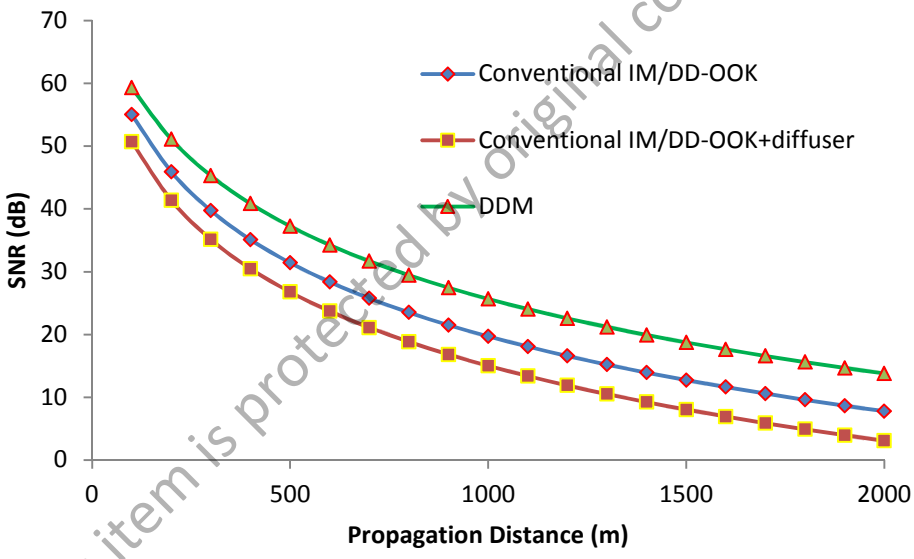

Figure 4.17: Performance of SNR versus propagation distance without presence of turbulence

The Figure 4.17 shows the comparison of SNR corresponding with propagation distance without the presence of turbulence. As discussed in Section 4.3.1, the lowest SNR is produced by CIM/DD-OOK+Diffuser due to decreasing of signal power. This condition will change when involve the turbulence effect. The Figure 4.18 shows the performance of SNR against the propagation distance with the presence of turbulence. In this condition, the reduction of the scintillation index as indicated in Equation 5.8 resulting the increasing of mean SNR but from the both Figure 4.17 and Figure 4.18

shows the DDM outperform CIM/DD-OOK and CIM/DD-OOK+Diffuser.

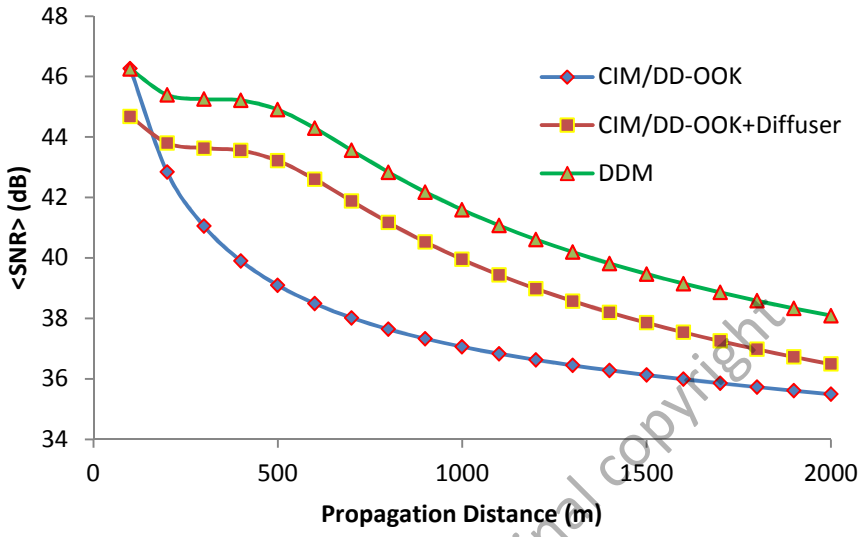

Figure 4.18: Performance of SNR versus propagation distance with presence of turbulence

4.3.4 Bit Error Rate (BER)

In digital transmission, the number of bit errors can be defined as the number of received bits of a data stream over a communication channel that have been altered due to noise, interference, distortion or bit synchronization errors. Meanwhile the bit error rate or bit error ratio (BER) is the number of bit errors divided by the total number of transferred bits during a studied time interval. BER is a unitless performance measure, often expressed as a percentage. However for the bit error probability p_e, can be described as the expectation value of the BER. The BER can be considered as an approximate estimate of the bit error probability. This estimate is accurate for a long time interval and a high number of bit errors.

The general expression for the bit error probability of any binary communication is given (Cough, 2001).

$$P_e = P(1) \int_{-\infty}^{V_T} P(0|1)dI + P(0) \int_{V_T}^{\infty} P(1|0)dI \quad (4.27)$$

Therefore the BER characteristic can be is defined as

1) Ratio of the number of wrong bits over the number of total bits
2) Probability of error is the theoretically predicted expected BER.
3) The more the signal is affected, the more bits are incorrect.
4) The BER is the fundamental specification of the performance requirement of a digital communication system
5) It is an important concept to understand in any digital transmission system since it is a major indicator of the health of the system.

4.3.4.1 Conventional Intensity Modulation/Direct Detection –On Off Keying technique

The conventional OOK are using the bit '1' and '0' to indicate the signal data. Therefore, it will involve two possibility the incoming signal whether decide signal '1' or signal '0'. Assuming a Gaussian additive noise the probability of the received signal, x conditioned '0' and '1' are as follows:

- μ_1 = mean of x when bit '1' is transmitted
- μ_0 = mean of x when bit '0' is transmitted
- σ_1^2 = variance of x when bit '1' is transmitted
- σ_0^2 = variance of x when bit '0' is transmitted

In order to determine the bit '1' and bit '0', it need the threshold to deceide. The rule is:

a) If x > "Threshold", will choose bit '1' was sent

b) If x < "Threshold", will choose the bit '0' was sent

Thus the two conditional probability density function (PDF) for CIM/DD-OOK can be written as

$$P(0|1) = \frac{1}{\sigma_1\sqrt{2\pi}} \int_{-\infty}^{I_D} exp\left(-\frac{(I-I_1)^2}{2\sigma_1^2}\right) dI = \frac{1}{2} erfc\left(\frac{I_1-I_D}{\sigma_1\sqrt{2}}\right) \quad (4.28)$$

$$P(1|0) = \frac{1}{\sigma_0\sqrt{2\pi}} \int_{I_D}^{\infty} exp\left(-\frac{(I-I_0)^2}{2\sigma_1^2}\right) dI = \frac{1}{2} erfc\left(\frac{I_D-I_o}{\sigma_0\sqrt{2}}\right) \quad (4.29)$$

where complementary error function $erfc\ (x) = \frac{2}{\sqrt{\pi}} \int_x^{\infty} exp(-y^2) dy$ and I_D is the threshold value.

The P(0|1) is represent the conditional error of the system will occur if the receiver decided the incoming signal as '0' but indeed the transmitter sent the bit '1'. Meanwhile for P(1|0) is indicate that the receiver decide the incoming signal as bit '1' but indeed the transmitter sent the bit '0'. Therefore BER can be written as

$$BER = \frac{1}{4}\left[erfc\left(\frac{I_1-I_D}{\sigma_1\sqrt{2}}\right) + erfc\left(\frac{I_D-I_o}{\sigma_0\sqrt{2}}\right)\right] = \frac{1}{2} erfc\left(\frac{Q}{\sqrt{2}}\right) = \frac{1}{2} erfc\left(\sqrt{\frac{SNR}{2}}\right) \quad (4.30)$$

where the Q(x) is Gaussian Q-function with $Q(x) = \frac{1}{\sqrt{2\pi}} \int_x^{\infty} e^{-(\frac{t^2}{2})} dt$

4.3.4.1 Dual Diffuser Modulation technique

As show in Table 4.2, the DDM technique still utilize the basic bit same as conventional OOK signaling that are bit '1' and bit '0' but the expected received signal is change. If transmitter sent bit '1' the receiver should received signal '1' and if the

transmitter sent bit '0' the receiver should received signal '-1'. This condition can recognized as bipolar signaling. Now, the two conditional PDF for DDM technique can be written as

$$P(0|1) = \frac{1}{\sigma_1 2\sqrt{2\pi}}\, e^{-\frac{(I-I_1)^2}{4\sigma_1^2}} \tag{4.31}$$

$$P(1|0) = \frac{1}{\sigma_0 2\sqrt{2\pi}}\, e^{-\frac{(I-I_0)^2}{4\sigma_1^2}} \tag{4.32}$$

By considering equally likely condition, we obtain the BER in absence atmospheric turbulence

$$P(0|1) = P(1|0) = Q\left(\sqrt{\frac{2E_b}{N_o}}\right) \cong \frac{1}{2} erfc\left(\sqrt{\frac{E_b}{N_o}}\right) = \frac{1}{2} erfc\left(\sqrt{SNR}\right) \tag{4.33}$$

Interms of E_b and N_o and $\frac{E_b}{N_o} = SNR_o$ can be obtained in Equation 4.22.

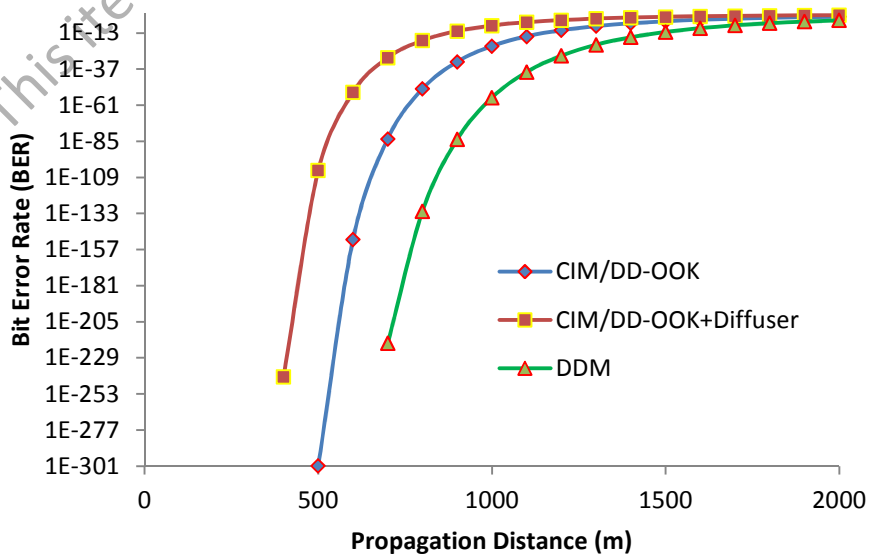

Figure 4.19: Performance of BER versus the propagation distance without the presence of turbulence

The Figure 4.19 shows the comparison BER performance against the propagation distance without the presence of turbulence. The DDM shows the better BER results with outperform CIM/DD-OOK and CIM/DD-OOK+Diffuser. This is because of the effectiveness threshold detection as discussed in Section 4.3.2. In addition, the SNR of DDM which is discussed in Section 4.3.3 produce better result yielding the improvement of conventional modulation technique. The Table 4.3 shows the summary of comparison modulation performance interm of signal power, bit detection, SNR and BER.

Table 4.3: Comparative performance between DDM and CIM/DD-OOK technique

	CIM/DD-OOK	DDM
Signal Power	$i_s = \Re(\frac{\pi D^2}{8} I(0,L))$	$i_s = 2\Re(\frac{\pi D^2}{8} I(0,L))$
Bit detection	Bit '1' = 1 Bit '0' = 0	Bit '1' = 1 Bit '0' = -1
SNR	$\frac{\Re^2((\frac{\pi D^2}{8})(\frac{2P_o}{\pi W^2(L)}))^2}{2e\Re\left(\left(\frac{\pi D^2}{8}\right)\left(\frac{2P_o}{\pi W^2(L)}\right)\right)B + \frac{4k_b}{R}}$	$\frac{\left(\frac{2^2\Re^2((\frac{\pi D^2}{8})(\frac{2P_o}{\pi W^2(L)}))^2}{4e\Re\left(\left(\frac{\pi D^2}{8}\right)\left(\frac{2P_o}{\pi W^2(L)}\right)\right)B + \frac{4k_b T_n B}{R_L}}\right)}{\sqrt{1+q_c\Lambda_1}}$
BER	$\frac{1}{2}erfc\left(\sqrt{\frac{SNR}{2}}\right)$	$\frac{1}{2}erfc\left(\sqrt{SNR}\right)$

4.4 Summary

In this chapter, the development of DDM technique have been discussed with combination of conventional OOK signaling technique and PCB technique. Generally, the DDM technique utilize two transmitters and two receivers. At transmitter, one of source signal will be inverted and both transmitter will via the diffuser to create 'new' beam propagation. This will increase the quality FSO signal when experiencing the atmospheric turbulence effect. Meanwhile at receiver, the subtractor will be equipped which change the behavior signal received similar to bipolar signaling that involve '1' and '-1'. In this chapter also discuss the comparison performance between CIM/DD-OOK and DDM technique with consider four area of performances that are signal power, threshold signal level, signal to noise ratio and bit error rate. The comparison mathematical derivation can be view in Table 4.2. For the performance of both CIM/DD-OOK and DDM technique in the presence of atmospheric turbulence is discussed more detail in next Chapter 5 that encompass theoretical and simulation performance.

CHAPTER 5

PERFORMANCE OF DUAL DIFFUSER MODULATION IN FSO THROUGH THE ATMOSPHERIC TURBULENCE CHANNELS

5.1 Introduction

In this chapter, we study the performance of DDM under atmospheric turbulence condition. The mathematical derivation for signal to noise ratio (SNR) and bit error rate (BER) will be discussed with considering absence and presence of turbulence. The performance of DDM is represented via two methods. The first method is theoretical result which generates from the derivation SNR and BER. The second method is the simulation result by using the Optisystem software tool.

5.2 Atmospheric Turbulence Model

The past report show that there are several turbulence model that has been used in FSO study relate to atmospheric channel research for communication. The log-normal model is most commonly reported model for describing the atmospheric turbulence induced scintillation (S. Karp, 1988; Osche, 2002; S. Karp, 1970; Goodman, 1985). This model is valid only in weak atmospheric turbulence and as the strength of turbulence increases, multiple scattering effects, not accounted for by the log-normal model, must be taken into account. Beyond the weak turbulence regime, the gamma-gamma and negative exponential models can be used for describing the signal fluctuation under a wide range of atmospheric turbulence conditions (S. Karp, 1988, M. Uysal , 2006; Andrews 2001 & 2005).

As discuss in Chapter 2, the atmospheric turbulence creates the thermal inhomogeneities along the path which lead to the fluctuations that yield from energy conversion of solar energy (L. Wasiczko, 2004). The process of turbulence begins with the solar power heats the atmosphere irregular with different cells. This produces the different temperatures and create the variations in the index of refraction of the atmosphere. As a result over the light source FSO, the fluctuations occur in the amplitude of the received optical signal (R. Iniguez *etl.*,(2007). The effects of atmospheric turbulence can be quantified by determining the scintillation index, which is related to the mean and standard deviation of the intensity distribution which can defined by (L. C. Andrews & R. L. Phillips, 1998)

$$\sigma_I^2 = \frac{\langle I^2\rangle - \langle I\rangle^2}{\langle I\rangle^2} = \frac{\langle I^2\rangle}{\langle I\rangle^2} - 1 \qquad (5.1)$$

Generally the atmospheric turbulence is divided into three main regimes which depend on the turbulence strength (S. Rasouli; 2006). Table 5.1 shows the categories atmospheric turbulence where basically varies from 10^{-15} to 10^{-13} $m^{-2/3}$.

Table 5.1: Categories turbulence strength (Cvijetic, N., Wilson, S.G., & Brandt-Pearce, M. 2007)

Atmospheric turbulence regime	Turbulence strength $C_n^2\, m^{-2/3}$
Weak	10^{-15}
Moderate	10^{-13}
Strong	10^{-12}

The performance of an FSO system with an atmospheric turbulence channel can be evaluated mathematically with knowledge of the probability density function (PDF) of the randomly fading intensity signal (E. Jakeman, 1980). There are several PDF models have been proposed to deal with more general intensity fluctuation conditions, such as: *K* distribution, log normal distribution, or gamma-gamma distribution (J.H. Churnside & S.F. Clifford, 1987; M.A. Al- Habash, L.C. Andrews & R.L. Phillips, 2001).

5.2.1 Log Normal Distribution

For the weak turbulence, the intensity is lognormally distributed. The probability density function (PDF) valid for $I > 0$ and can be written in (L. C. Andrews, R. L. Phillips, & C. Y. Hopen, 2001).

$$p(I) = \frac{1}{\sqrt{2\pi\sigma_I^2}} \frac{1}{I} \, exp\left\{-\frac{(ln(I/I_0)-E[l])^2}{2\sigma_l^2}\right\} \quad I \geq 0 \tag{5.2}$$

5.2.2 Gamma-Gamma Distribution

The Gamma Gamma Distribution is preferred for the weak to strong regime. It obtained by a modulation between the small-scale intensity *y* and the large-scale intensity *x* (L. C. Andrews, 2001):

$$I = xy \tag{5.3}$$

where *x* and *y* are assumed to be gamma distributed and statistically independent. A conditional PDF for the intensity is given by the small-scale intensity, which is assumed to have a fluctuating mean that is smeared, or modulated, by the distribution of the large-scale fluctuations. The unconditional PDF for the intensity is a doubly stochastic

process and is obtained by taking the expected value of the unconditional PDF, which results in the GG distribution (M. A. Al-Habash, 2001):

$$p_I(I) = \frac{2(\alpha\beta)^{(\alpha+\beta)/2}}{\Gamma(\alpha)\Gamma(\beta)} I^{\frac{(\alpha+\beta)}{2}-1} K_{\alpha-\beta}\left(2\sqrt{\alpha\beta I}\right) \text{ For I>0} \quad (5.4)$$

where I is the normalized intensity, $\Gamma_{(x)}$ is the gamma function, and $K_\mu(x)$ is the modified Bessel function of the second kind. $\alpha$and β are the parameters of the PDF, which represent the effective numbers of large and small scale scatterers, respectively. They are related to the scintillation index by calculating the second moment of the Gamma Gamma distributed intensity (L. C. Andrews, 2001; M. A. Al-Habash, 2001):

$$\langle I^2 \rangle = \left(1+\frac{1}{\alpha}\right)\left(1+\frac{1}{\beta}\right) \quad (5.5)$$

In this work, the PDF Gamma-Gamma is choose in the calculation. Appendix A and B show the example calculation of Gamma gamma probability density function and determine the value alpha and beta in MATLAB codes.

5.2.3 The Exponential Distribution

This PDF will use in case for the limit of strong intensity turbulence which usually the number of scattering is large (F. E. Goodwin, 1970; H. Hemmati, 2007). The exponential distribution sometime also known as a fully developed speckle regime. This saturation regime is obey the Rayleigh distribution that using the negative exponential statistic (G. R. Osche, (2002).).

$$p(I) = \frac{1}{I_o} exp\left(-\frac{I}{I_0}\right) \qquad I_0 > 0 \quad (5.6)$$

where $E[I] = I_0$ is the mean received intensity. The value of the scintillation index, $S.I$ = 1 when under this saturation regime.

$$\sigma^2_{flux}\left(L + L_f, \Omega_G\right) = \exp\left[\sigma^2_{\ln x}\left(L + L_f, \Omega_G\right) + \sigma^2_{\ln y}\left(L + L_f, \Omega_G\right)\right] - 1$$

5.3 Performance Analysis

The performance analysis will investigate the respond of the system when experiencing under the turbulence effect. There are two critical performance that can be analyzed that are signal to noise ratio and bit error rate. The SNR will measure the presence of noise over the signal and the BER will determine how many bit error can occur (Nistazakis,2009).

5.3.1 Signal to Noise Ratio (SNR)

In the presence of atmospheric turbulence, the received signal exhibits additional power losses (refraction, diffraction) and random turbulence fluctuations. The SNR will determine as a mean SNR. In this case it will consider the SNR without presence of turbulence and also the flux variance as shown in Equation 5.7. The mean SNR can be written as

$$\left\langle SNRP \right\rangle = \frac{SNR_0}{\sqrt{\left(\frac{Pso}{\left\langle Ps \right\rangle}\right) + \sigma^2_{flux}\left(L + L_f, \Omega_G\right) SNR_0^2}} \tag{5.7}$$

where the SNR_o and $\sigma^2_{flux(L+L_f,\Omega_G)}$ can be obtained in Equation 3.24 and Equation 4.24.

$$\langle SNRP \rangle = \frac{SNR_o}{\sqrt{1+q_c\Lambda_1+1.63\sigma_I^{12/5}\Lambda_1+\sigma^2_{flux}\left(L+L_f,\Omega_G\right)\mathrm{SNR}_0^2}} \tag{5.8}$$

where Pso is the signal power in the absence of atmospheric effects and $\sigma_I^2(L+L_f,\Omega_G)$ is the intensity flux variance on the photo detector. Angle bracket $\langle\ \rangle$ represents the mean. The power ratio $\frac{Pso}{\langle Ps \rangle}$ provides a measure of SNR deterioration caused by atmospheric induced beam spreading given by

$$\frac{Pso}{\langle Ps \rangle} = 1+1.63\sigma_R^{\frac{12}{5}}\Lambda_1 \tag{5.9}$$

5.3.2 Probability of Error, P_e

When determine the BER performance under the turbulence effect, it has to consider the whole probability of error. Since the signal of noise ratio using the mean value as shown in Equation 5.8, therefore it will involve the integeral of BER to obtain the mean of BER. The probability error of DDM performance in the presence of turbulence with using the Gamma-Gamma distribution can be written as:

$$\Pr(E) = \langle BER \rangle = \frac{1}{2}\int_0^\infty p_I(I)erfc\left(\sqrt{\left\langle \frac{E_b}{N_o} \right\rangle I}\right)dI \tag{5.10}$$

where $p_I(I)$ is a gamma-gamma distribution as shown in Equation (5.4) and the $\left\langle \frac{E_b}{N_o} \right\rangle = \langle SNRP \rangle$. When aperture averaging effects are considered, parameters α and β of the gamma-gamma PDF are defined as

$$\alpha = \frac{1}{\exp\left[\sigma_{\ln X}^2\left(L + L_f, \Omega_G\right)\right] - 1} \tag{5.11}$$

$$\beta = \frac{1}{\exp\left[\sigma_{\ln Y}^2\left(L + L_f, \Omega_G\right)\right] - 1} \tag{5.12}$$

where $\sigma_{\ln x}^2\left(L + L_f, \Omega_G\right)$ and $\sigma_{\ln y}^2\left(L + L_f, \Omega_G\right)$ are relate to large and small scale log intensity variances obtained in Equation 4.21 and Equation 4.23 respectively. The Appendix C shows the example calculation using the MATLAB code to obtain probability of error with some calculation value has been made early using excel. This because there is no simple mathemathical form for complex integral gamma gamma and error function as shown in Equation 5.10.

5.4 Theoretical Results

In this section, the theoretical analysis will focus on three main effect. The first is effect over power signal where to analyze how strong the signal when experiencing turbulence. The more strong signal the better signal quality. The second effect is analyze the bit error rate. Under the strong turbulence the BER can increase rapidly due to high scintillation index. Here it will measure the capability with and without diffuser effect. The low BER will indicate the better system performance. The last effect is propagation distance performance. This is one of crucial element in FSO communication that relate on range link. The more far FSO system can transmit the signal, it will give the advantage to the system to operate effectively at long range link. All the analysis performance will be compare between CIM/DD-OOK and DDM technique. In the analysis, the percentage of improvement will be used as well to indicate the improvement of the system. Percentage of improvement can be described as

$$\frac{Improvement\ value}{original\ value} \times 100\% \quad (5.13)$$

The Table 5.2 shows the typical parameters to evaluate the DDM under strong turbulence condition.

Table 5.2: Parameters for DDM technique performance under strong turbulence

Parameters	Symbols	Value
Wavelength	λ	1550 nm
Distance	L	2000 m
Electron charge	e	1.6×10^{-19} C
Plank constant	h	6.6×10^{-34} J.s
Speed of light	c	3×10^{8} Km/s
Photodetector efficiency	η	0.7
Power transmitt	P_o	0 dBm
Diffuser strength	l_c	0.001
Collecting lens	W_G	0.01 m
Radius of curvature	F_o	∞
Spot beam at transmitter (z=0)	W_o	0.025 m

5.4.1 Effective Power

By using the Equation 5.10 we calculate the effective power with target below the BER 10^{-9} at standard error free transmission. The Figure 5.1 shows the comparison performance between partially coherent beam with employ the OOK modulation and the DDM technique. Under the weak turbulence condition the effect of the diffuser is very effective. The dotted red line represents the common acceptable bit error transmission which is at 10^{-9}.

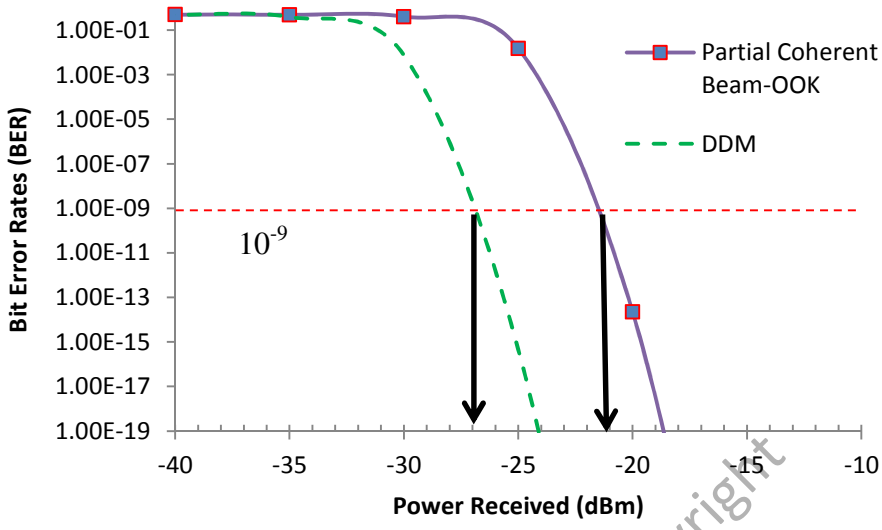

Figure 5.1: Effective power received under weak turbulence

For partially coherent beam, the received power at BER 10^{-9} is approximately -21dBm. However the received power of the DDM technique can improve to -27dBm. This is due to increasing of magnitude power of signal as show in Figure 4.11. This indicates the DDM technique is able to detect weak power at receiver and subsequently increase the receiver sensitivity.

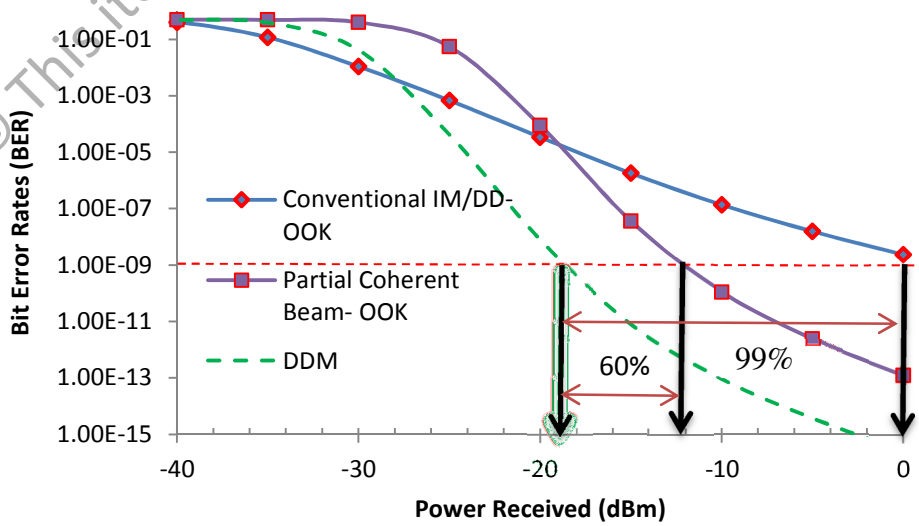

Figure 5.2: Effective power received under strong turbulence condition

However, under the strong turbulence, the fading signal is increased as shown in Figure 5.2. The comparative performance between CIM/DD-OOK, PCB-OOK and the DDM technique. As we can see, all the curve are below -20dBm at BER 10^{-9} due to the effect of strong turbulence condition. The worst performance is CIM/DD-OOK where the received power is approximately 0dBm meanwhile for and the DDM technique approximately -14dBm and -18dBm respectively. Therefore the DDM technique improves approximately about 99% and 60% percent with using Equation 5.13.

In Figure 5.3 shows the performance of various power transmits under strong turbulence. As notice in the graph, the CIM/DD-OOK require higher power than 5dBm to obtain the maximum error free transmission 10^{-9}. Meanwhile the DDM technique can operate under 0dBm. This indicates that the DDM only requires small power transmit to operate. As a result if small power transmitted the FSOC system eliminate the need of high power sources which mean reduce the cost and at the same time can maintain the high power received at the receiver. The gaps between the close performance of the DDM technique is approximately 98% if compare with partially coherent beam-OOK.

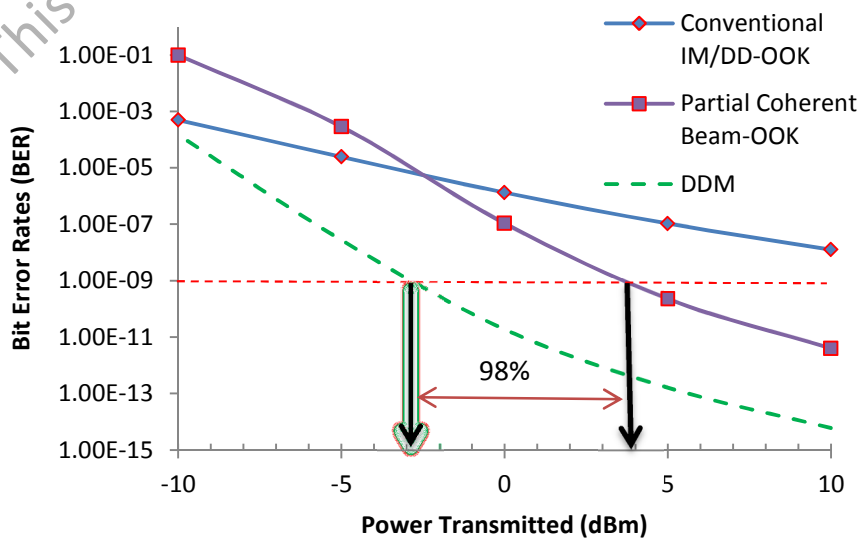

Figure 5.3: Minimum power requirement at transmitter for minimum acceptable BER 10^{-9}

In Figure 5.4 shows the performance of various diffuser strengths under strong turbulence condition. The coherent represent the FSO without the diffuser effect which is well known as fully coherent beam and incoherent shows the very strong diffuser is employed. Meanwhile for the diffuser effect the moderate diffuser is selected as value l_c = 0.01. As we can see the received power for fully coherent beam is approximately at -9dBm and the effect received power can be increased by using the diffuser which approximately at -18dBm. This is due to the effect of diffuser capable to reduce the scintillation index and as a result improve the bit error rate performance as elaborate detail in Figure 3.5, Figure 3.6 and Figure 3.7 in Chapter 3.

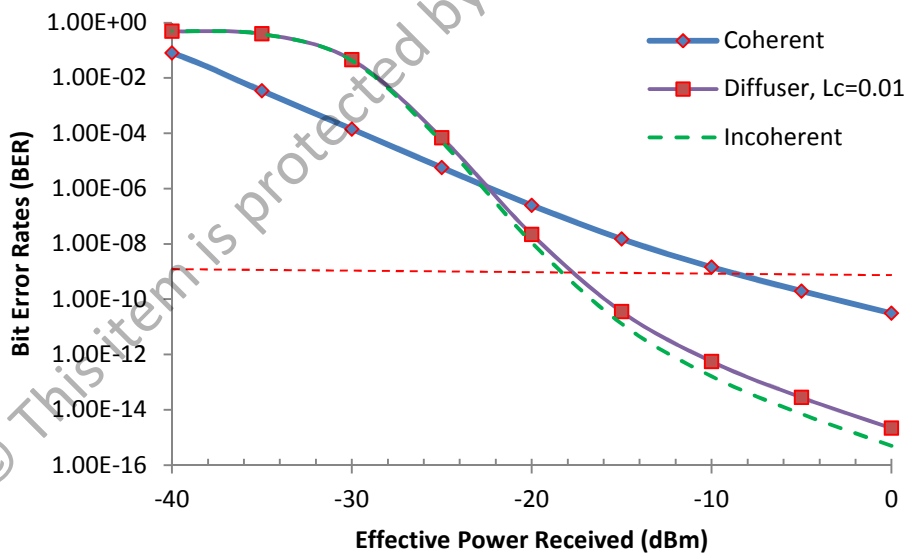

Figure 5.4: Effect of diffuser strength over power received

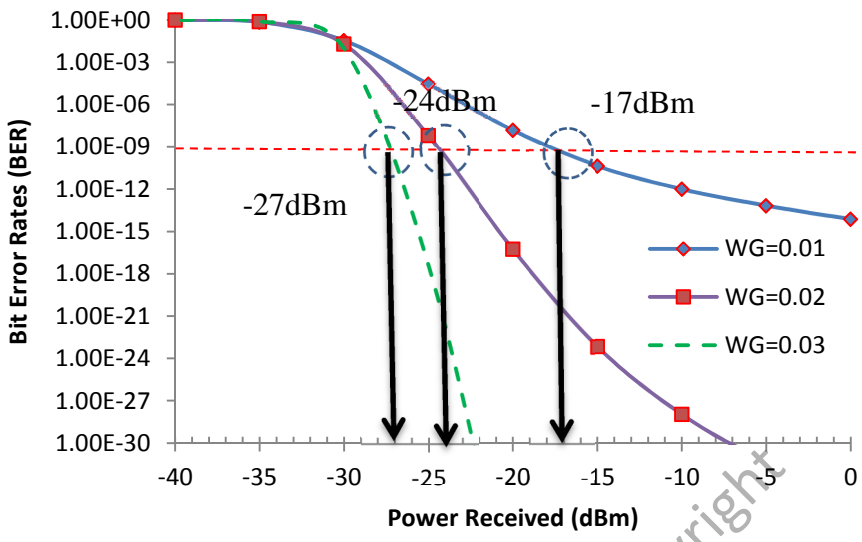

Figure 5.5: Aperture averaging effect on receiving power for DDM technique

The Figure 5.5 shows that effective power received corresponds to the aperture averaging effect. There are three different values of the radius Gaussian lens at receiver 0.01m, 0.02m, and 0.03m to be analytical. The effect of aperture averaging in DDM technique can reduce the further bit error rate. This is because with the increasing of radius Gaussian lens it will reduce the scintillation index and at the same time increase the capability to detect weak signals at the receiver. For instance BER 10^{-9}, for W_G = 0.01m the power received is approximately -17dBm. As the W_G increase double to 0.02m the received power can detect low power to -24dBm and more low power can be detected where can reached up to -27dBm with W_G =0.03m.

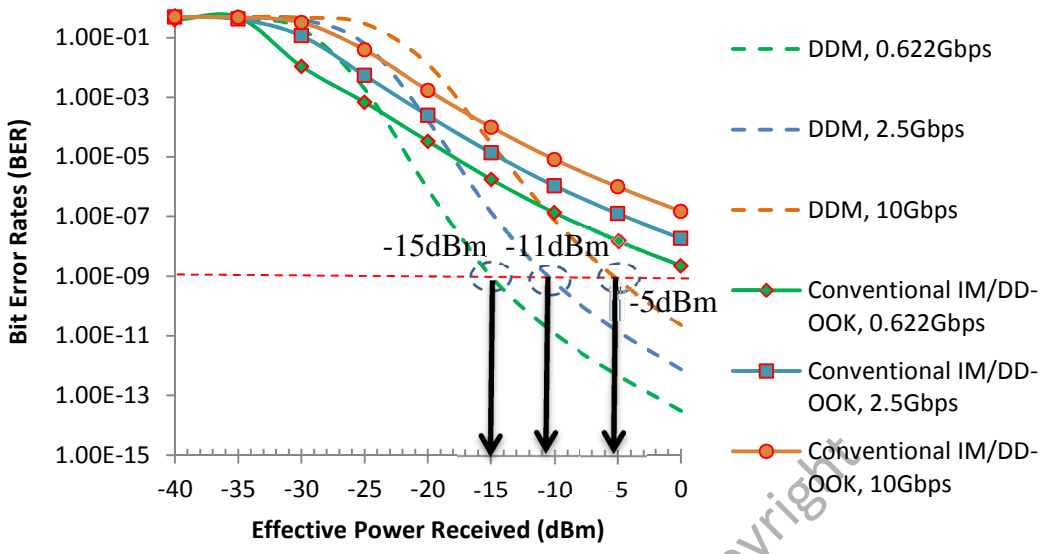

Figure 5.6: Effective power received from selected of bit rate value

The Figure 5.6 shows the effective power received for several value of bit rate that are 622 Mbps, 2.5Gbps and 10Gbps. This selected value of bit rate is referring to the standard Synchronous Digital Hierarchy (SDH) in fiber optic communication transmission. As we can see from the pattern graph the increasing of bit rate will deteriorate the quality of received power. For a fix distance 2km with W_G= 0.01 the CIM/DD-OOK in very poor performance as compared to DDM technique. For BER 10^{-9}, the CIM/DD-OOK only survive on bit rate 0.622Gbps with received power at 0dBm meanwhile the rest bit rate need higher power received in order to operate under error free transmission. However by using the DDM technique it can support high bit rate with received power -5dBm for 10Gbps, -11dBm for 2.5Gbps and -15dBm for 0.622Gbps respectively.

Figure 5.7 shows the effective power received for various propagation distances. Here the distance can up to 3km due to the consideration theoretical analysis result only focus on turbulence effect and moreover the beam divergence is small where below

0.5mrad. In a real situation of FSO must consider all effect such as atmospheric attenuation, pointing error, noise loses and etc. Interm of beam divergence is usually in range of 0.5mrad to 15mrad. For BER 10^{-9}, the receive power for CIM/DD-OOK at 3km is the worst where need higher received power more than 0dBm but the for the propagation distance 1km and 2km can still perform better which at 0dBm and -15dBm respectively. Once again the DDM technique manages to have a good quality signal with power received respectively at -26dBm (1km), -17dBm (2km) and -5dBm (3km).

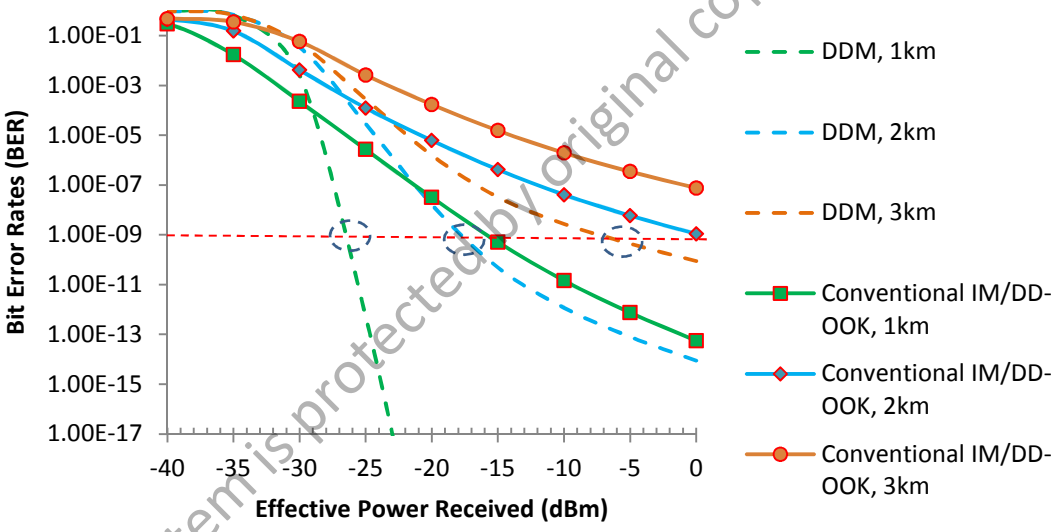

Figure 5.7: Effective power received due to propagation distance

5.4.2 Effective Bit Rate

In a bit rate analysis, we evaluate the data rate from 0.622Gbps up to 10Gbps. The Figure 5.8 shows the performance of DDM compare with CIM/DD-OOK and PCB-OOKfor receiving power fix at -10dBm under strong turbulence condition. Clearly the DDM shows the superior performance where at BER10^{-9} the DDM can support higher bit rate above 10Gbps. Meanwhile the PCB-OOK only operate approximately at

1.25Gbps and the CIM/DD-OOK is the poor performance which is under acceptable BER 10^{-9}. In order to enhance the performance it can be implemented whether by using higher power, reduce propagation distance and increase diameter aperture receive.

In the Figure 5.8 show also the improvement of magnitude BER. If considering at bit rate 2.5Gbps as reference, the CIM/DD-OOK only reach $1.09x10^{-9}$ but the curve PCB-OOK and DDM technique are increase with magnitude BER x2 and x6 respectively. This indicate that when the FSO system operate under strong turbulence effect and if the power receive is set fix at -10dBm, clearly the DDM technique shows the superior performance if compare to conventional OOK modulation technique where at 2.5Gbps the magnitude of BER for DDM technique increase with 12 magnitudes or equivalent to 100 percent improvement and the CIM/DD-OOK with diffuser only 2 magnitudes which give the 33 percent improvement.

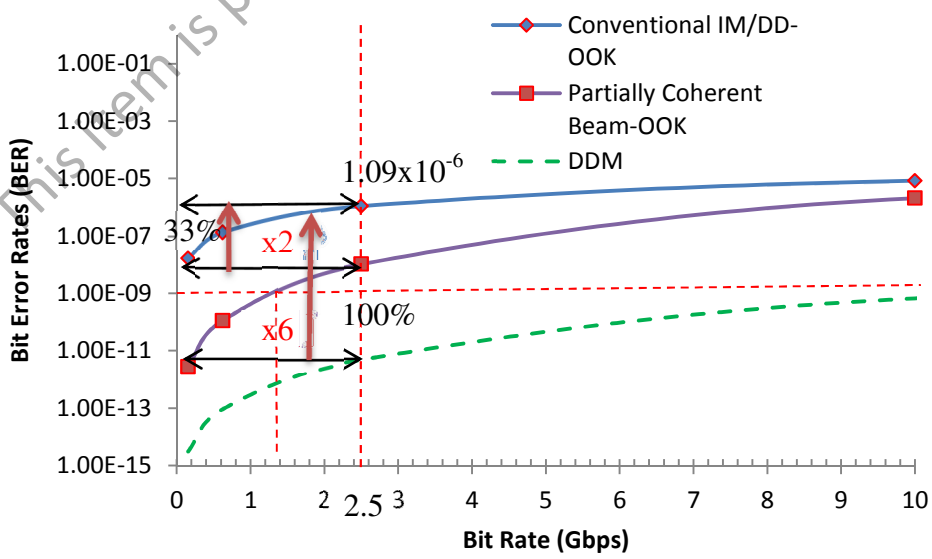

Figure 5.8 : Comparison bit rate under strong turbulence at fix power received -10dBm

The Figure 5.9 shows the performance of DDM to investigate the effective bit rate at various power transmit levels. The optimum performance of bit rate for DDM can be achieved at 5dBm power transmit where at BER 10^{-9} the data bit rate can support higher up to approximately 10Gbps. The significance of this result is to provide the estimation of performance bit rate for DDM when we fix the distance at 2km. From the result clearly shows that DDM capable to operate at low power transmit due to the advantage of DDM efficient in detecting weak signal as explained in Figure 4.11.

The effect of diffuser strengths can also contribute the performance of bit rate as shown in Figure 5.10. The coherent signal represent the signal without using the diffuser and incoherent signal indicate the strong diffuser is used where lead to beam diverge bigger than origin shape. Under the strong turbulence condition the effect of the diffuser strength is small and very effective under weak to moderate turbulence. It points out that no matter how strong the diffuser used it will not improve the turbulence effect. As we can see for coherent beam which denote the CIM/DD-OOK without employ the diffuser shows at BER 10^{-9} the performance of data bit rate is very poor where cannot provide good transmission. However, by using the DDM it can spread the effect of the diffuser up to 1Gbps.

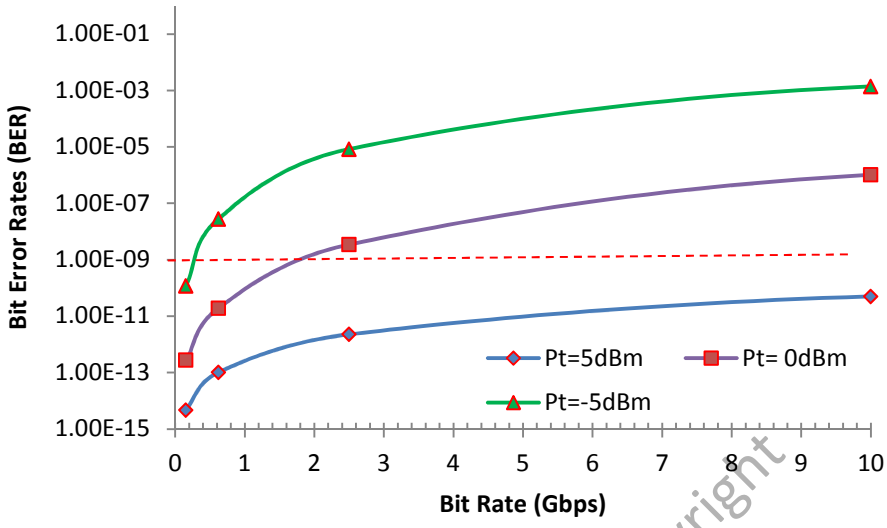

Figure 5.9 : BER versus bit rate under strong turbulence condition for various power transmit level of DDM

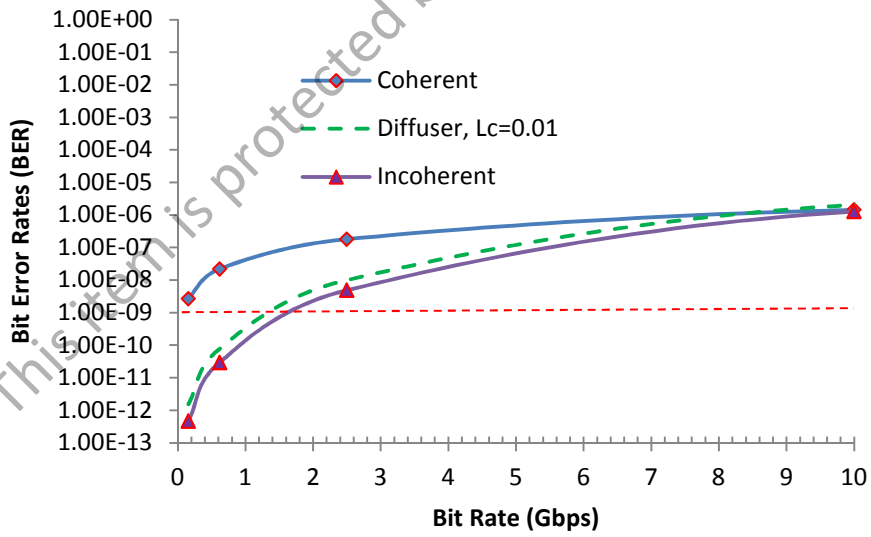

Figure 5.10 : BER versus bit rate under strong turbulence condition for different diffuser strength

5.4.3 Effective Propagation Distance

The distance propagation is one of important role to mitigate the effect of turbulence. In general of FSO measurement performance, shorter distance can provide excellent quality of signal transmission if compare to the long propagation distance. However in a real situation it is necessary for FSO to have rgood quality transmission were able to promulgate at far distance. Figure 5.11 shows the BER versus the various propagation distances under weak turbulence condition. As we can see from the graph all the performances of comparison graph shows in beter quality signal with the DDM is the preeminent. This is because in weak turbulence region the effect scintillation index is very low and thus the amount of signal fading small. Consequently it can expand the length of the propagation distance.

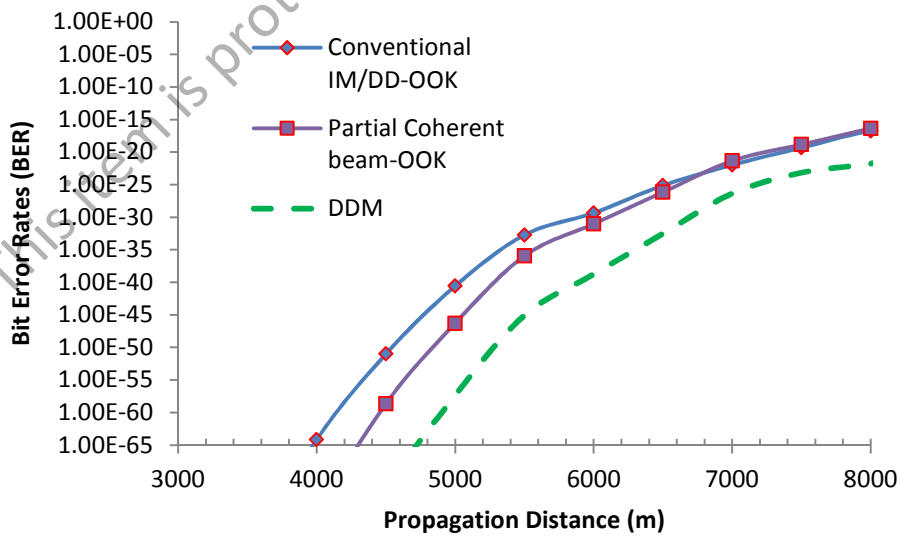

Figure 5.11 : Performance of various propagation distances under weak turbulence condition

Nevertheless in strong turbulence region, the propagation distance shrinkage due to the amount of signal fading escalations. This circumstance can be exemplified in Figure 5.12. For BER 10^{-9}, the CIM/DD-OOK only perform approximately at 1.3km and the partial coherent beam-OOK at 1.7km. Meanwhile for the DDM it can attain more good propagation distance up to 2.1km. Figure 5.13 shows the performance of DDM for BER versus various propagation distances in different wavelength transmission under strong turbulence condition. According from the graph it unambiguously shows the 1550nm wavelength perform better than the 850nm wavelength where at BER 10^{-9} the propagation distance of DDM only reach 1.6km but for 1550nm the propagation distance climb up several hundred meters until 2.1km. The is because the 1550nm has the lower scintillation index if compare to 850nm and thus led to better quality of signal.

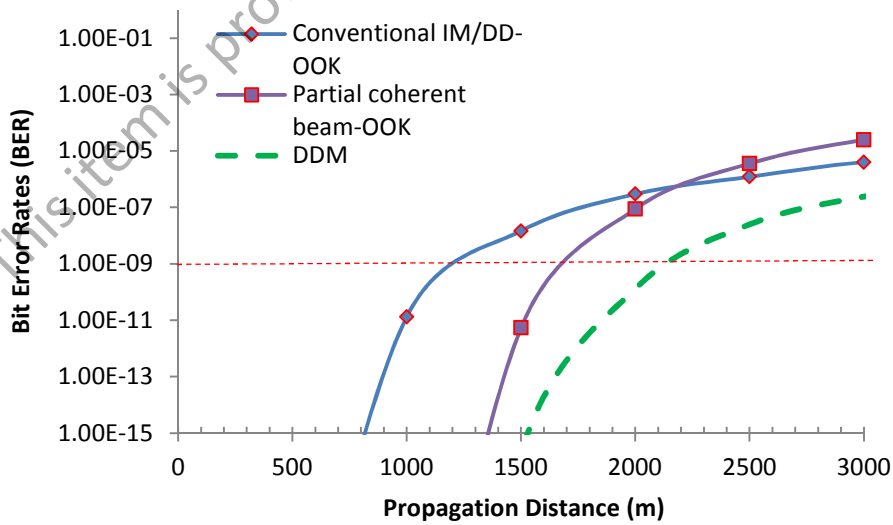

Figure 5.12 **:** Performance of various propagation distances under strong turbulence condition

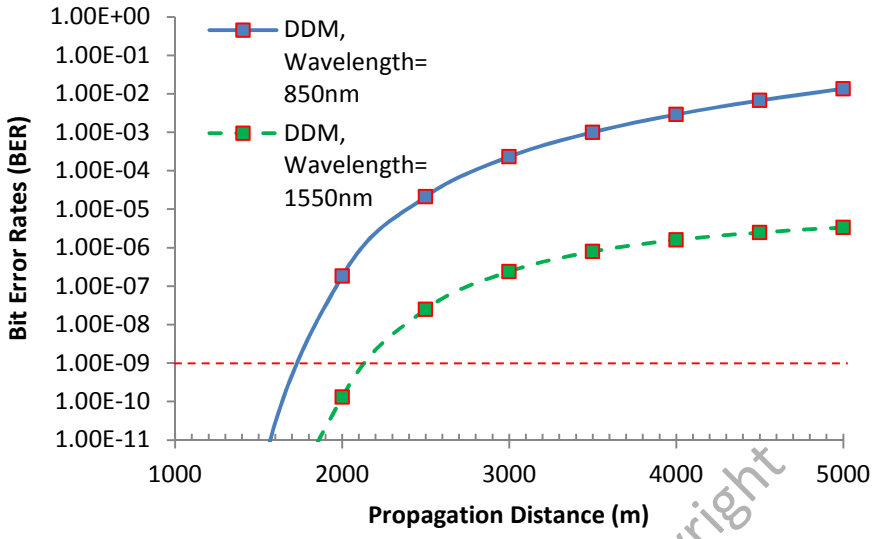

Figure 5.13 : Comparison of different wavelength performance DDM for various propagation distances under strong turbulence condition

5.5 Simulation Results

The performance of DDM technique was simulated using the Optisystem software. Figure 5.14 shows the structure of DDM setup for simulation analysis. We used the Continuous Wave (CW) laser as the source signal with launching power transmit at 0dBm. The wavelength was pick at 1550nm due to the better performance in the reduction scintillation index if compare to 850nm. In generating the data we used Pseudo-Random Bit Sequence (PRBS) with select Non-Return Zero (NRZ) as a modulation format. The external modulator Mach-Zehnder Modulator (MZM) is used to modulate the electrical signal into an optical signal before propagate through the free space optic medium.

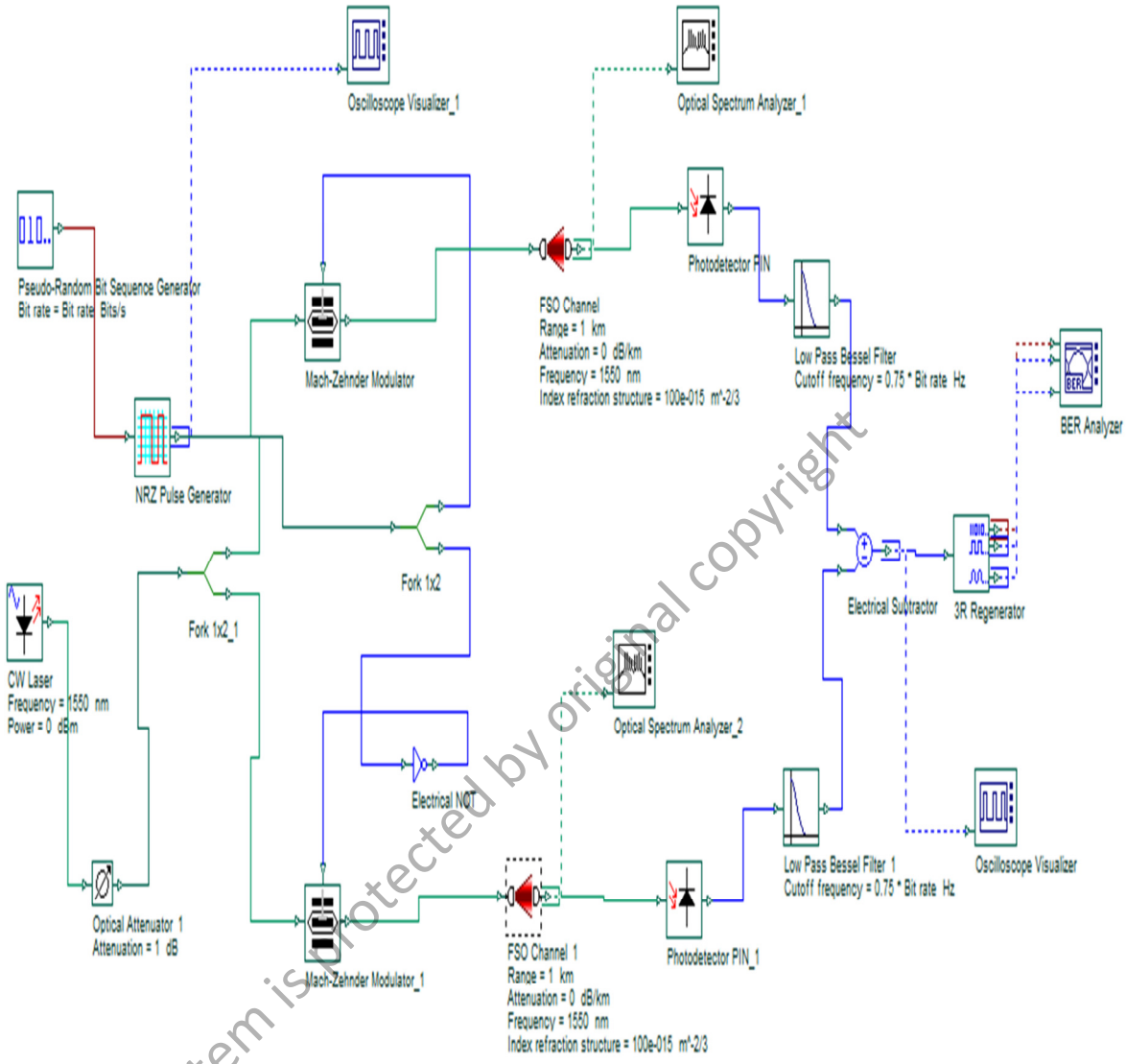

Figure 5.14 : Setup simulation for DDM technique with parameter L = 1km, l_c = 0.001, data rate = 622Mbps, θ = 1mrad and C_n^2 = 100 x 10^{-15} $m^{-2/3}$

In the FSO Channel component we set up both in the same parameters. The propagation range is set at 1km and the attenuation of atmospheric is set to 0 dB/km . This is because we focus only atmospheric turbulence effect in FSOC with not consider other atmospheric effect. For the intensity scintillation we set at 100 x 10^{-15} $m^{-2/3}$ for strong turbulence condition and for weak turbulence 1 x 10^{-15} $m^{-2/3}$. Under geometrical loss factors, the transmitter aperture and receiver aperture are set 2.5cm and 8cm respectively. Meanwhile the beam divergence is pick at 1mrad and other parameters

such as transmitter loss, receiver loss, additional loss and propagation delay are remaining in default value. The noise that generated at receiver were set at random and the dark current value at 10nA with responsivity 1 A/W and thermal noise 100 x 10^{-24} W/Hz. The performance of the system can be evaluated through BER analyzer, oscilloscope visualizer and eye patterns.

5.5.1 Effective Power

Figure 5.15 shows the comparison performance effective received the power of the DDM technique with the CIM/DD-OOK. As expected the DDM is performing better than the CIM/DD-OOK. For BER 10^{-9}, the value of receiving the power of the CIM/DD-OOK is approximately at -24.5 dBm and the DDM at -27 dBm. As a result of using the DDM the received power improved approximately 43% percent.

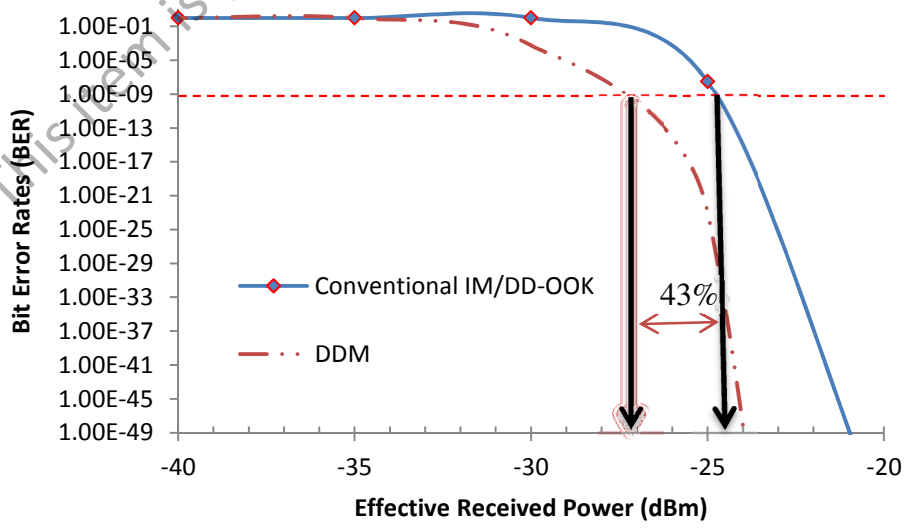

Figure 5.15: Comparison the DDM technique with the CIM/DD-OOK

The Figure 5.16 (a) shows the comparison of BER versus signal power between DDM and the CIM/DD-OOK technique. At BER 10^{-9}, the received power for CIM/DD-OOK and DDM are -85.2dBm and -88.2dBm respectively. This gives the gap signal power approximately 3dBm. Interms of noise power performance, the Figure 5.16 (b) shows the performance of BER versus noise power between CIM/DD-OOK and DDM. The gap noise power between CIM/DD-OOK and DDM is approximately 0.6dBm.

The Figure 5.17 shows the BER versus the effective power received for aperture averaging effect on DDM. The more large receiver the more effective received power can be achieved. For BER 10^{-9}, the aperture diameter 2cm is the poor performance where the received power is at -15.2 dBm. However as the diameter lenses are increase the received power can be more effective where the power received at 5cm and 8cm value are -23.7dBm and -27.5dBm.

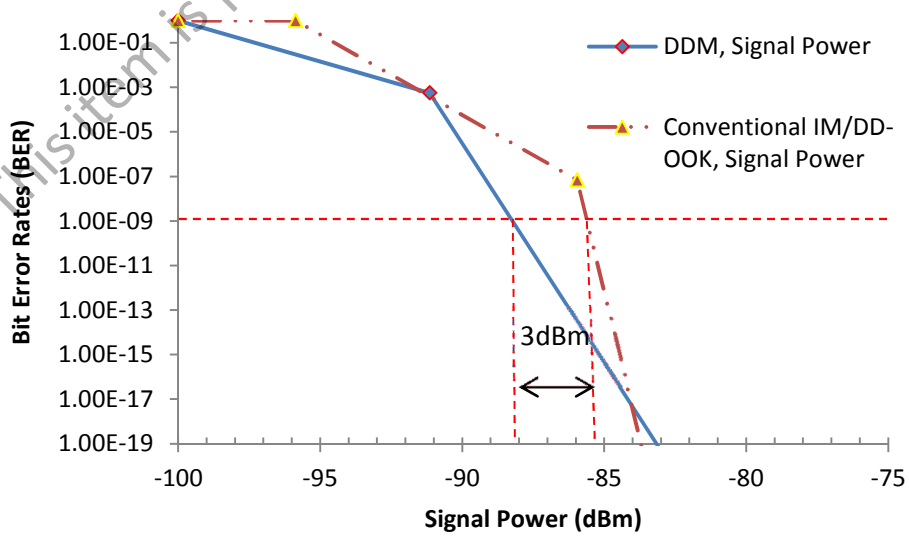

Figure 5.16 (a) : Comparison BER versus Signal Power

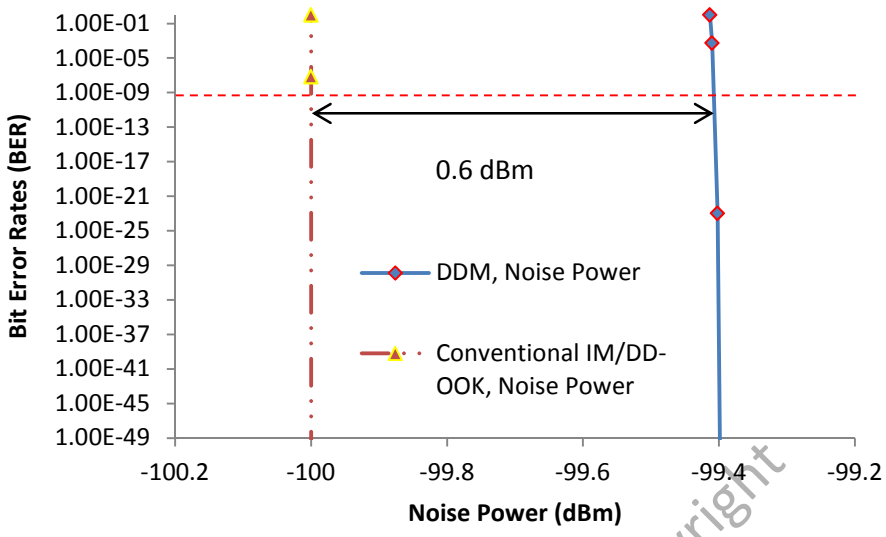

Figure 5.16 (b) : Comparison BER versus Noise Power

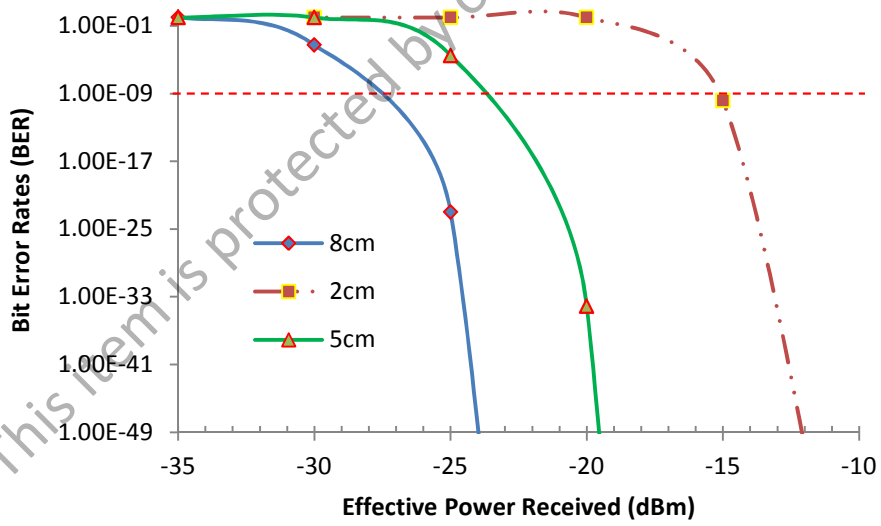

Figure 5.17 : Effect of aperture averaging effect over power received for DDM

In order to analyze more further the performance of DDM due to the influence of averaging effect, the results are visualized through eye patterns and oscilloscope analyzer. Basically if the opening of eye pattern is high it indicates the performance of the system a good and the minimum BER usually below than 10^{-9}. Otherwise if the opening of eye pattern a drop mean the system turn to bad performance and in worst

condition the eye pattern can be flat with the BER is close to 1 value. Meanwhile for oscilloscope result, generally shows the three patterns of signal which is consist of signal and noise power. The blue line represents the signal plus noise power meanwhile the red line represents the only signal power and the green line represent only noise power. The Figure 5.18 (a) and (b) shows the performance of eye pattern and oscilloscope result for 8cm diameter lens.

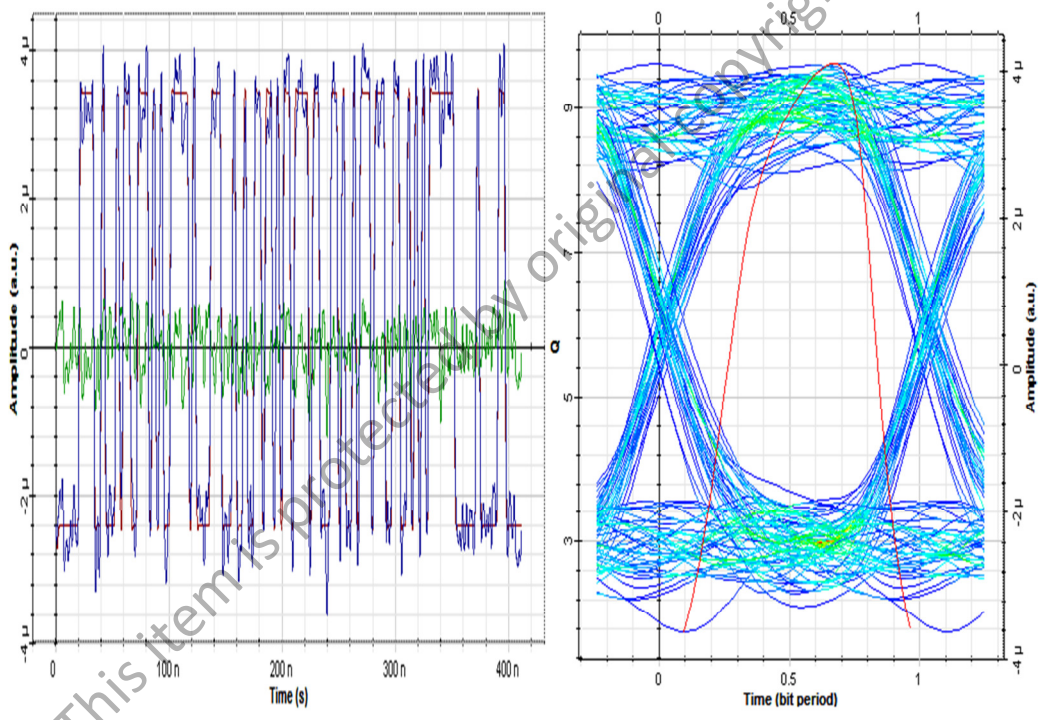

5.18 (a) 5.18 (b)

Figure 5.18 (a) and (b): Performance of eye pattern and signal power with noise power due to aperture averaging effect for diameter lens D=8cm for parameter simulation L = 1km, θ=1mrad, Pt=0dBm, λ=1550nm, Bit rate =622Mbps and $Cn^2=1x10^{-13}$ $m^{-2/3}$

The opening of eye pattern is high which indicate the performance of system is good and this condition can be viewed effectively in oscilloscope result where the signal power (red line) is high if compare with the noise power (green line). This shows that

the level of noise power is still low and allow the detector to receive the signal power with high rate.

Figure 5.19 (a) and (b) shows the performance of eye pattern and oscilloscope result due to aperture averaging effect for diameter lens D=5cm. When the diameter lens is decreasing the effect averaging also decrease as indicate the eye pattern in Figure 5.19 (a). The eye opening seems to close with the eye height drop. Meanwhile in oscilloscope result pattern the gap between signal power and noise power are becoming close. This indicates the performance is deteriorating where the noise power is increased but the signal power is decreasing.

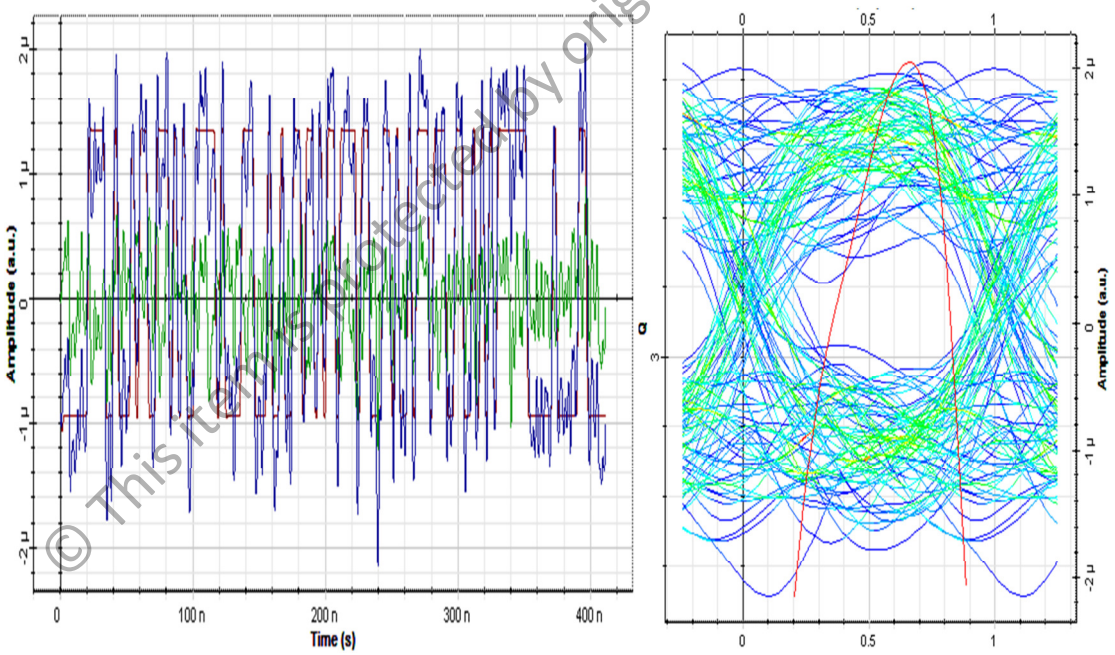

5.19 (a) 5.19 (b)

Figure 5.19 (a) and (b): Performance of eye pattern and signal power with noise power due to aperture averaging effect for diameter lens D=5cm for parameter simulation L = 1km, θ=1mrad, Pt=0dBm, λ=1550nm, Bit rate =622Mbps and $Cn^2=1x10^{-13}$ $m^{-2/3}$

For the worst condition as shown in Figure 5.20 (a) and (b) for the aperture averaging effect with diameter lens D=2cm. At this stage there is no eye opening pattern

and usually the BER is equal to 10^0. For the noise power pattern of oscilloscope results show that the it surpasses the signal power. This indicates that the level of the signal power is very weak and the noise power dominates the overall signal. Here also show that at this point the signal plus noise (blue line) shape pattern turn to similar to noise power.

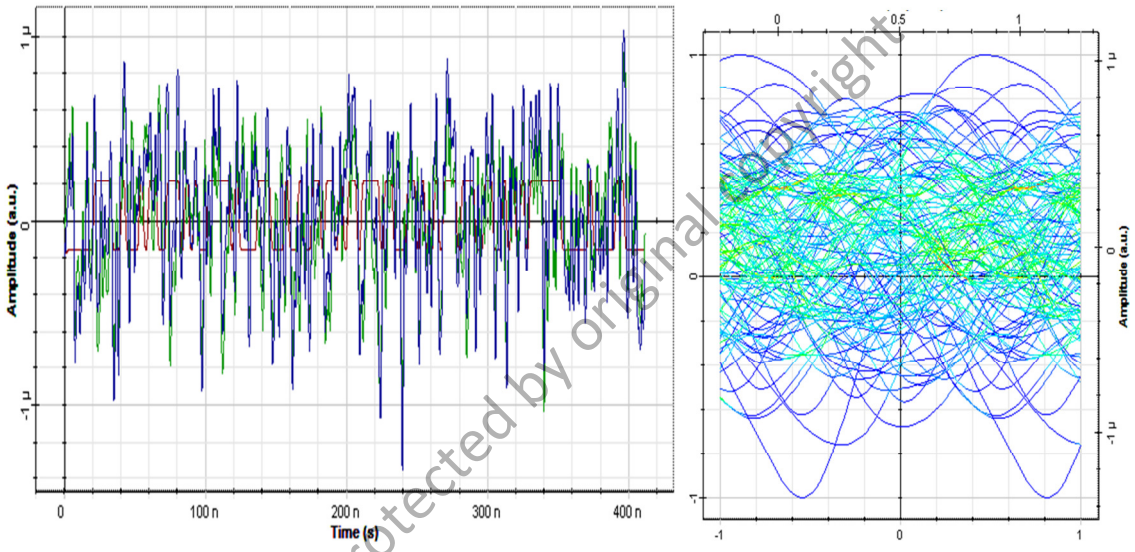

5.20 (a) 5.20 (b)

Figure 5.20 (a) and (b): Performance of eye pattern and signal power with noise power due to aperture averaging effect for diameter lens D=2cm for parameter simulation L = 1km, θ=1mrad, Pt=0dBm, λ=1550nm, Bit rate =622Mbps and $Cn^2=1x10^{-13}$ $m^{-2/3}$

5.5.2 Effective Bit Rate

In bit rate analysis, we simulated the data bit rate from 155Mbps until 10Gbps. Here we fix the diameter lens at D= 8cm with beam divergence value 1mrad. The turbulence is set at $1x10^{-13}$ $m^{-2/3}$ under strong turbulence region and the diffuser effect is chosen at l_c=0.0001 which is equivalent to 1dB attenuator which is represented as a diffuser effect at the transmitter. Figure 5.21 shows the simulation result for BER versus bit rate under strong turbulence condition. The comparison is between CIM/DD-

OOK and DDM along with eye pattern performance. As we can see the DDM optimize the performance of CIM/DD-OOK. For instance the higher bit rate of 2.5Gbps, the DDM can support better than CIM/DD-OOK where the indicator of eye opening shows the CIM/DD-OOK is low if compare with DDM is still high. Interms of BER performance, the CIM/DD-OOK is 3.27 x 10^{-12} and DDM is 2.17 x 10^{-37}. This shows that the DDM improve the BER CIM/DD-OOK performance with 25 magnitude.

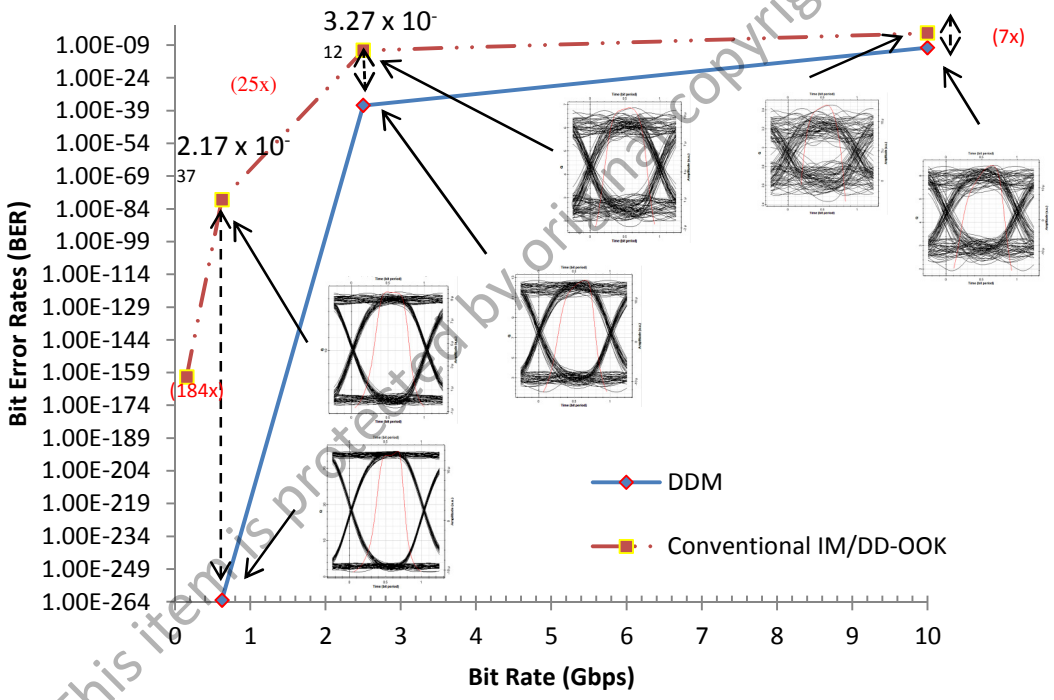

Figure 5.21 : BER versus data bit rate under strong turbulence condition

5.5.3 Effective Range

The analysis for effective range was simulated from the range from 1km to 3km. Figure 5.22 shows the BER versus the propagation distance under strong atmospheric turbulence. In the short propagation distance of 1km both of the performance BER for CIM/DD-OOK and DDM is excellent where 1.1 x10^{-80} and 4.36 x 10^{-268} respectively.

As the distance increase to 2km, the BER for CIM/DD-OOK is drop to below the acceptable error free 10^{-9} which yield 4.89 x 10^{-4}. However the DDM still manages to perform better with the BER 5.51 x 10^{-17}. This show the improvement with 13 magnitude of BER.

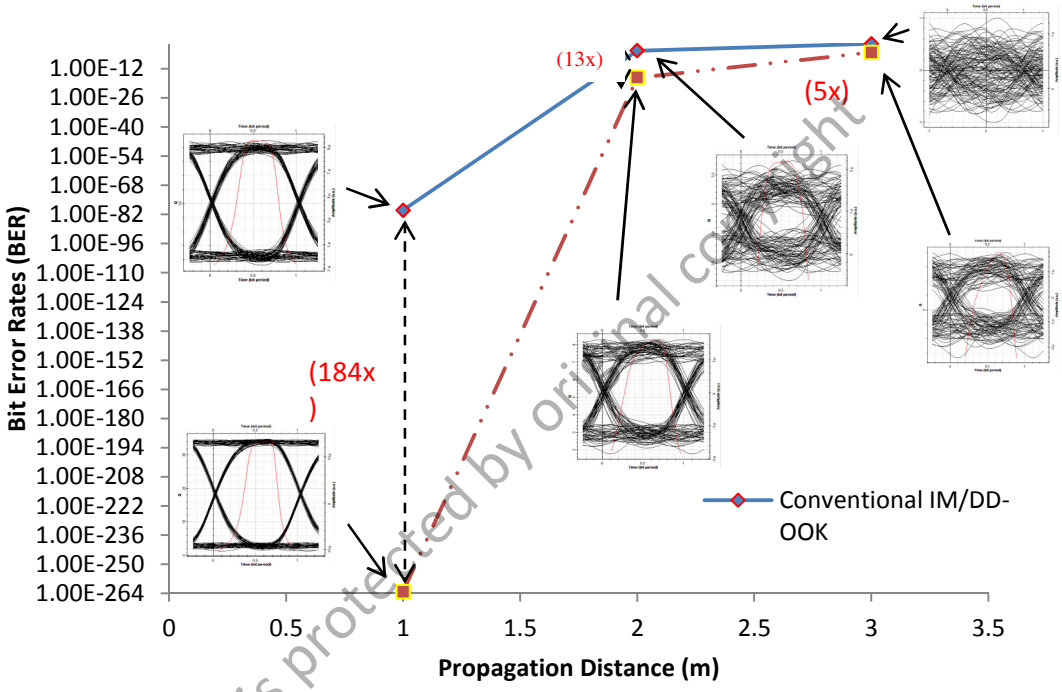

Figure 5.22: BER versus propagation distance under strong turbulence condition

5.5.4 Comparison Theoretical and Simulation Result

The new DDM technique is validated via a simulation 'Optisystem' tool. The curve that label as 'Theoretical' can be obtained in Equation 5.23 whereas the curve that label as 'Simulation' is generated through configuration in Figure 5.14. The beam divergence is select at 1mrad with the aperture receiver 8cm and diffuser strength value is l_c=0.0001. In Figure 5.23 shows the comparison theoretical and simulation result of the effective power received. The curve for simulation is almost similar with theoretical

results. The differences occur due to the certain consideration is not included in theoretical but count in simulation. For instance the noises, in theoretical we only consider shot noise and thermal noise but in simulation it includes the dark current noise. The effect of the attenuator on transmitter also is not similar to the phase diffuser effect which contribute the power received at the receiver.

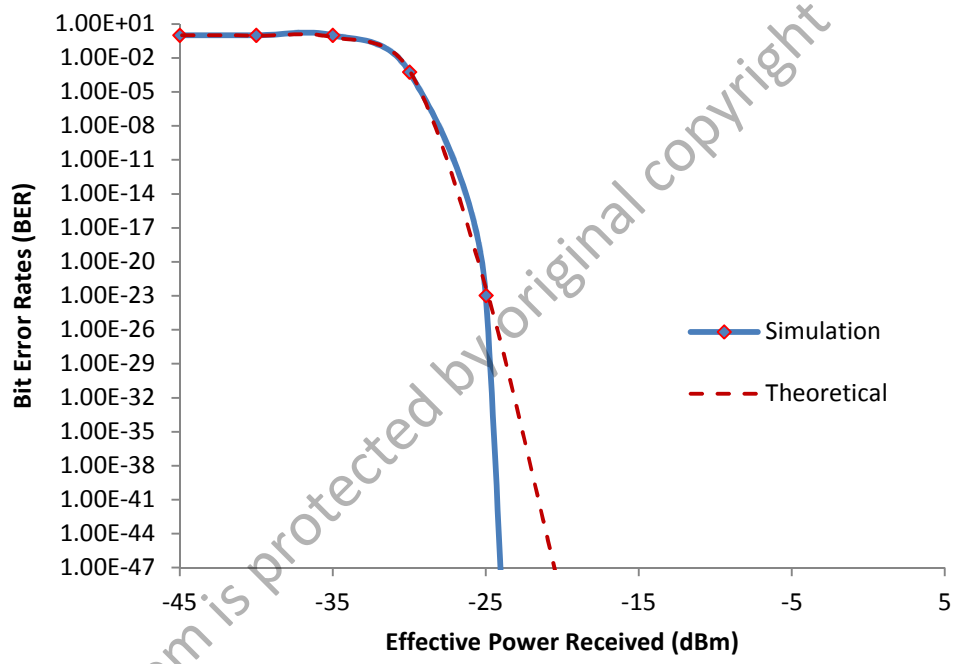

Figure 5.23: Comparison of theoretical and simulation result of the effective power received.

The Figure 5.24 shows the comparison theoretical and simulation result of the effective bit rate. Generally the both curve simulation and theoretical are showing the same pattern with a little bit different when the BER at 1 x 10^{-14} until BER $10^{-1.}$ This is because in simulation the consideration involve such as the sample rate, sequence length, sample per bit and number of samples which not include in theoretical formula.

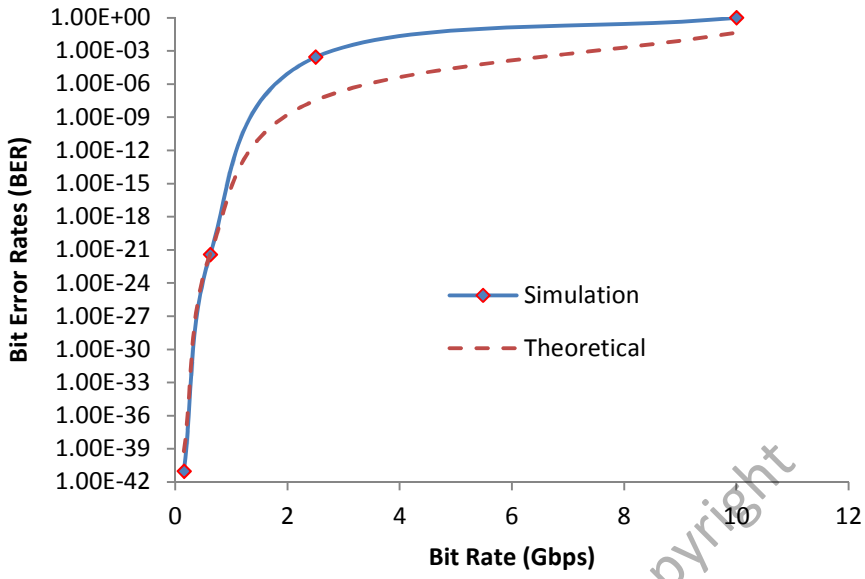

Figure 5.24: Comparison theoretical and simulation result of the effective bit rate

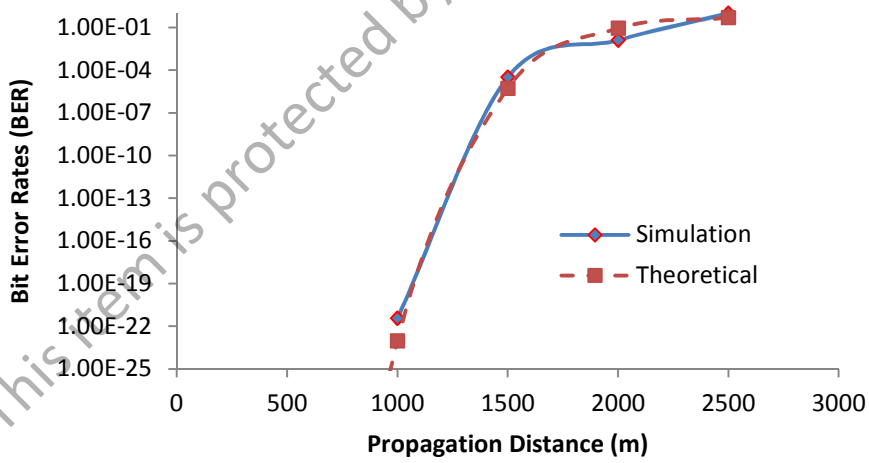

Figure 5.25: Comparison theoretical and simulation result of the effective bit rate

The Figure 5.25 shows the comparison theoretical and simulation result of the increment of propagation distance. It indicates the better matching between simulation and theoretical. The inconsistency the curve between theoretical and simulation is due to effects of geometrical loss where in simulation we only take account effect of the

transmitter and receiver aperture diameter and beam divergence whereas in theoretical include the intensity of the signal.

5.6 Summary

In this chapter we have studied the performance of DDM under the turbulence condition. The curve graphs were produce to evaluate the BER performance by using the Equation 5.25, Equation 5.26, Equation 5.27 and Equation 5.28 with assume the receiver perfectly synchronized. The result shows that for the receiving power performance at acceptable BER 10^{-9} under the strong turbulence condition, the DDM technique able to detect weak signal up to -18dBm. Meanwhile for CIM/DD-OOK with and without diffuser are at -14dBm and 0dBm respectively with different received power approximately 4dBm and 18dBm or equivalent to 99% and 66% improvement. In a bit rate analysis, the evaluation data rate from 622Mbps up to 10Gbps. In case of fix receive power at -10dBm for strong turbulence condition, clearly the DDM technique shows the superior performance if compare to conventional OOK modulation technique where at 2.5 Gbps the magnitude of BER for DDM technique increase with 12 magnitudes or equivalent to 100% improvement and the CIM/DD-OOK with diffuser only 2 magnitudes which give the 33% improvement. Meanwhile for the analysis result of receiving power DDM at 3km distance propagation with consider 0dBm power transmit, wavelength 1550nm and diffuser strength at l_c = 0.01 the received power is 4.59dBm compare with conventional OOK that using diffuser only -7.6dB which equal to 3dBm improvement or around 40 %. Meanwhile interm of BER performance, the DDM can further the distance propagation with approximately 42 % improvement.

CHAPTER 6

CONCLUSION

6.1 Introduction

This chapter will summarize the findings of the research which has been done so far with the contribution of the dissertation research. The recommendations for future work research were also discussed.

6.2 List of Contribution Research

The major contributions of this dissertation for the free space optic communication could be summarized as follows:

i. The development of a new modulation technique, which extend the diffuser effect, enhance the power received and can fix to zero threshold level are easy to apply in practical implementation since the new modulation technique are sharing the same technology with the CIM/DD-OOK without need a complex process.

ii. A new mathematical model of the SNR and BER based on the newly modulation technique has been developed and thoroughly analyzed.

iii. A new design of modulation technique using the Optisystem simulation tool.

6.3 Conclusion

In this dissertation, the new Dual Diffuser Modulation technique has been successfully developed as fullfill the first objective. This technique employ two transmitters and two receivers with equipped inverter at transmitter and subtractor at receiver. Meanwhile the phase screen diffuser is mount at laser exit at transmitter. In order to counter the problem of CIM/DD-OOK, the DDM overcome the weakness of conventional OOK signaling. This new modulation is better against the turbulence effect and can withstand under the strong turbulence regime.

Three important elements which make this new modulation technique can become as a compromising future commercializing modulation technique. The firstly is the new modulation technique has overcome the threshold level problem in CIM/DD-OOK where can fix the threshold signal level to zero. It is easier to identify the received signal whether bit '1' or bit '0' without need a complex process such as an adaptive threshold. The secondly is the using of phase screen diffuser is one of alternatives to reduce the channel fading effect *(*Ricklin and Davidson 2002). The phase screen diffuser capable in reduces the scintillation index which can result low BER performance. The phase screen diffuser is very effective especially under weak and moderate turbulence condition. However as the turbulence increase to strong region, the effects of diffuser become weak and at the some point the performance of partially coherent beam (with diffuser effect) will be same as a perfectly coherent beam (without diffuser effect) but with the new modulation technique the effect of the diffuser can extend even in a strong turbulent regime. The thirdly is the power received can increase almost double if compare with CIM/DD-OOK.

This condition also actually overcomes the problem of using the partially coherent beam where the beam divergence is more expensive (Yaqing, 2011) if using the diffuser and as a result the power transmit will be reduced. The combination of optimization diffuser effect, higher power received and threshold signal level fixes to zero has formed the new modulation technique robust against the atmospheric turbulence effect. This has been discuss extensively in Chapter 3 and Chapter 4.

The development of a new modulation technique has been established in a mathematical model to analyze the performance of an FSO system interm of effective power received, effective data bit rate and link propagation coverage. This is the second goal objective of the this research. The model of mathematical encircles the signal to noise ratio (SNR) and bit error rate (BER) with considering the Gamma-Gamma distribution model. The model of the scintillation index on laser communication application and intensity and average power beam also has been derived.

The third objective is to analyze the theoretical and simulation has been carried out as well. After the successfully developing a new modulation technique, the study in theoretical and simulation has been carried out to analyze the performance in an FSO system under the presence of turbulence effect. In the theoretical part, the performances are based on SNR and BER along with study of scintillation index and power beam effect for the new modulation technique. Meanwhile in simulation part, the analysis is used Optisystem software where the performance can be analyzed in eye diagram shape, power received and oscilloscope signal pattern. At the same time also the study between theoretical and simulation can become as a validation stage to verify the finding has related each other.

The findings show that the comparison between with and without diffuser effect CIM/DD-OOK and the new modulation technique can improve approximately 99 % and 60 % for received power. Interm of data bit rate, the result shows that when the FSO system operate under strong turbulence effect and if the power receive is set fix at -10dBm, the DDM technique is better than conventional OOK modulation technique where at 2.5Gbps, the magnitude of BER for DDM technique increase with 12 magnitudes or equivalent to 100 % improvement and the CIM/DD-OOK with diffuser only 2 magnitudes which give the 33 % improvement. Meanwhile for the analysis result of receiving power DDM at 3km distance propagation with consider 0dBm power transmit, wavelength 1550nm and diffuser strength at lc = 0.01, the received power is -4.59dBm compare with conventional OOK that using diffuser only -7.6dBm which equal to 3dBm different or around 100 % improvement. Interm of BER performance, the DDM can further the distance propagation with approximately 42 % improvement. Therefore, the new DDM technique is perform better than the conventional intensity modulation for direct detection on off keying (CIM/DD-OOK) to overcome the degradation of signal fading due to strong turbulence condition.

6.4 Recommendations for Future Work Research

Although the objectives of this dissertation have been achieved, the work has never been enough to cover the entire optical wireless communications research areas. The work and time constraint will need to do so is beyond the scope of this dissertation. Therefore there a few recommendations can be carried out to extend the future work study:

a) The study can be investigated to the pulse interval modulated in FSO. This is one of the alternative solutions to reduce the channel fading effect. In the case of OOK signaling technique, the pulse interval modulation encoded the data in the interval between pulses. This technique could become the effective solution for the complex symbol decision circuit needed for an optimum CIM/DD-OOK FSO system in turbulent atmospheric channels.

b) The study also can extend to the polarization shift keying modulated in FSO. This study might be providing the best solution of channel fading where the atmospheric turbulent channel does not result in change of the polarization state of a traversing field. This can be done by encoding the data on the polarization state of an optical beam.

c) Other than the modulation technique to reduce the channel fading effect, the hybrid radio over FSO (RoFSO) can be investigated. This study was based on principle a multiple subcarrier system, can further prove the viability of subcarrier modulated FSO as a tool for increasing communication system's capacity.

d) The hybrid FSO/RF also as a robust system to ensure the system can be operated continuously. The FSO is acting as a main transmission channel and the RF as a backup link. Under the fog or thick haze can cause the FSO link loss transmission but with the capability of RF it can maintain the transmission signal even in the poor weather condition.

REFERENCES

A. A. Farid and S. Hranilovic (2007), Outage capacity optimization for freespace optical links with pointing errors, *J. Lightwave Technol*., vol. 25, pp. 1702–1710, July.

A. C. Schell, (1961). The multiple plate antenna. *PhD Dissertation*, Massachusetts Institute of Technology, Cambridge

A. Dogariu & S. Amarande, (2003). Propagation of partially coherent beams: turbulence-induced degradation. *Opt. Lett.* 28~1, 10–12.

A. Garcia-Zambrana, (2007). Error rate performance for STBC in free-space optical communications through strong atmospheric turbulence. *IEEE Communication Letters,* vol. 11, pp. 390-392, May.

A. Prokes, (2009). Modeling Of Atmospheric Turbulence Effect On Terrestrial Fso Link *Radioengineering Journal*, Vol 18, No.1 April.

Andrews, L. C., Phillips, R. L. (1998). *Laser Beam Propagation through Random Media*. Bellingham: SPIE Press.

A. K. Majumdar & J. C. Ricklin (2008), Free-Space Laser Communications: Principles and Advances. New York: Springer.

A. Nordbotten (2000), LMDS systems and their application, *IEEE Communications Magazine*, vol. 38, pp. 150 -154,.

B. Flecker, M. Gebhart, E. Leitgeb, M. S. Sheikh, & C. Chlestil (2006), Results of attenuation-measurements for Optical Wireless channels under dense fog conditions regarding different wavelengths, *Proc. SPIE* 6303, 63030P.

Carbonneau & D. R. Wisely, (1998). Opportunities and challenges for optical wireless: the competitive advantage of free space telecommunications links in today's crowded marketplace. *Wireless Technologiesand Systems: Millimeter-Wave and Optical*, P. Christopher, L. Langston and G. S. Mecherle, eds, Proc. SPIE 3232, 119–128.

Cvijetic, N., Wilson, S.G., & Brandt-Pearce, M. (2007). Receiver Optimization in Turbulent Free-Space Optical MIMO Channels With APDs and Q-ary PPM. IEEE Photonics technol. lett., , 19, (2), pp. 103–105.

D. Kedar & S. Arnon. (2004). Urban optical wireless communication networks: the main challenges and possible solutions. *IEEE Communications Magazine,* vol. 42, pp. s2-s7, May.

D. Kedar and S. Arnon. (2003). Optical wireless communication through fog in the presence of pointing errors. *Applied Optics,* vol. 42, pp. 4946-4954, Aug.

D. L. Fried, (1967). Aperture averaging scintillation. *J. Opt. Soc. Am. 57,* 169-175.

Dennis Killinger, (2002). *Free space optics for laser communication through the air*. *Optics & Photonics News,* pp. 36-42.

D. Rockwell, A. and S. Mecherle, G. (2009), Optical wireless: Low-cost, broadband, optical access.

E.B. Zyambo, D.C. O'Brien, C.E. Faulkner, D.J. Edwards (2001), Design of a highspeed optic al wireless LAN at long wavelengths, in *Optical Wireless Communications III*, Proc. SPIE 4214, 115-123.

E. J. Lee & V. W. S. Chan, (2004). Optical communications over the clear turbulent atmospheric channel using diversity. *IEEE Journal on Selected Areas in Communications,* vol. 22, pp. 1896-1906, Nov.

E. Jakeman, (1980). On the statistics of *K*-distributed noise. *J. Phys*. A 13, 31-48.

F. E. Goodwin, (1970). A review of operational laser communication systems. *Proceedings of IEEE,* vol. 58, pp. 1746-1752, Oct.

Free Space Optic.org (FSO) (2009). *History of Free Space Optics*. Citing Internet Sources from URL http://www.freespaceoptics.org/freespaceoptics/default.cfm

fSona (2009). *FSO Technology Guide.* Citing Internet Sources from URL http://www.fsona.com/technology.php?sec=fso_guide

G. Gbur & E. Wolf, (2002). Spreading of partially coherent beams in random media. *J. Opt. Soc. Am. A* 19, 1592–1598.

G. R. Osche, (2002). *Optical Detection Theory for Laser Applications*. New Jersey: Wiley.

H. Manor, S. Arnon (2003), Performance of an optical wireless communication system as a function of wavelength, *Appl. Opt. 42*, No. 21, 4285-4294.

H. Hemmati, (2007). Interplanetary laser communications. *Optics and Photonics News,* vol. 18, pp. 22-27, Nov.

H. Willebrand and B. S. Ghuman, (2002). *Free Space Optics: Enabling Optical Connectivity in today's network*. Indianapolis: SAMS publishing.

H. Yamamoto & T. Ohtsuki, (2003) Atmospheric optical subcarrier modulation systems using space-time block code. *IEEE Global Telecommunications Conference, (GLOBECOM '03)* vol. 6, New York, pp.3326-3330.

Hamed Al-Raweshidy, (2002). *Radio over Fiber Technologies for Mobile Communications Networks*. Artech House.

I. B. Djordjevic, B. Vasic, and M. A. Neifeld, (2007). LDPC coded OFDM over the atmospheric turbulence channel. *Optical Express,* vol. 15, pp. 6336-6350.

I. I. Kim, H. Hakakha, P. Adhikari, E. Korevaar, and A. K. Majumdar, (1997). Scintillation reduction using multiple transmitters. *Proceeding of SPIE,* vol. 2990, pp. 102-113.

I. I. Kim, J. Koontz, H. Hakakha, P. Adhikari, R. Stieger, C. Moursund, M. Barclay, A. Stanford, R. Ruigrok, J. J. Schuster, and E. J. Korevaar, (1997). Measurement of scintillation and link margin for the TerraLink laser communication system. *Wireless Technology and Systems: Millimeter Wave and Optical, Proceedings of SPIE,* vol. 3232, pp. 100-118.

I. Kim, M. Mitchell, and E. J. Korevaar. (1999). Measurement of scintillation for free-space laser communication at 785 nm and 1550 nm. *Optical Wireless Communications II, Proceedings of SPIE,* vol. 3850, pp. 49-52.

I. Kim, (2009), 10 G FSO systems position technology for the future, *Lightwaveonline* pp. 19-21.

Isaac I. Kim, Bruce McArthur, and E. Korevaar. (2001). Comparison of laser beam propagation at 785 nm and 1550 nm in fog and haze for optical wireless communications. *SPIE Proceeding: Optical Wireless Communications III,* vol. 4214, pp. 26-37.

J. Alda (2003), Laser and Gaussian beam propagation and transformation, *Encyclopedia of Optical Engineering*, Marcel Dekker, New York.

J. C. Ricklin & F. M. Davidson, (2002). Atmospheric turbulence effects on a partially coherent Gaussian Beam: implications for free-space laser communication. *J. Opt. Soc. Am. A* **19**, 1794–1802.

J. C. Ricklin & F. M. Davidson. (2002). Atmospheric turbulence effects on a partially coherent Gaussian Beam: implications for free-space laser communication. *Journal Optical Society Am*. A 19, 1794-1802

J. Elon Grave and S. Drenker, (2002). Advancing Free space Optical communication with Adaptive optics. *Lightwaveonline,* vol. 19, pp. 105-113, Sept.

J. H. Churnside, (1991). Aperture averaging of optical scintillation in the turbulent atmosphere. *Appl. Opt*. 30**,** 1982–1994.

J. Richard Kerr & James R. Dumphy, (1973). Experimental effects of finite transmitter apertures on scintillations. *J. Opt. Soc. Am. 63,* 1-8.

J. T. Li & M. Uysal. (2003). Optical wireless communications: System model, capacity and coding. *Vehicular Technology Conference,* vol. 1, pp. 168-172.

J. W. Goodman, (1985). *Statistical Optics*, Wiley, New York.

J. W. Goodman, (1985). *Statistical Optics*. New York: John Wiley,

J.H. Churnside & S.F. Clifford, (1987). Log-normal Rician probability-density function of optical scintillations in the turbulent atmosphere. *J. Opt. Soc. Am*. A 4, 1923-1930.

Johnson, D.A. (2009). *Handbook of Optical Through The Air Communications.* Citing Internet Sources from URL http://www.imagineeringezine.com/ttaoc/detector.html.

L. C. Andrews & R. L. Phillips, (1998). *Laser Beam Propagation through Random Media*, SPIE Press, Bellingham, WA.

L. C. Andrews & R. L. Phillips, (2005) *Laser beam propagation through random media*, second ed. Washington: SPIE Press,

L. C. Andrews, (1998). *Special Functions of Mathematics for Engineers*, SPIE Press, Bellingham, WA.

L. C. Andrews, R. L. Phillips, & A. R. Weeks, (1997). Propagation of a Gaussian-beam wave through a random phase screen. *Waves Random Media* **7**, 229–244.

L. C. Andrews, R. L. Phillips, & C. Y. Hopen, (2000). Aperture averaging of optical scintillations: power fluctuations and temporal spectrum. *Waves Random Media* **10,** 53–70.

L. C. Andrews, R. L. Phillips, & C. Y. Hopen, (2001) *Laser beam scintillation with applications*. Bellingham: SPIE,

L. Mandel & E. Wolf, (1995). *Optical Coherence and Quantum Optics*, Cambridge University Press, Cambridge

L. Wasiczko, I.I. Smolyaninov, S.D. Milner, C.C. Davis (2004)., Studies of freespace optical links through simulated boundary layer and long-path turbulence, in *Optics in Atmospheric Propagation and Adaptive Systems VI*, Proc. SPIE 5237, 127-135.

M. A. Al-Habash, L. C. Andrews, & R. L. Phillips, (2001). The mathematical model for the irradiance probability density function of a laser beam propagating through turbulent media. *Optical Engineering,* vol. 40, pp. 1554-1562.

M. A. Al-Habash, L. C. Andrews, & R. L. Phillips, (2001). Mathematical model for the irradiance PDF of a laser beam propagating through turbulent media. *Opt. Eng*. 40, 1554–1562.

M. Abtahi, P. Lemieux, W. Mathlouthi, and L. A. Rusch, (2006). Supprression of turbulence-induced scintillation in free-space optical communication systems using saturated optical amplifiers. *Journal of Lightwave Technology,* vol. 24, pp. 4966-4973, Dec.

M. Razavi and J. H. Shapiro, (2005). Wireless optical communications via diversity reception and optical preamplification. *IEEE Transaction on Communications,* vol. 4, pp. 975-983.

M. Naboulsi, H. Sizun, and F. de Fornel (2004), Fog attenuation prediction for optical and infrared waves, *Opt. Eng.*, 43_2_, 319–329.

M. Salem, T. Shirai, A. Dogariu, and E. Wolf, (2003). Long-distance propagation of partially coherent beams through atmospheric turbulence. *Opt. Commun.* **216**, 261.

M. Uysal, J. T. Li, & M. Yu, (2006). Error rate performance analysis of coded free-space optical links over gamma-gamma atmospheric turbulence channels. *IEEE Transactions on Wireless Communications,* vol. 5, pp. 1229-1233, June.

M. Uysal, S. M. Navidpour, and J. T. Li, (2004). Error rate performance of coded free-space optical links over stong turbulence channels. *IEEE Communication Letters,* vol. 8, pp. 635-637.

Mahon, R., et al (2008). Interference effects and aperture averaging in retroreflected light", *Opt. Eng*. 47(4), 046002-1 -046002-9.

M.A. Al- Habash, L.C. Andrews & R.L. Phillips, (2001). Mathematical model for the irradiance probability density function of a laser beam propagating through turbulent media. *Opt. Eng.* 40, 1554-1562.

N. Perlot (2007), Evaluation of the scintillation loss for optical communication systems with direct detection, *Opt. Eng.* 46-2, 025003.

Nykolak, G. Raybon, B. Mikkelsen, B. B. Brown, P. F. Szajowski, J. J. Auborn, & H. M. Presby, (2001). 160- Gb/s free-space transmission link. *Optical Wireless Communications III*, E. J. Korevaar, eds, Proc. SPIE 4214, 11-13

Nistazakis, H.E., Tsiftsis, T.A., & Tombras, G.S. (2009), Performance analysis of free-space optical communication systems over atmospheric turbulence channels *IET Commun.*, 3, pp. 1402–1409

O. Bouchet T. Marquis, M. Chabane, M. Al Naboulsi, & H. Sizun (2005), FSO and quality of service software prediction, *Proc. SPIE* 5892, 589204.

O. Korotkova, L. C. Andrews & R. L. Phillips. (2000). Speckle propagation through atmosphere: effects of a random phase screen at the source. *Proc. SPIE* Vol. 4821

O. Korotkova, L. C. Andrews, & R. L. Phillips, (2003). Phase diffuser at the transmitter for lasercom link: effect of partially coherent beam on the bit-error rate. *Proc. SPIE* 4976, 70–77.

O. Korotkova, L. C. Andrews, and R. L. Phillips, (2003). Phase diffuser at the transmitter for lasercom link: effect of partially coherent beam on the bit-error rate. *Proc. SPIE* 4976, 70–77.

Q. Cao, M. Brandt-Pearce, S. G. Wilson, and L. C. Brown, (2006). Free-space optical MIMO system using an optical pre-amplifier. *IEEE Global Telecommunications Conference* pp. 1-5, Nov.

R. Iniguez, Roberto, IDRUS, Sevia M., SUN & Ziran. (2007). Optical wireless communications : IR for wireless connectivity. *New York : CRC Press*, 320 s. ISBN 0-8493-7209-7.

R. K. Tyson, (2002). Bit-error rate for free-space adaptive optics laser communications. *J. Opt. Soc. Am. A* **19**~4, 753–758.

Ricklin, J. C., Bucaille, S. & Davidson, F. M., (2004). Performance loss factors for optical communication through clear air turbulence. *Proc. SPIE* 5160, 1-12.

S. Bloom, E. Korevaar, J. Schuster, & H. Willebrand. (2003). Understanding the performance of free-space optics. *Journal of Optical Networking,* vol. 2, pp. 178-200, June.

S. Betti, G. De marchis, and E. Iannone (1995), Coherent Optical Communication Systems, 1st ed. Canada: John Wiley and Sons Inc.,

S. Karp, E. L. O'Neill, & R. M. Gagliardi, (1970) Communication theory for the free-space optical channel. *Proceedings of the IEEE,* vol. 58, pp. 1626-1650.

S. Karp, R. M. Gagliardi, S. E. Moran, & L. B. Stotts. (1988). Optical Channels: fibers, clouds, water and the atmosphere. *New York: Plenum Press*.

S. M. Navidpour, M. Uysal, and M. Kavehrad, (2007). BER performance of free-space optical transmission with spatial diversity. *IEEE Transaction on Communications,* vol. 6, pp. 2813-2819.

S. Rasouli and M. Tavassoly (2006), Measurement of the refractive-index structure constant, Cn^2, and its profile in the ground level atmosphere by moire technique, *Proc. SPIE* 6364, 63640G.

S. Trisno, I.I. Smolyaninov, S.D. Milner, C.C. Davis (2005)., Characterization of time delayed diversity to mitigate fading in atmospheric turbulence channels, in *Free-Space Laser Communications V*, Proc. SPIE 5892, 388-397.

Saleh, B. E., Teich, M. C., (1991) .*Fundamentals of Photonics*. New York: John Wiley & Sons.

Sorensen, N., & Gagliardi, R. (1979), 'Performance of optical receivers with APD', IEEE Trans. Commun., , COM-27, (11), pp. 1315–1321

Schulz, T. J., (2005). Optimal beam for propagation through random media. *Optic. Letter*., 30(10), 1093-1095.

Tyson, R. K., Canning, D. E. and Tharp, J. S. (2005), Measurement of the bit-error rate of an adaptive optics, free-space laser communications system, part 1: tip-tilt configuration, diagnostics, and closed-loop results, *Opt. Eng*. 44(9), 096002-1 – 096002-6.

T. Shirai, A. Dogariu, & E. Wolf, (2003). Directionality of some model beams propagating in atmospheric turbulence. *Opt. Lett.* **28**, 610.

T. Shirai, A. Dogariu, and E. Wolf, (2003) Mode analysis of spreading of partially coherent beams propagating through atmospheric turbulence. *J. Opt. Soc. Am. A* **20**, 1094.

T. Shirai, A. Dogariu, and E. Wolf, (2003). Directionality of some model beams propagating in atmospheric turbulence. *Opt. Lett.* **28**, 610.

T. Yoshimura, (1986) Statistical properties of dynamic speckles. *J. Opt. Soc. Am. A* **3**, 1032–1054.

V. G. Sidorovich, V. V. Ragulsky, M. V. Vasil'ev, A. A. Leshchev, and M. A. Sadovnikov, (2002). Mitigation of aberration in a beam-shaping telescope and optical inhomogeneity in a free-space optical path using an extended light source coupled to the telescope. *Proc. SPIE* **4635**, 179–191.

Vetelino, F. S., Young, C., Andrews, L. & Recolons, J. (2007), Aperture averaging effects on the probability density of irradiance fluctuations in moderate-to-strong turbulence, *Appl. Opt*. 46, 2099-2108.

V. W. S. Chan, (2006). Free-space optical communications. *IEEE Journal of Lightwave Technology,* vol. 24, pp. 4750-4762, Dec.

W. K. Pratt. (1969). *Laser Communication Systems*, 1st Edition. New York: John Wiley & Sons, Inc.

Wang, S. C. H. & Plonus, M. A., (1979). Optical beam propagation for a partially coherent source in the turbulent atmosphere. *Journal Optic Society Am.,* 69, 1297-1304.

Willebrand, B. S. Ghuman (2002), Free-*Space Optics: Enabling Optical Connectivity in Today's Networks*, Sams Publishing, Indianapolis, In.

X. Zhu & J. M. Kahn, (2001) Pairwise codeword error probability for coded free-space optical communication through atmospheric turbulence channels. *IEEE International Conference on Communications (ICC),* vol. 1, pp. 161-164.

X. Zhu & J. M. Kahn, (2003). Mitigation of turbulence-induced scintillation noise in free-space optical links using temporal-domain detection techniques. *IEEE Photonics Technology Letters,* vol. 15, pp. 623-625.

X. Zhu & J. M. Kahn, (2003). Performance bounds for coded free-space optical communications through atmospheric turbulence channels. *IEEE Transaction on Communications,* vol. 51, pp. 1233-1239, Aug.

X. Zhu & J. M. Kahn. (2002). Free-space optical communication through atmospheric turbulence channels. *IEEE Transactions on Communications,* vol. 50, pp. 1293-1300, Aug.

Y. Baykal & M. A. Plonus, (1985) Intensity fluctuations due to a spatially partially coherent source in atmospheric turbulence as predicted by Rytov's method. *J. Opt. Soc. Am. A* **2**, 2124–2132.

Y. Li, Z. Wu, R. Wu & J. Zhang, (2011). Characteristics of the partially coherent Gaussian Schell-model beam propagating in atmospheric turbulence. *Beijing*

Yaqing Li, Zhensen Wu, Rui Wu & Jinpeng Zhang, (2011). Characteristics of the partially coherent Gaussian Schell-model beam propagating in atmospheric turbulence. *Beijing*.

Z. Kolka, O. Wilfert, and V. Biolkova (2007), Reliability of Digital FSO Links in Europe, *Int. J. Electronics, Communications, and Computer Engineering*, **1**_4_, 236–239.

PUBLICATIONS

Journals

- A.K Rahman, S.A Aljunid, Anuar M.S, Fadhil H.A (2014), Improving Performance In Free Space Optical Communication (FSOC) Channel Through The Dual Diffuser Modulation (Ddm) Due To Atmospheric Turbulence, *Journal of Theoretical and Applied Information Technology,* Vol. 60 No.1, February.

- A.K Rahman, S.A Aljunid, Anuar M.S, Fadhil H.A (2014), Enhance the Performance of Free Space Optical (FSO) Communication due to Atmospheric Turbulence via the Dual Diffuser Modulation (DDM), *Key Engineering Materials,* Vols. 594-595 pp1027-1031, Trans Tech Publication, Switzerland.

- A.KRahman, S.A. AlJunid, M.S Anuar, Fadhil H.A., A.R.Arief, C.B.M.Rashidi (2013), Alleviation atmospheric turbulence effect on Free Space Optical Communication (FSOC) channel using the novel modulation Dual-Diffuser Modulation (DDM) Technique, *Wulfenia Journal*, 2014.

Proceedings

- A.K Rahman, S.A Aljunid, Anuar M.S, Fadhil H.A (2013), Improve the BER Performance Of Free Space Optical Communication (FSOC) Due To Atmospheric Turbulence Effect Through The Robust Modulation, 3rd *International Conference and Exhibition on Sustainable Energy and Advanced Materials (ICE-SEAM 2013*), Melaka.

Awards

- Gold Medal, New Dual-Diffuser Modulation (DDM) Technique Free Space Optic (FSO) For Agriculture Application, *Ekspo Rekacipta Dan Pameran Penyelidikan 2013, 6 - 7 January (2014)*, University Malaysia Perlis

APPENDIX A

Example MATLAB codes for Gamma-Gamma probability density function (pdf)

```
clear
clc
x=4.2;                  % alpha value
alpha=x;
y=1.4;                  % beta value
beta=y;
k=(a+b)/2;
k1=alpha*beta;
G=2*(k1^k)/(gamma(alpha)*gamma(beta));
I=0.01:0.01:5;                                  % intensity
K1=I.^(k-1);
Z=2*sqrt(k1*I);
GammaGamma=G.*K1.*besselk((alpha-beta),Z);      % Gamma gamma pdf
Plot (I, GammaGamma)
Xlabel ('Intensity, I')
Ylabel ('Gamma gamma pdf, GammaGamma(I)')
```

APPENDIX B

Example MATLAB codes to determine the value of alpha 'α' and beta 'b' under different turbulence regimes

```
clear
clc


L=0:0.05:80;
for = i=1:length (L)
        x=L (i);
        A=(0.49*x) / (1+1.11*x^(6/5))^(7/6) ;
        B=(0.51*x) / (1+0.69*x^(6/5))^(7/6) ;
        Sci_ind (i) = exp (A+B) – 1;
        alpha (i) = (exp(A) - 1)^-1;
        beta (i) = (exp(B) - 1)^-1;
end
semilogx (L, alpha, L, beta)                %plot function
xlabel ('Log intensity variance \sigma_1^2')
ylabel ('Parameters: \alpha, beta')
```

APPENDIX C

Example calculate the probability of error (BER) using MATLAB and excel calculation input

```
clear
clc

syms x
alpha=2.417;          %calculate using excel then insert in MATLAB
a=alpha;
beta=4.813;           %calculate using excel then inser in MATLAB
b=beta;
k=(a+b)/2;
k1=a*b;
K=(k1.^k)/(gamma(a).*gamma(b))

%Calculate the Probability of BER in presence of atmospheric turbulence
SNRP=0.007835225;     % SNR with diffuser effect calculate using excel
fun=@(x)(((erfc((SNRP.*x)/(2.*sqrt(2))))).*(x.^(k-1))).*(besselk((a-
b),2.*sqrt(k1.*x)));
q=integral(fun,0,inf)
p=K*q
```